Università degli Studi della Tuscia di Viterbo

Dipartimento per la Innovazione nei sistemi biologici, agroalimentari e forestali (DIBAF)

Corso di Dottorato di Ricerca in

SCIENZE, TECNOLOGIE E BIOTECNOLOGIE PER LA SOSTENIBILITÁ - XXXV ciclo

In vitro evaluation of AECOPD experimental vaccine response against NTHi and *Moraxella catarrhalis* by using human advanced models for COPD

Settore scientifico-disciplinare
BIO/19

Tesi di dottorato di:

Dott. Andrea Ariolli

Firma

Coordinatore del corso

Prof. Andrea Vannini

Firma

Tutore

Prof. Antonio Tiezzi

Firma

Co-tutori

Dott.ssa Anna Rita Taddei

Firma

Dott. Alfredo Pezzicoli

Firma

A.A. 2022/23

Utilizzo di modelli umani avanzati per studi sulle infezioni croniche delle vie respiratorie causate da NonTypeable *Haemophilus influenzae* (NTHi) e *Moraxella catarrhalis,* i principali batteri patogeni associati alle esacerbazioni acute nella BPCO (BroncoPneumopatiaCronicoOstruttiva)

Abstract

Understanding host-pathogen interaction is a fundamental step in drug development and its success is often limited by the suitability of the models used to study infections. For instance, beyond ethical debates the use of animals is costly and sometimes not adequate for the desired purposes. Consequently, in the last decades the interest of industry and scientific research has been directed toward the development of innovative *in vitro* alternatives, pushing over traditional preclinical cell culture methods. NonTypeable *Haemophilus influenzae* and *Moraxella catarrhalis* are two common respiratory pathogens often associated with acute exacerbations in Chronic Obstructive Pulmonary Disease (COPD) and Otitis Media. The mechanisms behind the persistence of these bacteria are not yet completely understood, making their eradication complicated. The human airway epithelium is the first line of defence against inhaled pathogens, providing physical, chemical, and immunological barriers against infections. Given its characteristics, modeling this anatomical region *in vitro* could be useful in the characterization of mucosal infections as well as in preclinical drug evaluation. By using highly physiological *in vitro* models fully replicating the human airways cellular architecture, we aimed at recreating COPD-related persistent bacterial infections to mimic the chronicity stage of the disease, with the final scope of using our system to evaluate specific antibodies efficacy in counteracting bacterial pathogenesis. Traditional Air-Liquid-Interface (ALI) respiratory epithelial models' integrity is generally limited to a relatively short timeframe after bacterial infection, representing an obstacle to the investigation of long-term bacterial persistence strategies. We hypothesized that, beyond the absence of immune system components, this limit could be related to the closed spatial configuration of the traditional ALI system. Indeed, mucociliary escalator and cellular extrusion, reported to be key defence mechanisms in pathogen clearance, are hindered by the spatial configuration of the support leading to debris accumulation and fast epithelial disruption after infection. To overcome this limit, we explored a 'personalized' use of the ALI system firstly described by Yonker et al. (2017), consisting in the assembly of the epithelium on the basal part of the porous membrane. Inverting the model configuration allowed us to obtain a system devoid of any physical obstacle to the natural epithelial clearance. This configuration switch did not affect tissue differentiation, as assessed by confocal microscopy analysis that highlighted the presence of key markers representative of the small airways' cellular architecture. Moreover, according to a flow cytometry-based analysis, the inverted model resulted to be more resistant against *Moraxella catarrhalis* infections, apparently as a consequence of the delayed and more controlled onset of the bacterial invasion of the tissue. Interestingly, fluorescence and electron microscopy analysis revealed the ability of *Moraxella catarrhalis* to invade the airway epithelium according to a mechanism involving cellular invasion and formation of intra-epithelial and surface-associated biofilm-like communities. Analysis of these samples highlighted the presence of extracellular material embedding bacterial clusters and sign of macroscopical remodeling of the epithelium. Furthermore, LSCM and TEM analysis demonstrated that these biofilm-like structures are impermeant to labeling with immunoglobulins and that extracellular double strand DNA is part of the biofilm architecture. Despite exhibiting a lower invasiveness, NonTypeable *Haemophilus influenzae* (NTHi) was observed to persistently colonize the airway epithelium as it was detected intra- and extra-cellularly after two weeks of infection apparently without causing substantial damage and displaying different colonization phenotypes (planktonic, aggregated, biofilm-like). A reduction in overall NTHi presence in the tissue was observed after one week of infection in inverted models only, possibly as a consequence of the fact that natural clearing processes could be functional in this configuration. Finally, two different bacterial quantification strategies were explored in order to overcome biofilm-related issues encountered when applying traditional CFU counting methods; this was done with the final scope of quantifying bacterial biomass associated with the respiratory model in the presence of specific treatments intended to be used as anti-bacterial intervention strategy. This work aims to serve as a basis for future validation of organotypic ALI airway models as relevant tools to characterize infections and evaluate the efficacy of treatments against pathogen infectivity.

Key words: advanced *in vitro* models, airways, host-pathogen interaction, microscopy, biofilm.

Disclaimer

Sponsorship: This work was funded by GlaxoSmithKline Biologicals SA.

Transparency statement: Andrea Ariolli is a PhD student at the University of Tuscia (UNITUS) and participates in a post graduate studentship program at GSK, Siena, Italy.

Contents

1. Introduction

This PhD thesis research project is aimed at setting up and implementing advanced cellular models that could be relevant for the characterization of long-term human airways infections caused by the main pathogens associated with COPD exacerbations. Moreover, this work aims to serve as basis for future validation of organotypic ALI airway models as relevant tools to evaluate the efficacy of treatments against pathogen infectivity.

1.1 Background and state of the art

Chronic obstructive pulmonary disease (COPD) is an increasingly prevalent type of obstructive respiratory disease characterized by long-term breathing complications and impaired airflow caused by the progressive narrowing of the small airways and breakdown of lung tissue (Decramer et al., 2012). A common feature of COPD disease is acute exacerbation (AECOPD), defined as a period of acute worsening of symptoms (Ritchie & Wedzicha, 2020) that can lead to periodic hospitalization and higher mortality in COPD patients (Njoku et al., 2020). Beyond the definition of COPD as a heterogeneous disease characterized by several causes and features, the relationship between the lung microbiome and AECOPD has been highlighted by numerous evidences over time (Dy & Sethi, 2016). Bacterial and viral infections are reported to be the main cause of exacerbations, respectively being responsible for approximately half of the cases each (Bouquet et al., 2020); Nontypeable *Haemophilus influenzae* (NTHi) and *Moraxella catarrhalis* (Mcat) are two pathogens frequently associated with AECOPD and otitis media (OM) (Bakaletz & Novotny, 2018; Blakeway et al., 2017; Huang et al., 2017; Mayhew et al., 2018); their presence in stable COPD patients increases the chance of a subsequent exacerbation (Malvisi et al., 2021) and they can act as co-pathogens (Armbruster et al., 2010; Nicchi et al., 2022).

There is currently no cure for COPD, but treatments can help slow down the progression of the condition and manage the symptoms. A recent report showed that pneumococcal and influenza vaccination significantly reduced the likelihood of a COPD exacerbation suggesting that patients could benefit from this type of treatment (Walters et al., 2017). With the aim of reducing the frequency of AECOPD episodes in COPD patients, GSK developed an investigational multicomponent vaccine based on recombinant antigens of NTHi and *Moraxella catarrhalis*. Whereas the goal of vaccination in reducing and preventing bacterial infection is

obvious, the immune mechanisms behind the effectiveness of the treatment are not fully understood. Indeed, COPD respiratory tissues are susceptible to dysregulation of innate immune effectors and have impaired cilia beating and turnover of the mucus layer rendering the eradication of the bacterial pathogens complicated (Aghapour et al., 2018). Moreover, despite both NTHi and *Moraxella catarrhalis* are known to adopt various strategies to persist in the host such as intracellular survival and biofilm formation (Ahearn et al., 2017; Perez et al., 2014), the ways by which these pathogens contribute to lung inflammation causing exacerbations have not yet been fully elucidated (Weeks et al., 2021).

In this context, as well as in others concerning more generally infectious disease research and drug discovery, the exploitation of advanced *in vitro* tissue models that accurately replicate physiological and morphological characteristics of specific human anatomical districts represents a promising choice to study bacterial pathogenesis. Indeed, beyond ethical debates the use of animals is costly and sometimes not adequate for the desired purposes (Van Norman, 2020); moreover, despite their proved utility, traditional cell culture methods such as suspensions or 2D monolayers (mainly involving the use of cell line monocultures) limitedly mimic in *vivo* conditions leaving many translational issues unsolved (Barrila et al., 2018; Moysidou et al., 2020). However, research strongly relies on cell-based assays, and the growing need to investigate diverse biological processes with higher accuracy has encouraged the development of advanced *in vitro* systems, able to better recapitulate several features of the *in vivo* microenvironment (Barrila et al., 2018). Different innovative cell culturing approaches underlie this progress, including scaffold-based configurations, hydrogels, organotypic cultures and organs-on-chips (Moysidou et al., 2020).

Given the strong impact that respiratory diseases have on human health worldwide (Wisnivesky & De-Torres, 2019), the precise characterization of the biological mechanisms underlying human airways patho-physiology represents today an important challenge. Cellular models mimicking airway environment and immunity have been extensively employed for the investigation on the infections caused by various respiratory tract pathogens (Barron et al., 2021), including NTHi (Ahearn et al., 2019; Baddal et al., 2015; Goyal et al., 2015; Hotomi et al., 2010; Kaufhold et al., 2017; Ketterer et al., 1999; Marrazzo et al., 2016; Morey et al., 2011; Raffel et al., 2013; Starner et al., 2006; Wang et al., 2002) and Mcat (Aebi et al., 1998; Balder et al., 2007; Balder et al., 2009; Brooks et al., 2008; de Vries et al., 2013; Holm et al., 2004; Holm et al., 2003; Lafontaine et al., 2000; N'Guessan et al., 2007; Nicchi et al., 2022; Spaniol et al., 2008; Tan et al., 2006; Tan et al., 2005).

Ketterer et al. (1999) used primary and transformed airway epithelial cells to study the early stage infection behavior of different NTHi strains, observing specific cell-type binding features and highlighting the role of host cytoskeletal rearrangements in the bacteria internalization process. Wang et al. (2002) assessed mucin gene up-regulation driven by NTHi cytoplasmic proteins and activation of p38 mitogen kinase in HeLA and A549 cells. Starner et al. (2006) observed NTHi biofilm formation on polarized Calu-3 cell monolayers after five days, exhibiting decreased susceptibility to antibiotics. Morey et al. (2011) investigated NTHi invasion mechanisms in A549 and undifferentiated NHBE cells, underlining the ability for this pathogen to survive intracellularly in a metabolically active but non-proliferative state; this observation was confirmed by Goyal et al. (2015) that also assessed NTHi escape from endocytic vacuoles and apoptosis triggering at later stages of infection. Raffel et al. (2013) highlighted the importance of the host's microenvironmental cues in modulating NTHi invasiveness of differentiated airway epithelial cells, suggesting a role of the NTHi Sap transporter protein complex in nutrient availability sensing and pathogenic behavior, consequently promoting survival and affecting the host's immune clearance ability. Baddal et al. (2015) characterized the mechanism of NTHi strain FI 176 infection using Normal Human Bronchial Epithelial cells (NHBE)-derived ciliated airway epithelial models by performing dual RNA-sequencing to simultaneously monitor bacterial and eukaryotic infection-linked transcriptomes alterations; according to this study, specific genes involved in NTHi FI 176 pathogenicity have been identified; moreover, the strain has been shown to cause high cell death rates and disruption of NHBE-derived models within seventy-two hours of infection. Marrazzo et al. (2016) proposed a system to investigate on mid/long-term NTHi infections: after infecting a 3D reconstructed human airway mucosa, bacteria were observed crossing the mucus layer and the epithelium, apparently targeting the stromal compartment to form macro structures and secrete vesicles. The effect of NTHi infections on the respiratory epithelial integrity was investigated by Kaufhold et al. (2017); the authors observed a down-regulation E-cadherin mRNA and protein-levels in infected primary Alveolar Epithelial Cells type II, highlighting an important role of the destruction of cell junctions in NTHi infections.

Relying on the use of cellular models, several aspects of Mcat pathogenesis have been investigated. Different studies addressed the issue of bacterial adhesion to the host, identifying specific molecules involved in the process. Holm et al., (2004; 2003) highlighted the relation between MID/Hag and OMPCD proteins and bacterial adherence to A549 and other cell lines; MID/Hag protein was demonstrated to have a role also in Mcat adhesion to NHBE-derived ciliated epithelia (Balder et al., 2009). Binding to several human epithelial cell lines was also

observed to be mediated by two-partner secretion (TPS) system proteins (Balder et al., 2007). The phase variable proteins UspA1 and UspA2H were found to be involved in epithelial cell adhesion (Lafontaine et al., 2000) through interaction with eukaryotic proteins including carcinoembryonic antigen-related cellular adhesion molecules (CEACAMs) (Hill & Virji, 2003). UspA1- and lipooligosaccharide- (LOS) deficient Mcat mutants exhibited reduced epithelial cells adherence and invasion ability (Spaniol et al., 2008). Brooks et al. (2008) showed that the UspA1 cell-binding motifs are not conserved among UspA1- expressing Mcat isolates. N'Guessan et al. (2007) provided evidence for Mcat CEACAM-dependent induced apoptosis of alveolar epithelial cells. de Vries et al. (2013) characterized the molecular interplay between Mcat and respiratory tract epithelial cells during adhesion, highlighting host-pathogen transcriptional changes and inflammatory pathways.

The integration of *in vitro* traditional experimental methods involving the use of cellular models with a variety of different approaches allows the extrapolation of specific and useful knowledge, which can be combined to comprehensively define a complex biological process such as microbial pathogenesis. Insights into the virulence mechanisms of NTHi (Ahearn et al., 2017; Weeks et al., 2021; Zhang et al., 2020) and Mcat (Blakeway et al., 2017; Murphy & Parameswaran, 2009) have been reviewed by several authors, aiming to provide a basis to define strategies to combat or reduce their health-related burden; however, the exact mechanisms that drive colonization and persistence of these bacteria in the human niches are still not fully characterized.

To date, advances in scientific research have made it possible to progressively implement the relevance and the accuracy of airway-mimicking cellular models, moving from simple cell monocultures in submerged conditions (Lechner et al., 1981) to more complex culture methods that allow to obtain fully differentiated tissues retaining organ key functions and *in vivo* three-dimensional cellular architecture; these biomimetic tools are employed for many applications, including disease modelling (COPD, asthma, cancer, etc.), inhalation toxicity testing and host-pathogen interaction studies (Cao et al., 2021; Gard et al., 2021; Palma Medina et al., 2020; Sivarajan et al., 2021; Thacker et al., 2020). The increased understanding of the complex mechanisms related to microbial communities and their interaction with the host have broadened awareness on the importance of these approaches, even if feasibility and time-related drawbacks must be considered. However, despite disease or infection modelling accuracy escalates hand in hand with the ability to faithfully reproduce specific human environments, most of *in vitro* systems fail to integrate all the features of disease or infection (Shi et al., 2019),

giving rise to questions about the accuracy of the experimental observation that can be argued to be model-dependent. Based on these premises, it appears obvious that the approach to be used should represent a good compromise between being accurate, feasible and fit for purpose.

One important limitation of the current approaches adopted to study NTHi and Mcat as well as other bacteria pathogenesis in different human anatomical districts is the apparent difficulty in modelling its persistent or chronic stage. This limit could be related to the fact that most *in vitro* systems cannot tolerate microbial presence for a prolonged period of time, either if the aim is to mimic an infection or to reproduce a physiological microbiota within the cellular model by adding commensal bacteria. Distinct reasons can be hypothesized to underlie this issue: intrinsic (cell type-related) model weakness, physical impedance to natural clearance systems (culture system-related) and lack of functional immune components integrated in the model. Moreover, nutrient-rich culture media can incentivize infection overgrowth, with bacteria taking over on cells within hours (Aguilar et al., 2021). To date, beside the questionable choice of using antibiotics, only latest generation approaches such as organs-on-chips and microdevices allow to partially overcome the problem of the coexistence of cells with pathogenic or commensal bacteria in the same model, thanks to approaches comprising the inclusion of immune cells and constant or frequent flow removing bacterial excess and helping to inhibit fast bacterial overgrowth (Aguilar et al., 2021); however, these types of approaches are characterized by a high degree of difficulty in implementation, standardization and replicability; in fact, with regard to modelling respiratory infections, most models are based on the use of monotypic cell lines.

In the wide range of approaches used for reproducing the human airway environment *in vitro*, we identified air-liquid interface (ALI) organotypic human airway tissue models as advanced and suitable tools for the characterization of respiratory infections caused by NonTypeable *Haemophilus influenzae* and *Moraxella catarrhalis*. Overviews and perspectives on this cell-based system were exhaustively reviewed by Cao et al. (2021). Briefly, by following specific protocols, it is possible to grow primary epithelial cells sampled from the human respiratory tract to obtain differentiated organotypic tissue models exhibiting morphology and functions similar to those *in vivo*. The implementation of these procedures is based on the use of semi-permeable membrane supports (e.g., Corning Transwell) that allow the cell monolayers to be exposed to air while being nourished by the culture medium placed in the basal compartment. Air exposure is a key stimulus for the differentiation of the monolayer into a polarized tissue

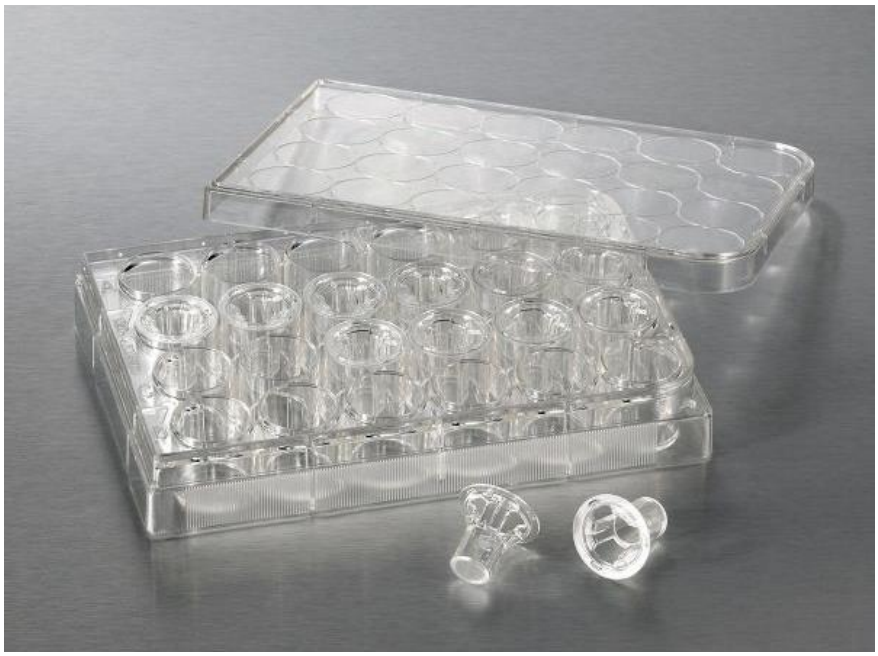

Figure 1 - 24-well plate with transwell inserts for air-liquid interface cell culturing

composed of several cell types and adequately reproducing many *in vivo* characteristics including cilia beating and mucus production; the accuracy of these models also covers more complex aspects such as transcriptional profiling and toxicity dysfunctions, allowing the simultaneous inclusion of numerous aspects of the host-pathogen interactions in the experimental model. There are other cell culture-based approaches to reproduce human airways *in vitro*, such as organoids. Organoids are three-dimensional tissues that can be derived from different types of stem cells, "consisting of organ-specific cell types that self-organize through cell sorting and spatially restricted lineage commitment" (van der Vaart & Clevers, 2021); organoids are suitable for long-term maintenance under submerged conditions (Sachs et al., 2019) but are not exposed to air, as they have a globular structure in which the lumen is in the inner part, rendering exposure to inhaled substances and pathogens difficult to obtain (Cao et al., 2021).

Hence, the main objective of this work is to exploit in-house developed human airway biomimetic ALI-tissue models to study the infections caused by NTHi and Mcat. This research aims to provide a better understanding of the chronicity/persistence mechanisms associated with the pathogenic behavior of these bacteria, and to validate a relevant *in vitro* system for the evaluation of specific treatments against bacterial persistent infection (e.g.: specific antibodies simulating the effect of a vaccination).

1.2 The human respiratory mucosa

The human respiratory tract is composed by different regions in which various organs fulfil specific functions that allow airflow during ventilation. Airways are commonly divided into upper and lower tract. Nose, paranasal sinuses, pharynx and larynx (constituting the upper airways) as well as trachea, bronchi and bronchioles (composing the lower airways) are referred to as “conducting portion”, while the respiratory bronchioles and the alveolar ducts and sacs represent the “respiratory” or “gas-exchange portion” (Ball et al., 2022; Kia'i & Bajaj, 2022; Morgenroth & Ebsen, 2008).

Along its entire length the respiratory mucosa is characterized by the presence of epithelial cells lined with basal cells adhered to the underlying basal membrane, a specialised form of extracellular matrix providing tissue structural support. The in-depth knowledge about the different cell types and subclasses or their differentiation stages and capabilities is constantly updating (Davis & Wypych, 2021). However, it is now well established that each airway region has a specific cell type relative composition and distribution that is related to its function (Fig. 2).

Basal cells constitute approximately 6-31% of the human airway cell population (Boers et al., 1998); these are undifferentiated cuboidal-shaped stem cells able to differentiate into many other cell types (ciliated, goblet, etc.), carrying out self-renewal function after epithelial damage. Ciliated and non-ciliated secretory pseudostratified columnar epithelial cells line the majority of the respiratory tract, from the upper airways to the bronchi. Ciliated cells are the most common cell type found in the conducting airways; each of these cells owns approximately 200-300 microtubule-based structures with hair-like phenotype called cilia (Serafini & Michaelson, 1977), actively beating with a regular and coordinated rhythm. The function of these cells is fundamental in maintaining homeostasis: cilia act in synergy with mucus-producing goblet cells to perform the primary innate defence mechanism of the lung (Bustamante-Marin & Ostrowski, 2017), referred to as mucociliary clearance (MCC) and consisting in the transport toward the pharynx and the clearance of mucus-trapped foreign particles. Goblet cells are the most common secretory cells in the tracheobronchial district; mucus produced by these cells coats the luminal side of this region and contains, beside a major percentage of water, various substances including mucins and antimicrobial products (Barron et al., 2021; Davis & Wypych, 2021). Below the mucus it is located an amphiphilic surfactant layer which function is to reduce surface tension; this substance is produced by club (or clara)

cells, a dome-shaped cell type which has the ability to act as a stem cell and, depending on the stimuli, to differentiate into ciliated or goblet cell as well as to de-differentiate into basal cell. Among the other types, the tracheobronchial epithelium comprises also Tuft cells; these are microvillous cells presumed to have chemosensory, neuronal, and immunological functions (Davis & Wypych, 2021). In addition to the cell types already described, another one can be found in the proximal airways, the pulmonary neuroendocrine cell (PNEC). These cells are very rare as they are estimated to comprise approximately 0.5% of the total epithelial population; their function is to mediate communication between immune and nervous system (Davis & Wypych, 2021). New cell types were discovered recently, the highly rare ionocytes (Plasschaert et al., 2018) and hillock cells (Montoro et al., 2018). The structure and the cellular composition of the epithelium progressively vary with the degree of branching, switching from pseudostratified to cuboidal in the small bronchi and bronchioles, with reduction of ciliated cells and predominance of secretory clara cells.

The alveolar district is mainly composed by two types of cells: type I and type II Pneumocytes, also referred to as Alveolar Epithelial Cells (AEC). Type I Pneumocytes have a squamous, thin phenotype and line the alveoli allowing for gas-exchange, while type II Pneumocytes are cuboidal-shaped surfactant secreting cells and their function is to prevent alveolar collapse (Proud, 2008).

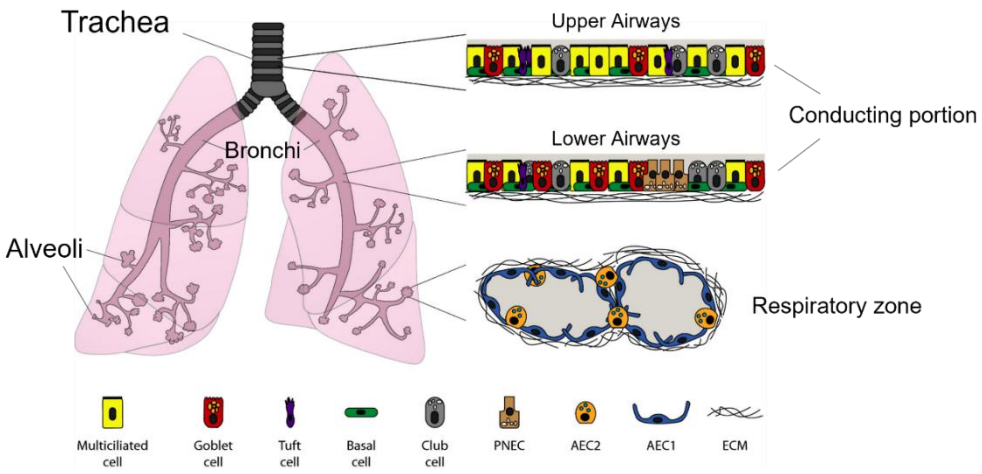

Figure 2 - Schematic representation of the human respiratory tract. Adapted from van der Vaart and Clevers (2021)

1.3 Immunity in the respiratory system

The respiratory system is directly exposed to the external environment and is therefore the first line of contact with inhaled pathogens and particles, providing physical, chemical and immunological barriers; its function is crucial in relation to the effect of respiratory exposure on human health and disease (Gohy et al., 2020; Parker & Prince, 2011).

1.3.1 The epithelial barrier

The epithelial physical barrier function is related with cell apical-basolateral polarity axis orientation and it is allowed by the transcellular apical junctional complex (AJC), a cell-to-cell contact zone defining the border between basolateral and apical elements of the plasma membrane (Koval, 2017). Specifically, barrier integrity is maintained by tight junctions (TJ), adherens junctions (AJ), gap junctions (GJ) and desmosomes (Fig. 3). Tight junctions are constituted by the interaction of claudins, occludins and junctional adhesion molecules with the cytoskeleton. Epithelial non-permeability is ensured by these structures that are also involved in the regulation of paracellular transport of ions and solutes (Gohy et al., 2020). Adherens junctions and desmosomes serve as cell-to-cell basolateral adhesion structures; AJ's network is composed by transmembrane E-cadherin interacting with actin cytoskeleton (Ganesan et al., 2013). Gap junctions constitute an inter-cellular pathway for the transport of cytosolic molecules (Koval, 2017). Impermeability of the epithelial barrier is fundamental for preventing the access of pathogens into the organism, and its impairment and function deficiency is associated with chronic inflammatory diseases (Gohy et al., 2020).

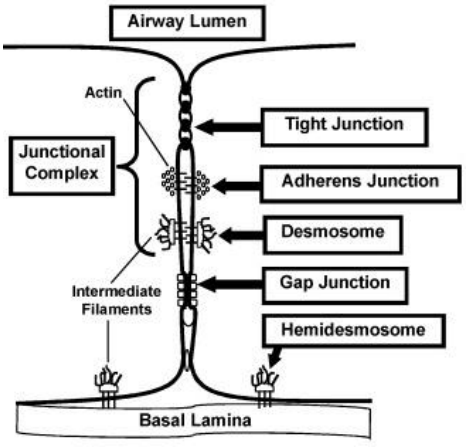

Figure 3 – Airway epithelial junctional complex (Berube et al., 2010)

1.3.2 Respiratory immune system

Barron et al. (2021) summarized the functions of each airway epithelial and immune cell type for the maintenance of epithelial barrier homeostasis and for the protection against pathogens. Airway epithelial cells, in addition to constituting a physical barrier, are involved in the secretion of proinflammatory cytokines and chemokines that are able to trigger inflammatory response, recruit innate immune cells and activate adaptive immunity; moreover, they can produce antimicrobial compounds such as mucins, lysozyme, lactoferrin and others. The production of immune signalling molecules and antimicrobial substances is modulated in response to the stimulus caused by different intra- or extra-cellular pathogen-sensing mechanisms, based on the recognition of pathogen-associated molecular patterns (PAMPS) (Parker & Prince, 2011) or host derived damage-associated molecular patterns (DAMPS) (Leiva-Juárez et al., 2018) by cytoplasmic or transmembrane proteins generally referred to as pattern-recognition receptors (PRRs). Examples of PRRs include Toll-like receptors (TLRs), nucleotide-binding oligomerization domain [NOD-like] receptors (NLRs), retinoic acid-inducible gene-I-like receptors (RLRs), TNFRs and others. (Gohy et al., 2020; Hartl et al., 2018; Parker & Prince, 2011). PRRs are constitutively expressed by airway epithelial cells, alveolar macrophages, antigen presenting cells and neutrophils; the function of these receptors is strictly related to their localisation within cellular environment (Pinkerton et al., 2017).

The noxious stimuli detection role is carried out also by airway resident dendritic cells (DCs); located below the epithelium throughout the entire length of the respiratory tract, these cells express tight junction proteins and are able to sample the luminal environment thanks to pattern recognition receptors displayed on protruding extensions that can cross the epithelium. Moreover, they can stimulate the adaptive immune response upon the acquisition of antigen-presenting capabilities: after undergoing a phenotypic switch, they can migrate to lymph nodes and prime naive adaptive immune cells (Barron et al., 2021; Schleimer et al., 2007). In the lower airways (mainly alveolar region), resident macrophages integrate PAMP sensing and immunomodulatory signal release functions; moreover, they carry out phagocytic and antigen-presenting functions, helping to maintain the respiratory environment free from particles and microbes (Hartl et al., 2018).

In the early stages of pathogen airway colonization, innate immune cells such as neutrophils, dendritic and natural killer cells are recruited to the infection site in order to clear the airways, boost inflammation and induce adaptive response (Barron et al., 2021). Neutrophils are the

earliest attracted cells in order to counteract the infection by killing and removing pathogens. These cells display intracellular pathogen clearance mechanisms upon phagocytosis, as well as extracellular killing capability implemented by the secretion of highly oxidative and proteolytic granules; moreover they are able to release pathogen-immobilizing extracellular "traps", made of decondensed chromatin, histones and other components; this process called NETosis eventually lead to neutrophil death (Hartl et al., 2018). Monocytes followed by lymphocytes (T and B cells) are involved in the late infection counteracting stage (Hartl et al., 2018). T-cells move to the airways after activation and can have multiple functions: helper T-cells are involved in the regulation and the modulation of the immune response (Holt et al., 2008), cytotoxic T-cells destroy infected cells, memory T-cell circulate in the bloodstream to maintain protection against re-infection. The function of B-cells is to produce antibodies to counteract the infection, with distinct plasma-cell populations residing for a prolonged period of time in the tissues. Substantial amounts of immunoglobulins are produced and released by mucosal B-cells. IgA is the prevalent immunoglobulin found in mucosal secretions to protect the organism from external threats by preventing or inhibiting pathogen adhesion and consequently facilitating mucociliary clearance; this molecule can undergo epithelial transcytosis and translocate to the luminal compartment (Gohy et al., 2020; Pilette et al., 2004). In addition to peripheral lymphoid tissue, mucosal regions such as the lungs and the gut are characterized by the presence of a particular immune component referred to as mucosal associated lymphoid tissue (MALT), constituting a specialized supplementary shield against infections (Barron et al., 2021; Cerutti et al., 2011).

1.3.3 The inflammasome

The term inflammasome refers to a family of high-molecular-weight cytosolic protein complexes involved in the elicitation of an inflammatory response by acting as signalling platforms following potentially damaging stimuli (Parker & Prince, 2011). Recent research has increasingly highlighted its importance in the process of the innate immune response against pathogens as well as in chronic diseases and cancer (Broz & Dixit, 2016; Pinkerton et al., 2017; Vladimer et al., 2013; Wen et al., 2021). These protein complexes can assemble following the detection of pathogenic ligands by specific proteins (NLRs) that direct the process and define the type of inflammasome (Vladimer et al., 2013). Canonical inflammasome activation leads to caspase-1 recruitment and subsequent cleavage and activation of the pro-inflammatory cytokines IL-1B and IL-18 (Wen et al., 2021); non-canonical inflammasome activates upon specific stimuli and involves the recruitment of caspases -4, -5 and -11 (Broz & Dixit, 2016).

In addition, caspase recruitment links inflammasome activation to a particular form of programmed lytic cell death referred to as ‘pyroptosis’, occurring after caspase cleavage and activation of the pore-forming protein gasdermin-D. However, pyroptosis can occur independently from inflammasome-mediated processes (Galluzzi et al., 2018). Different authors reviewed the current understanding of inflammasome-related processes in the lungs (Pinkerton et al., 2017; Xu et al., 2018); examining the relationships between respiratory diseases and inflammasome-associated host responses, it was shown that the latter plays a fundamental role in pathogen clearance, while being associated with several chronic inflammatory diseases when occurring under uncontrolled conditions. Programmed cell death such as apoptosis, necroptosis and pyroptosis are reported to be a host defence mechanism against pathogen invasion (Jorgensen et al., 2017). The inflammasome immune recognition function is thought to be fundamental in particular at the inner-outer environment interface areas such as mucosal barriers, to ideally trigger the immune system and start a proper response; even if the host defence role of the inflammasome machinery has been mainly characterized in immune cells, the occurrence of the process in epithelial cells is being recently acknowledged. The inflammasome relation with pyroptosis highlights its importance in epithelial tissues; this cell death mechanism can ensure barrier integrity maintenance through elimination of infected cells that could function as pathogen replicative niches; cellular extrusion appears to have a role in this process at least in intestinal epithelia (Churchill et al., 2022). Inflammasome and pyroptosis defensive role have been described for intestinal epithelia but there is limited and continuously updating knowledge about this process in specific respiratory epithelium cell types. Recent data suggests that airway epithelia can undergo canonical (Robinson et al., 2020) and non-canonical (Phuong et al., 2021; Wang et al., 2018) inflammasome-mediated pyroptosis (Churchill et al., 2022); however, as far as several specific types of inflammasomes and their mechanism of activation and functioning have been defined, the available information about these processes and their relation with airway diseases is still limited and continuously being updated.

1.3.4 Epithelial cell extrusion

Epithelial layers are routinely subjected to a mechanism referred to as cell extrusion, required to eliminate dying or redundant cells while preserving the barrier function of the mucosal interfaces; this process is fundamental in maintaining homeostasis as many circumstances may necessitate its proper functioning (Gudipaty & Rosenblatt, 2017). Epithelia are subjected to turn over between dead and dividing cells, thus it is important to maintain a constant cell number.

Moreover, extrusion is critical in the host defence against pathogens to avoid or reduce their transit across the epithelial barriers. Thus, extrusion dysfunction can have a substantially negative impact on the correct resolution of different homeostatic and disease-related processes (Gudipaty & Rosenblatt, 2017). Epithelial cell extrusion has been described by many authors (Eisenhoffer et al., 2012; Gudipaty & Rosenblatt, 2017; Ohsawa et al., 2018; Saw et al., 2017). This process occurs through actomyosin contraction that squeeze out the cell following stimuli of different types including apoptotic, crowding- or infection-induced. Obviously, although to date there is fairly firm knowledge about extrusion and the different mechanisms by which it occurs, this process has yet to be adequately investigated, especially given the heterogeneity of epithelial tissues as well as of its characteristics and outcomes in relation to disease. Despite extrusion is described as a fundamental mechanism for the maintenance of tissue homeostasis, it has been shown to have potential effects in favor of infectivity of some pathogens. Inflammatory-mediated cell death (pyroptosis) and extrusion was shown to have a role in in the dissemination of intracellular replicating bacteria during *Salmonella* infection of colonic (C2ebb1) polarized epithelial cells (Knodler et al., 2010), providing a model for infection-mediated mucosal inflammation and explaining how this pathogen exploits the process of extrusion to complete its life cycle and infect other cells. Extrusion could occur in a dysregulated manner leading to adverse effects for the host; it can expose the underlying matrix or cellular junctions and provide additional attachment niches for pathogens (Pentecost et al., 2006; Wurster et al., 2021); moreover, excessive triggering of cellular shedding could lead to blockage of the lumen as in the case of bronchiolitis caused by RSV in the airways (Gudipaty & Rosenblatt, 2017; Liesman et al., 2014). On the other hand, several other pathogens adopt persistence strategies to inhibit extrusion or avoid its consequences (Muenzner et al., 2005). Recently, the occurrence of the extrusion process in response to mucosal infections has been investigated. Bastounis et al. (2021) characterized a mass extrusion mechanism in primary or cell line-derived epithelial monolayers as a result of a collective cell response against *Listeria monocytogenes* infection, involving cellular biomechanics and innate immune signalling. Lawrence et al. (2022) established a multi-component human intestinal organoid (HIO) model of *Salmonella enterica* Typhimurium infection, highlighting a death- and extrusion-enhancing activity of human neutrophils. Aparicio-Yuste et al. (2022) highlighted the role of the extra-cellular-matrix stiffness on the extrusion process occurring in response to epithelial monolayer infections. To date, the understanding of cell extrusion process and its relationship with the resolution of various conditions is constantly improved, as it is an important topic to be considered and further investigated, especially with regard to host-pathogen interaction studies and mucosal tissue modeling.

1.4 Modelling the human respiratory tract

Given the importance of the respiratory tract in regard to human health, scientific research has been directed toward the development of reliable and predictive models to study airway diseases (Cao et al., 2021). In this context, animal models represent a widely used tool. However, the success of the animal-to-human translation process has been consistently affected by the significant anatomical, physiological and disease-specific differences between humans and animals that also led several respiratory drugs to fail safety and/or efficacy evaluations in clinical trials, despite demonstrating promising performance in preclinical animal studies (Artzy-Schnirman et al., 2021; Barnes et al., 2015; Cao et al., 2021; Shanks et al., 2009). Moreover, today, the three R's principles of Reduction, Refinement and Replacement of animal experiments are extensively becoming a routinely faced objective for scientists, encouraging the development of adequate alternatives (Hubrecht & Carter, 2019). *In vitro* cell cultures represent an increasingly promising system in many biomedical research contexts, including respiratory disease-related research.

In vitro airway models are laboratory-grown cell-based systems developed to provide a structural, morphological, and functional surrogate of specific districts of the respiratory tract. These models auspiciously represent the alternative to animal testing for new therapeutics safety and efficacy evaluations, and can be employed to investigate many diverse biological processes and/or related pathological conditions, such as tissue differentiation (Prytherch et al., 2011), tissue regeneration (Chakraborty et al., 2021; Puchelle et al., 2006), inflammation, infection and chronic disease (Miller & Spence, 2017; Osei et al., 2020; Yonker et al., 2017). Airway model development has gained increasing importance as over time traditional cell culturing methods, such as 2D systems involving the use of monotypic cells (Lechner et al., 1981) were recognized to be primitive and not adequate to accurately mimic *in vivo* tissue anatomy and physiology, a fundamental feature required to perform highly informative and useful studies. The issue of airway and lung model implementation has been addressed by numerous review articles (Artzy-Schnirman et al., 2021; Barron et al., 2021; Berube et al., 2010; Cao et al., 2021; Hasan et al., 2018; Lacroix et al., 2018; van der Vaart & Clevers, 2021); currently emerging methodologies can involve the use of several cell types (immortalized, primary) and sources (proximal and distal epithelium, immune cells), cultured or co-cultured exploiting particular cell scaffolds or micro-fabricated devices and extra-cellular matrices or hydrogels to bioengineer *in vivo* resembling tissues or organs. Airway advanced models include organotypic Air-Liquid-Interface tissue cultures, organoids, organs-on-chips.

An important step in advancing the relevance of the models has been the shift from submerged to Air-Liquid-Interface cultures, thanks in part to the use of particular supports (e.g., Transwell system) that allow cells to be fed from the basolateral side while they are exposed to air. In this context, one the most widespread approach involves the *in vitro* reproduction of the airway epithelium starting from primary cells of tracheo-bronchial or alveolar origin. Airway exposure is a key stimulus for differentiation of the tissue that is comprised of different types of cells with specific functions. ALI-based systems are characterized by the advantage of providing well-differentiated, organotypic features such as barrier properties, metabolic functions, in vivo-like transcriptional profile and toxicity responses (Cao et al., 2021); moreover, this tools are suitable for pathogen or noxious agent exposure as it occurs *in vivo*, representing a good option to model infections and investigate on host-pathogen interaction.

Another aspect to be taken into account when approaching to advanced *in vitro* modelling is the importance of reproducing the three-dimensional native environment for cell differentiation and organ development, as it is fundamental to maintain tissue-specific functioning of the cells (van der Vaart & Clevers, 2021). This consideration led to the development of the organoid culturing approach; organoids are defined as “self-organizing, 3D culture systems that are highly similar to actual human organs”, generated starting from stem cells (Kim et al., 2020). Human airway organoids exhibit realistic *in vivo* features and are suitable for a variety of applications (Aguilar et al., 2021; Sachs et al., 2019); however, this approach implies submerged condition model generation and maintenance as well as inward polarization (luminal side located inside), rendering pathogen exposure tricky (Cao et al., 2021). Interestingly, methods to reverse epithelial polarity in intestinal (Co et al., 2021) or airway (Stroulios et al., 2022) organoids were described, representing an important advancement in organoid implementation. Recent review articles addressed the latest, most advanced step in the improvement of the *in vivo* mimicking capability of cellular models, that has been due to driving forces represented by the converging advances in the areas of tissue engineering, microfabrication, and the aforementioned cell culture techniques, leading to the development of the so-called "organs-on-chips” (Ko et al., 2022; Leung et al., 2022; Wu et al., 2020). Organs-on-a-chip (OoCs) can be defined as microfabricated devices consisting of microchannels for guiding and manipulating solutions to administrate nutrients to and discharge waste from chambers lined with natural or engineered tissues designed to closely reconstruct the structure of specific organs and recapitulate their essential physiological functions (Esch et al., 2015; Ko et al., 2022; Wu et al., 2020). This approach allows the development of models that mimic the

mechanical and biochemical stimuli present *in vivo* as well as having higher control over the cell culturing environment thanks to its microscale. Examples of organ models implemented with microfluidic technologies include liver (Chong et al., 2018; Hegde et al., 2014; Ho et al., 2013; Kang et al., 2015; Lee et al., 2007; Lu et al., 2018; Ma et al., 2018), kidney (Jang et al., 2013; Jang & Suh, 2010; Nieskens & Sjogren, 2019; Schutgens et al., 2019), heart (Marsano et al., 2016; Schneider et al., 2019; Zhang et al., 2013; X. Zhang et al., 2016; Y. S. Zhang et al., 2016), gut (Imura et al., 2009; Jalili-Firoozinezhad et al., 2019; Kasendra et al., 2018; Kim et al., 2012; Shin et al., 2019; Sung et al., 2011) and lung (Benam et al., 2016; Blume et al., 2015; Guenat & Berthiaume, 2018; Huh et al., 2012; Huh et al., 2010; Humayun et al., 2018; Stucki et al., 2015; Xu et al., 2013; Yang et al., 2018), as well as multi-organs-on-chips (Lee et al., 2017; Satoh et al., 2017; van Midwoud et al., 2010).

Moreira et al. (2022) recently summarized the main advantages and drawbacks as well as the possible applications of each *in vitro* lung modelling platform, identifying stem cell-based approaches as the revolutionary choice in this field, overcoming many disadvantages of other common systems. However, such methodologies are still characterized by a lack of standardization, scalability, and time-effective protocols as well as by high expenses. Thus, as previously claimed by Artzy-Schnirman et al. (2021), the escalation in model complexity and accuracy goes hand-in-hand with a decrease in throughput capacity; therefore, according to our view, each research context should address its own necessities to properly select a fit-for purpose approach through a trade-off, taking into account several aspects such as model in vivo resembling ability, time, cost and throughput capacity.

2. Rationale

As discussed previously, simple models that rely on the use of a single cell type (e.g., epithelial, or immune cell line) are frequently used in the context of the characterization of respiratory infections caused by NTHi and Mcat. This approach is based on well-established methods that have several advantages including low time-consuming experimental set ups, investigation specificity, reproducibility, and uniformity of the observations at a relatively low cost. However, this approach has specific limitations that can directly influence the model's ability to reflect the complex interactions that occur *in vivo*, affecting the translational reliability of the experimental observations. One of the reasons behind this fact is that simple models often do not take into account the effect of the immune system. The inability to appropriately mimic an immune response, which can impact on the course of the infection, could lead to an incomplete explanation of the process. Another limitation is represented by the intrinsic scarce tolerance displayed by cellular models in response to infections, given the mostly high invasive behavior of pathogens, quickly overgrowing and/or takin over on cells. This issue represents an obstacle to the investigation on long-term bacterial persistence strategies, often associated with chronic diseases. Generally, within the context of bacterial infection characterization, acute and persistent infections are distinguished with regards to planktonic or biofilm bacterial growth phases (Roberts et al., 2015). Acute infections are characterized by rapid onset and decay and relative antibiotic treatment efficacy. Chronic infections are related to persistent and progressive pathology associated with a longer recovery time, in which both antibiotic treatment and the host's defence mechanisms appear less effective; over the years, biofilms have been reported to play a fundamental role in persistent infections (Hoiby et al., 2015) even if recent data suggests that biofilms could dominate in both acute and persistent respiratory infections (Kolpen et al., 2022). As discussed previously, mimicking bacterial infections has been proved to be a challenging objective, in which no defined *in vitro* assay guidelines are shared in the scientific community, leading to the implementation of animal models that often lead to scarce predictive ability and translational failure. It is generally accepted that biofilms are involved in 65 % - 80 % of human infections, furtherly complicating disease modelling (Shi et al., 2019). Biofilms are extensively studied and characterized mostly using *in vitro* approaches involving the attachment and growth of bacteria on abiotic surfaces; however, significant differences between *in vitro* and *in vivo* biofilms have been highlighted (Roberts et al., 2015). As claimed by many authors (Roberts et al., 2015; Shi et al., 2019) a paradigm shift

that relies on methods that better represent clinical conditions is required to better understand bacterial infection biology, especially if involving biofilm formation.

Non-typeable *Haemophilus influenzae* and *Moraxella catarrhalis* are two pathogens known to exhibit persistent behavior. NTHi is a non-encapsulated gram-negative human commensal that commonly colonizes the airway mucosa and that can switch to pathogenic lifestyle in airway diseases (e.g., COPD), especially when impaired immunity contribute to establish a growth-favourable environment; this pathogen has been identified by large cohort studies as a recurrent aetiological factor in COPD acute exacerbations, even if other cohorts indicate other obligate pathogens (*Moraxella catarrhalis*, *Streptococcus pneumoniae* and *Pseudomonas aeruginosa*) as the cause of COPD-related severity (Weeks et al., 2021). The mechanisms triggering NTHi and Mcat host susceptibility are not fully understood despite both pathogens are known to be able to adopt biofilm lifestyle. With regard to NTHi and Mcat, most infection experiments involving the use of human cells are performed within limited, defined timeframes (ranging from hours to days) either because of high susceptibility of the model to bacterial planktonic phase, or because the investigation is focused on the early infection phases. An NTHi strain isolated from a COPD patient was observed to form biofilm on Calu-3 cells monolayer (Starner et al., 2006) but the limited relevance of the cellular model restricts this observation to this experimental set up as cell lines do not faithfully represent human niches. Another NTHi strain (Otitis Media isolate) displayed highly cytotoxic activity when infecting a ciliated human bronchial epithelial model derived from primary cells, resolving in complete model disruption occurred in seventy-two hours (Baddal et al., 2015). As discussed previously, Mcat infections of the human respiratory tract were modelled relying on several cell types but observations were limited to the early infection stages or to specific interactions between a certain cell type and the bacteria (de Vries et al., 2013; Nicchi et al., 2022); other approaches allowed to highlight specific virulence determinants (Blakeway et al., 2020; 2017). However, to date, no evidence of airway resident NTHi or Mcat biofilm was provided using relevant cellular models.

Previous work carried out by Yonker et al. (2017) addressed the issue of developing a primary human co-culture model of an inflamed airway mucosa in the context of *Pseudomonas aeruginosa* infections: the authors relied on a ‘personalized’ use of the Transwell ALI system by culturing airway basal cells on the down-facing side of the support, in order to obtain an Inverted model and allowing to observe neutrophil epithelial recruitment and transmigration upon infection-induced stimulation (Fig. 4).

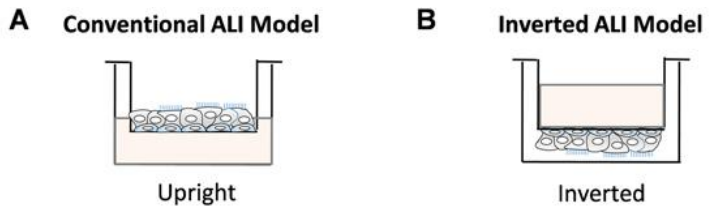

Figure 4 – Standard vs inverted ALI configuration (Yonker et al., 2017)

It has been hypothesized that the inverted configuration may be useful also in enhancing the possible effect of natural clearance mechanism such as cellular extrusion and mucociliary escalator, reported to be key defence mechanisms in pathogen clearance. In fact, these kinds of lab-grown tissues exhibit ciliary beating and mucus production as well as cellular extrusion ability, but the possible involvement of these mechanisms in controlling the infection process is hindered by the spatial configuration of the support leading to accumulation of debris and fast epithelial disruption, though variations in the results could occur and could be related to many aspects including MOI and cell source used. This issue represents an obstacle to the investigation on long-term bacterial persistence strategies, often associated with chronic diseases.

Based on these premises, the aim of this work is to implement standard and inverted organotypic ALI tissue models to characterize NTHi and Mcat respiratory infections; furthermore, this work aims to serve as a basis for future validation of advanced cellular models for evaluating the effect and efficacy of specific treatments on bacterial infectivity (e.g., antibodies simulating a vaccination). The integration of immune components in the system is out of the scope of this work but represents one of the future implementation goals.

3. Experimental Procedure

The main activities were directed to:

- Implement human airway epithelial models starting from primary epithelial cells of tracheo-bronchial origin, sourced from diseased (COPD) donors: in particular, standard and inverted models were grown according to slightly modified established protocols to obtain fully differentiated tissues.

- Characterize NTHi and Mcat infections of standard and inverted airway epithelial models: the effect of the configuration on the infection process was investigated by comparing infection-induced cytotoxicity in each type of model. In this context, traditional and relatively old methods such as LDH assay were observed to provide inconsistent results if applied to the models in question; for this reason, a flow cytometry-based evaluation was explored to provide proper readouts. Moreover, infection phenotypes were characterized relying on CSLM, TEM and SEM analysis.

- Quantify bacterial infection at different time points in order to evaluate antibodies functionality in preventing/reducing bacterial colonization of the infected tissues. In this context, the quantification method needs to be tailored to the pathogen's behavior. If the pathogen shows a biofilm phenotype (as observed in this study), traditional methods such as CFU counting could lead to inconsistency of the results. For this reason, two strategies were developed and applied to Mcat infections in order to provide a more reliable quantification method, especially in view of future works involving polymicrobial infections. The first strategy was based on the generation of a fluorescence-expressing strain, in order to be quantified through LSCM and image analysis; the second strategy was based on a RT-qPCR approach that aimed to quantify viable bacteria infecting the tissue samples, based on the amount of *16S rRNA* indirectly represented by threshold cycle values obtained from the reactions. Briefly, the aim of the experiments was to set up a reference curve by correlating threshold cycle values obtained from RT-qPCR carried out on total RNA purified from tissue models infected with defined amounts of bacteria (quantified by optical density readings at 600 nm and dilution plating).

4. Materials and Methods

4.1 Human small airways *in vitro* models

The cellular models used in this work were either purchased or developed in-house starting from primary human epithelial cells. SmallAir and MucilAir models were purchased by Epithelix. Primary human airway epithelial cells isolated from the upper (hAEC) or lower (hSAEC) airways of diseased (COPD) subjects were purchased by Epithelix. Cells were expanded in 75 cm^2 flasks, using human Airway Epithelial Cell Culture medium (hAEC; Epithelix) supplemented with Primocin (Invivogen), at 37°C in 5% CO_2 until approximately 80% confluence and trypsinized using Trypsin-EDTA (0.25%) (Gibco) for seeding between passage 4 and 6. Standard and inverted models were cultivated according to a similar protocol, with minor modifications required for the inverted as already described (Yonker et al., 2017). For both configurations, 6.5 mm Transwell with 0.4 µm Pore Polyester Membrane Insert (Corning product #3470) were used. The upside or the underside of the insert membranes, where human airway basal cells were applied, were coated with a Collagen Type I solution from rat tail (REFC3867-1V, Sigma-Aldrich) prior to seeding. In conventional ALI models, ~0.5 x 10^5 cells were seeded in the apical chamber of the inserts. In inverted configuration, transwells were flipped and ~1 x 10^5 cells were seeded on the top of the membrane; after one hour incubation at 37 °C to allow adhesion, extra medium and unattached cells were carefully aspirated, and the inserts were returned to the receiving wells containing 600 µl of medium. Cells were cultivated under submerged conditions adding hAEC medium in both apical and basal chamber of the transwells for 3-5 days to allow the formation of a confluent monolayer. Then, to induce cell differentiation the models were cultured at the Air-Liquid-Interface with complete Pneumacult-ALI medium (StemCell Technology) for two weeks changing the media every 2-3 days. Standard models were cultured by adding the medium only in the basal chamber; inverted models were cultured by adding the medium only in the apical chamber of the insert. During ALI differentiation, before every medium change the cultures were rinsed with DPBS, calcium, magnesium (ThermoFisher) to remove mucus excess. After two weeks, the medium was replaced with SmallAir medium (Epithelix). At this point, a Matrigel-embedded fibroblast feeder layer was added on the underside (standard configuration) or upside (inverted configuration) of the insert membrane; the addition of fibroblasts, beside allowing a better, full maturation of the tissue, is required to maintain the tissue differentiated over time, allowing long-term maintenance of the models. Normal Human Lung Fibroblasts (ATCC) or IMR90 cell line (ATCC) were used for this purpose. In some experiments, the addition of

fibroblasts was not required, and the models were used after two more weeks of ALI culturing with SmallAir medium, required to obtain an acceptable tissue maturation with a sustained ciliary beating.

Normal Human Lung Fibroblasts (ATCC) were cultured in 75 cm^2 flasks using Fibroblast Basal Medium (ATCC, PSC-201-030) supplemented with Fibroblast Growth Kit-Low serum (ATCC, PCS-201-041) and Primocin (InvivoGen) and used between passage 4 and 6. Cells were trypsinized and resuspended in a Small Air medium + 25 % Matrigel solution and kept on ice until seeding. For the standard configuration ALI model, medium was removed from the basal chamber, transwells were flipped and 20µlof solution containing ~3 x 10^3 cells were added on the top of the membrane. For the inverted, medium was removed and 40µlof solution containing ~2.5 x 10^3 cells were added directly in the apical chamber. After seeding, both standard and inverted cultures were incubated for 30 minutes at 37 °C to allow solidification of the Matrigel-embedded fibroblast solution, then standard culture inserts were returned to the receiving wells and Small Air medium was added respectively to the basal (standard configuration) or apical (inverted configuration) chamber to continue ALI culturing for at least two additional weeks.

IMR90 were cultured in 75 cm^2 flasks using complete EMEM medium (ATCC) supplemented with 10 % FBS and primocin (invivogen) and used between passage 3 and 6. Cells were subjected to γ-irradiation (6000 rads, treatment time calculated according to ^{137}Cs decay rate) with a Gammacell 3000 irradiator (ELAN) to reduce their mitotic activity, prior to be embedded in Matrigel solution and added to the epithelial cell cultures.

Cellular models were maintained at the ALI for at least 28 days prior to use in biological assays, with the basolateral medium being changed every second day, to ensure a differentiated cell population with a mucociliary phenotype. Cell polarity and TJ barrier function were verified by transepithelial electrical resistance (TEER) measurements using an epithelial volt ohmmeter (EVOM2; World Precision Instruments). Differentiation and polarization were evaluated by confocal scanning laser microscopy (Zeiss LSM 710) through the labelling of specific markers for the presence of cilia, tight junctions, goblet cells, basal cells, and club cells.

4.2 Bacterial cultures and model infections

The experiments were performed using these Gram-negative bacteria: Nontypeable *Haemophilus influenzae* NTHi FI 176 (isolate from the middle ear of a participant in a Finnish

otitis media outbreak cohort study) and *Moraxella catarrhalis* strain 415, isolated during the prospective, observational cohort AERIS study (Wilkinson et al., 2017) (NCT01360398).

All the strains used were routinely reconstituted from frozen stock cultures, plated on PoliVitex chocolate agar (bioMérieux), and incubated overnight at 37 °C with 5 % CO_2. For infection studies, Brain-heart infusion (BHI) was used as growth medium at 37°C, 180 rpm with 5 % CO_2. For NTHi growth, BHI was supplemented with 5 µg/ml hemin and 2 µg/ml of nicotinamide adenine dinucleotide (NAD, Sigma). Bacteria concentration was determined by both measuring O.D. at 600 nm and colony forming units (CFU) by dilution plating. For all host-pathogen interactions studies, bacteria were collected during the exponential growth phase. One day before the infection, cellular models' medium was replaced with Small Air medium without antibiotics. On the day of the infection, bacteria at an OD_{600} of 0.5 were pelleted and resuspended in Small Air medium without antibiotics; after removing culture medium from the basal side of the models, 50 µl of bacterial suspension (corresponding approximately to ~3×10^8 CFU/mL for Mcat AERIS 415 and ~1×10^9 CFU/ml for NTHi FI 176) or medium-only control was added to the apical side of the epithelia and incubated for 1 h at 37 °C and 5 % CO_2. Subsequently, the inoculum was removed, and the apical surface was washed three times with DPBS to remove non-adherent bacteria; models were then cultured with Small Air medium without antibiotics.

4.3 Laser Scanning Confocal Microscopy

Cellular models were washed three times with PBS and fixed with 4 % formaldehyde, except for mucin staining, where a methanol-acetone (1:1) fixation protocol was used. Membranes were cut with a scalpel and processed in a 48-well plate. Samples were permeabilized with a 1 % saponin (Sigma), 0.1 % Triton X-100 in PBS solution for 30 minutes and blocked with 3 % bovine serum albumin (Sigma), 0.1 % Triton X-100 in PBS for 45 minutes. Incubation with primary antibodies was performed for 1 h at room temperature; then, samples were washed in blocking solution and treated for 45 minutes with the appropriate Alexa Fluor-conjugated secondary antibody or chemical probe. Membranes were mounted on microscopy slides using ProLong gold antifade reagent (Thermo Fisher) and analyzed by confocal microscopy using either a Zeiss LSM 710 confocal microscope or Opera Phenix HCS Plus (PerkinElmer). Image analysis was performed using Harmony HCI software (PerkinElmer).

4.3.1 Image Analysis

Images obtained by acquiring whole transwell membranes with Opera Phenix HCS System were analyzed with Harmony HCI software with the aim of comparing the quantity of ciliated and goblet cells in models grown in standard or inverted configuration; dedicated analysis pipelines were developed to quantify the presence of each cell type through virtual segregation of the fluorescence signal related to ß -tubulin IV or MUC5CAC, respectively. Samples stained for each marker were acquired with a 40x water objective. Several acquired fields per sample were selected to set the pipelines parameters. Fluorescence threshold settings were arbitrarily established in order to have the most possible accurate readout. Cilia and goblet cells were quantified relying on the measurement of the fluorescence areas (μm^2) related to each correspondent marker, calculated on the maximum projection of the acquired Z-stacks of each field. Total sum of the fluorescence areas of 144 fields selected for the analysis was divided by the sum of the area of the fields in order to obtain a percentage of sample area positive for the marker.

4.4 Electron Microscopy

Protocols were adapted from Hammerschmidt et al. (2005) with little modifications. Membranes were pre-fixed in a cacodylate sucrose buffer (0.1 M Sodium Cacodylate, 0.09 M sucrose, 0.01 M $CaCl_2$, 0.01 M $MgCl_2$ and 0.075 % Ruthenium Red, pH of 6.9) containing 2 % paraformaldehyde (PFA), 2.5 % glutaraldehyde (GA) and 1.55 % L-lysine acetate (the latest added as last component just before fixation) for 20 minutes at 4 °C. The abovementioned reagents were supplied by Sigma. Then, without washing, samples were fixed in the same solution without L-lysine acetate overnight at 4 °C. For transmission electron microscopy (TEM), samples were post-fixed in 1 % OsO_4 (Electron Microscopy Science) + 0.075% Ruthenium Red in 0.1 M Cacodylate buffer, pH 6.9, 1 h at 4 °C, rinsed in bidistilled water for 15 minutes at 4 °C and dehydrated in a graded series of alcohol concentrations prior to embedding in LR White resin (Agar Scientific) at 50 °C for 36 hours. ultrathin sections (60-80 nm thick) were obtained using a Reichert-Jung ultracut E ultramicrotome and stained with uranyl acetate prior to examination with a JEOL 1200 EX II transmission electron microscope at an electron accelerating voltage of 100 kV equipped with an Olympus SIS Veleta CCD camera and the iTEM software for image acquisition and processing. For scanning electron microscopy (SEM) observations, samples were fixed and dehydrated as mentioned above. To dry the samples, they were processed using the method of liquid CO_2 in a Critical Point Dryer

(Balzer Union CPD 020), then they were coated with gold in a Sputter Coater (Balzer Union MD 010) and examined using a JEOL JSM 6010 LA at 5-15 kV voltage acceleration.

For Immuno-Gold labelling assays, membranes were fixed with 4 % PFA and 0.02 % GA in 0.1 M Phosphate Buffer (PB), pH 7.4, for 2 hours at 4 °C, then rinsed with 0.1 M PB and incubated in a 0.2 M sucrose solution overnight at 4 °C. Subsequently, samples were dehydrated and embedded in LR White resin (Agar Scientific) as described above. ultrathin sections were processed according to a two-step blocking procedure (low and high molecular weight, respectively) using firstly Glycine 0.05 M in PBS for 15 minutes and then Aurion blocking solution for 30 minutes. Samples were washed two times with incubation buffer and treated with the appropriate primary antibody for 3 hours at RT or overnight at 4 °C. Then, after being washed 6 times with incubation buffer, samples were treated with the appropriate secondary antibody for 2 hours and finally washed 6 times with PBS. Antibodies and dyes used in this study are summarized in table 1.

4.5 Flow Cytometry

For the flow cytometry analysis, infected or mock-infected airway epithelial models were processed according to previously defined infection time-points, indicated in the figure legends. Cellular models were detached and dissociated into cell suspensions according to the following protocol. DPBS without calcium, magnesium was added on the apical side of the models and cells were incubated at 37 °C in 5 % CO_2 for 5 minutes, then rinsed three additional times with the same buffer. Culture medium was removed and 300 µl of TrypLE Select Enzyme 10X (Thermo Fisher) were added to the apical and the basal side of each well; cells were incubated at 37 °C in 5 % CO_2 for 5-10 minutes and manually agitated. Cell detachment was observed with a light microscope. Then, the dissociation reagent was removed from the basolateral side of the models and detached cells and tissue portions were dissociated into cell suspensions by gently pipetting. Cell suspensions were transferred into 1.5 ml eppendorfs already containing 700 µl of DPBS and pelleted at 0.3 x g for 5 minutes. Cell pellets were resuspended in 300 µl of LIVE/DEAD Fixable Aqua Dead Cell (Thermo Fisher) staining solution (1:600 in PBS) and incubated at room temperature for ten minutes. Samples were resuspended in 4 % FA and incubated on ice for 20 minutes, then washed with PBS and resuspended in PBS 1 % BSA before the analysis. Data were collected using a BD FACS CANTO II (BD Bioscience) by acquiring the highest possible number of events per sample and exported as FCS files. Analysis was performed using Flow-Jo Software (v.8.6, TreeStar Inc). The first two gates were drawn to

identify the cell population of interest by using a dot plot forward versus side scatter area (FSC-A vs SSC-A). The second gate was drawn on single cells using a dot plot side scatter width versus side scatter area (SSC-W vs SSC-A) to exclude cell aggregates. Then, live and dead cells were identified with a dot plot SSC-A vs Live/Dead Aqua-A. Data were analyzed according to Welch and Brown-Forsythe ANOVA followed by Dunnet's T3 post-hoc multiple comparison test using the GraphPad Prism (software version 9.5.1).

Table 1 - Antibodies and markers used in this study

Primary antibodies	**Source**	**Identifier**
Rabbit anti-UspA2	This study	N/A
Rabbit anti-total NTHi serum	This study	N/A
Rabbit anti-NTHi FI 176	This study	N/A
Rabbit anti-Uteroglobin	Thermo Fisher	PA5102469
Mouse anti-β-Tubulin IV	Sigma-Aldrich	T7941
Mouse anti-MUC5AC	Sigma-Aldrich	MAB2011
Mouse anti-ZO1	Thermo Fisher	339100
Mouse anti-p63	Abcam	Ab735
Mouse anti-dsDNA	Abcam	ab270732
Secondary antibodies		
Goat anti-mouse 488	Thermo Fisher	A11029
Goat anti-rabbit 568	Thermo Fisher	A11011
Goat anti-rabbit 488	Thermo Fisher	A11008
Goat anti-mouse 20 nm gold	BBInternational	EM.GAF10
Goat anti-rabbit 20 nm gold	BBInternational	EM.GAF20
Dyes		

DAPI	Thermo Fisher	D1306
Phalloidin 647	Cell Signaling	8940S
LIVE/DEAD Fixable Aqua Dead Cell Stain	Thermo Fisher	L34957

4.6 Bacteria complementation

For the generation of a Mcat fluorescent strain, a cloning strategy to transform *Moraxella catarrhalis* AERIS 415 by complementation of mCherry protein gene into the bacterial genome was developed relying on the Polymerase Incomplete Primer Extension (PIPE) method (Klock & Lesley, 2009). The cloning strategy was set to create a vector with the fluorescent reporter gene mCherry and kanamycin resistance cassette to complement Mcat by site-directed mutagenesis. The strategy was developed analyzing Mcat BBH18 genome (KEGG) with Geneious software; the *ggt* pseudogene complementation locus (Tan et al., 2019) was selected. The procedure (outlined in figure 5) involved four steps: 1) cloning the whole complementation locus (comprising of 488 bp left and right flanking regions) in a pET15 plasmid; 2) cloning antibiotic resistance cassette (kanamycin) within the complementation locus flanking regions; 3) cloning mCherry expression cassette downwards kanamycin cassette; 4) transform wild type strain with the final construct. Kanamycin resistance cassette was isolated from an in-house engineered bacterial genome. MCherry expression cassettes including strain-specific constitutive promoter *OmpCD* and codon-optimized for the pathogen were supplied by Twist. For each insertion step, Vector and Insert were linearized respectively by V-PIPE and I-PIPE amplification using Kapa HIFI HotStart ReadyMix DNA polymerase (KAPA biosystems) with primers designed following PIPE rules (including extensions of at least 15 bases complementary to the paired oligonucleotide for hybridization) using a GeneAmp PCR system 9700 Thermocycler. PCR products were used to transform One shot Mach 1-T1 Chemically Competent *E. coli* cells (Thermo Fisher) as reported in manufacturer's instructions. Colonies were screened on ampicillin (100 µg/ml) LB plates and plasmids were amplified with Dream Taq Green PCR Master mix (Thermo-Fisher). PCR products were analyzed by 1 % agarose (Sigma) + SybrSafe (Thermo Fisher) gel electrophoresis using Gel Loading dye purple 6x (biolabs). Successful constructs were purified with E.Z.N.A. Plasmid DNA Mini Kit II (omega) and the region of interest was sequenced at the GSK sequencing facility according to Sanger method using a 96-capillary ABI 3730xl DNA Analyzer to ensure correct final construct

assembly. The final construct was amplified using Kapa HIFI HotStart ReadyMix DNA polymerase (KAPA biosystems) and purified with a Wizard SV Gel and PCR clean up system (Promega). PCR settings were adapted to each reaction and are summarized in table 3. Wild type Mcat was incubated with the purified construct for 6 hours at 37 °C to allow homologous recombination and subsequently screened on kanamycin supplemented agar chocolate plates. Transformed strains frozen stocks (16% glycerol) were prepared and stored at -80 °C.

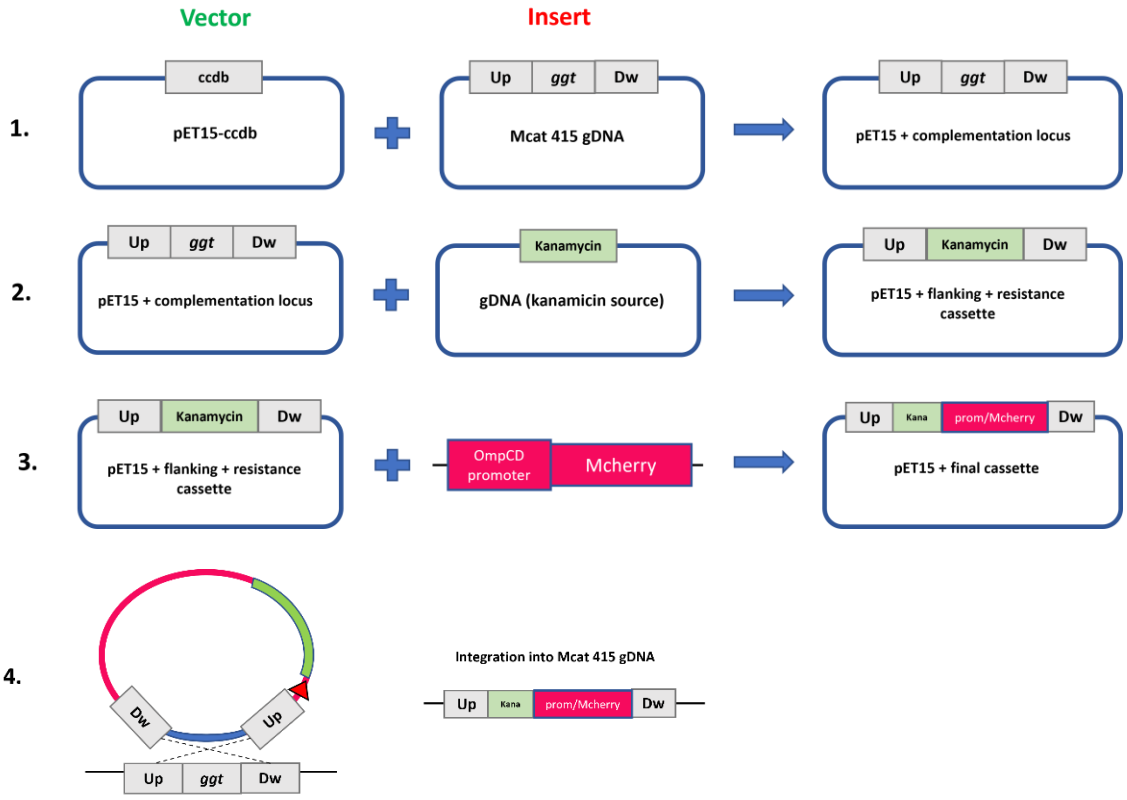

Figure 5 – Outline of the cloning strategy adopted to generate a mCherry-complemented Mcat 415 strain

Table 2 - Primers

Primer	Sequence (5' - 3')	Step	Stock concentration	Working concentration	Provider
V-PIPEUniv F	TAACGCGACTTAATTGGCCA GTGTGCCGGTCTCCG	1) V-PIPE	50 µM	0,5 µM	Metabion

pET15Korv	GACTCACTATAGGGGAATTGTGA	1) V-PIPE	50 µM	0,5 µM	Metabion
ggtUPfw	ATAGGGGAATTGTGACGATACGGTGTATTGCCTTGG	1) I-PIPE	50 µM	0,5 µM	Metabion
ggtDOrv	CCAAGATGCCATCAGTGCACTAACGCGACTTAATT	1) I-PIPE	50 µM	0,5 µM	Metabion
ggtDOfw	CTGTACCCATTCGCCAGTTG	2) V-PIPE	50 µM	0,5 µM	Metabion
ggtUPrv	CCTTCAGCATCATACCCCACC	2) V-PIPE	50 µM	0,5 µM	Metabion
Kana-UpFw	GTATGATGCTGAAGGATGCCGTCTGAAGGATCC	2) I-PIPE	50 µM	0,5 µM	Metabion
KanaDwRev	GGCGAATGGGTACAGTATCCATGGGGATCCTCATTATTC	2) I-PIPE	50 µM	0,5 µM	Metabion
ggtDOfw	CTGTACCCATTCGCCAGTTG	3) V-PIPE	50 µM	0,5 µM	Metabion
KanKOR3	TATCCATGGGGATCCTCATTATTC	3) V-PIPE	50 µM	0,5 µM	Metabion
OmpCDkana fw	GGATCCCCATGGATATGCGTTAGAAAGAAAATCGTAAATAATG	3) I-PIPE	50 µM	0,5 µM	Metabion
mCh2 Rev	GGCGAATGGGTACAGGATCCTCTAGATTATTTATAAAGTTCATC	3) I-PIPE	50 µM	0,5 µM	Metabion
McUPfw	CGATACGGTGTATTGCCTTGG	4)	50 µM	0,5 µM	Metabion
McDOrv	GTGCACTGATGGCATCTTGG	4)	50 µM	0,5 µM	Metabion
ggt LO F	GTGGGTACGCCTGCTATCC	Colony screening (Mcat)	50 µM	0,5 µM	Metabion
ggt RO R	CCATTGGACGGCGGTTGTATCC	Colony screening (Mcat)	50 µM	0,5 µM	Metabion
T7 PROM	TAATACGACTCACTATAGGG	Colony screening (E.Coli)	50 µM	0,5 µM	Metabion
SeqPetRev	GATATCCGGATATAGTTCCTC	Colony screening (E.Coli)	50 µM	0,5 µM	Metabion

Table 3 - PCR settings

	Temp (°C)	Time	
Initial denaturation	95	5'	
Denaturation	95 - 98	30''	25-30X
Annealing	55 - 70	30''	
Elongation	72	30'' - 3'30''	
Final elongation	72	0 - 5'	

4.7 RT-qPCR

Bacteria were grown in shaking conditions (as described above) till reaching exponential phase (OD_{600} = 0.5). Defined amounts of bacteria (OD_{600} = 4) were resuspended in TRI Reagent (Zymo Research) or PBS and serially diluted ten times (two-fold dilutions). 100 µl of lysed bacterial solution from each dilution plus 250 µl of lysis buffer were used to lyse airway models prior to extract and purify total RNA; 100 µl of PBS bacterial solution from each dilution were further diluted and plated for CFU counting. Prior to total RNA isolation, airway models were rinsed three times with DPBS (Thermo Fisher) to remove mucus excess. Samples were lysed in TRI Reagent (ZYMO RESEARCH) and Direct-zol RNA Microprep Kit (ZYMO RESEARCH) was used for RNA purification according to manufacturer's protocol. In addition to the DNase treatment recommended by the protocol, a second DNA digestion was performed using TURBO DNA-free kit (Thermo Fisher). To ensure the complete removal of the reagents used, the RNA purification step was repeated twice. Extracted RNA samples were quantified using a Nanodrop ND-1000 (Thermo Fisher). Then, 1 µg of total RNA was reverse transcribed to complementary DNA (cDNA) using the Superscript IV Reverse Transcriptase Kit (Thermo Fisher). A concentration of 2.5 ng/µl was determined as optimal for the subsequent qPCR reactions, which were performed using Platinum SYBR Green qPCR SuperMix-UDG with ROX (Thermo Fisher) as indicated by the manufacturer. Total RNA concentration of each sample was standardized prior reverse transcription into cDNA. A qPCR was carried out with primers targeting the *16s rRNA* gene (Fwd primer: 5'- TTCTACTCCCCTCTCACCTACTC-3'; Rev primer: 5'-GCGCGTAGGTGGTTATTTAAGTC-3') on each obtained cDNA sample and the reactions were performed in three technical replicates. The obtained Ct values were plotted against the CFU/well values referred to each optical density of bacteria lysed and added to the airway models to simulate an infection. The 'power' regression model (non-linear) was adopted to fit the data and to obtain the equation of a correlation curve, intended to be used for

the calculation of CFU values using Ct values in the interpolation equation. qPCR settings are summarized in table 4.

Table 4 - qPCR settings

Step	**T (°C)**	**Time**	**Cycles**
UDG incubation	50	2’	x1
Initial denaturation	95	2’	x1
Denaturation	95	15’’	x40
Annealing	60	30’’	
Melting curve	95	1’	x1
	55	1’	
	95	30’’	

5. Results and Discussion

5.1 Standard and Inverted small airway models exhibit comparable phenotype and differentiation features

Trans-Epithelial Electrical Resistance (TEER) is a common method to evaluate *in vitro* tissue epithelial barrier formation and integrity. TEER of standard and inverted models was measured during the differentiation process (Fig. 6). Even though data indicate that in standard models TEER values climb faster respect to inverted models during the first 7 days of culture, the overall trend between the two configuration is comparable and the values overlap after 31 days of ALI culturing, with inverted models displaying higher variation in the late differentiation stage (Standard = 305 ± 32 Ωcm^2; Inverted = 364 ± 71 Ωcm^2).

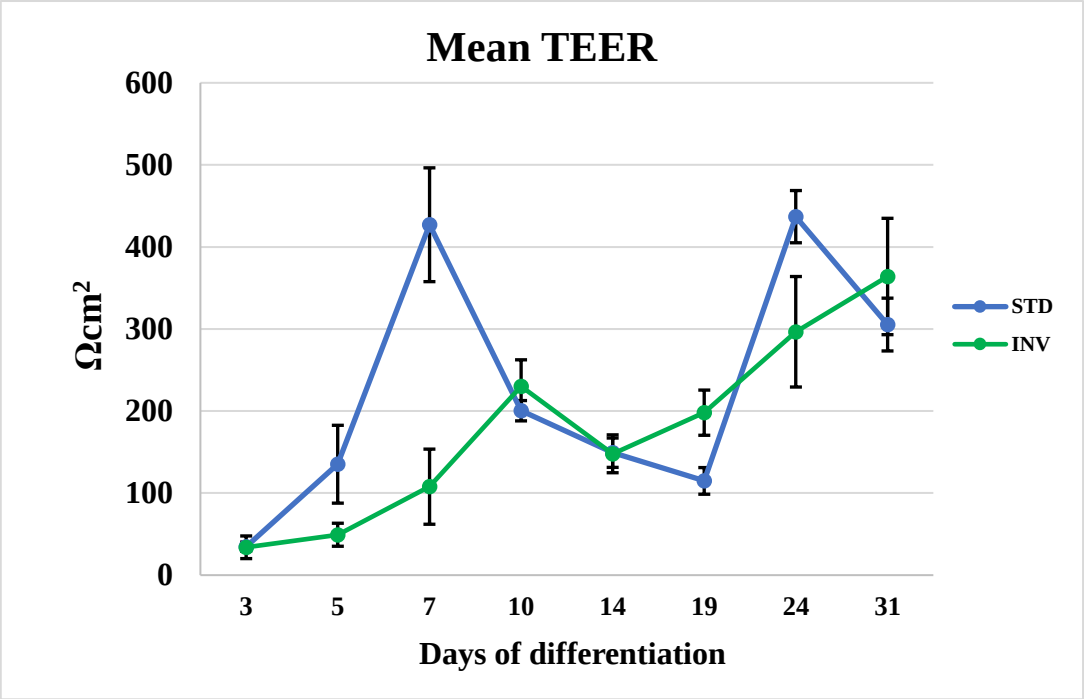

Figure 6 – TEER variation of standard and inverted models during differentiation. Results are expressed as mean values and standard deviation calculated on 25 replicates for each configuration.

To evaluate if cell differentiation occurred comparably in both configurations, standard and inverted models were characterized by laser scanning confocal microscopy (LSCM) for the presence of specific markers indicating the presence of ciliated cells (β-tubulin IV), goblet cells (MUC5AC), club cells (uteroglobin), basal cells (p63) and tight junctions (ZO-1). Ciliated and goblet cells are critical to the physiology and clearance of the airway epithelium, as they are the

main constituents of the mucociliary escalator; club cells are best known for secretion of surfactant with reduction of surface tension and participation in mucociliary clearance, but their functions also include detoxification and regulation of inflammation; in addition, their differentiation capabilities underline a role in tissue regeneration (Reynolds & Malkinson, 2010), although this function is mainly performed by basal cells. Zonula Occludens 1 (also known as Tight Junction protein 1) is part of the epithelial junctional complex, contributing to apical barrier function in airway epithelia. The assessment of the presence of the aforementioned cell types and the development of a pseudostratified structure with a functional apical barrier (junctional complex) is essential to the accuracy of the model and consequently to the relevance of the resulting observations during certain experimental conditions.

In both configurations, LSCM analysis showed proper tissue differentiation: inverted and standard models resulted positive for all the tested markers (Fig. 7, 8) with tissue architecture

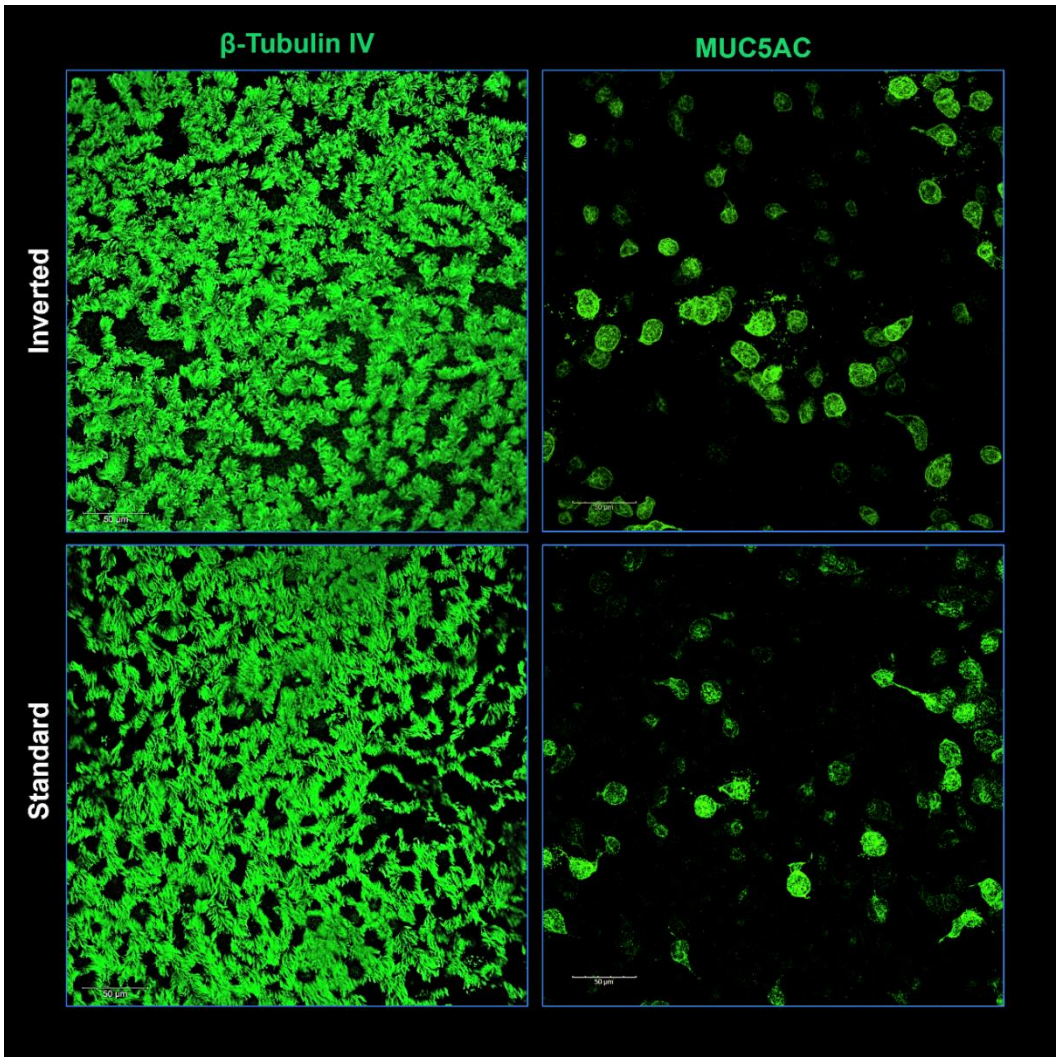

Figure 7 – Ciliated and goblet cells (highlighted in green) are present in both standard and inverted models. Images acquired with a 40x objective.

highly resembling the small airways pseudo-stratified epithelium (Fig. 9). Ciliated and secretory cells developed a polarized columnar morphology as highlighted by actin fluorescent

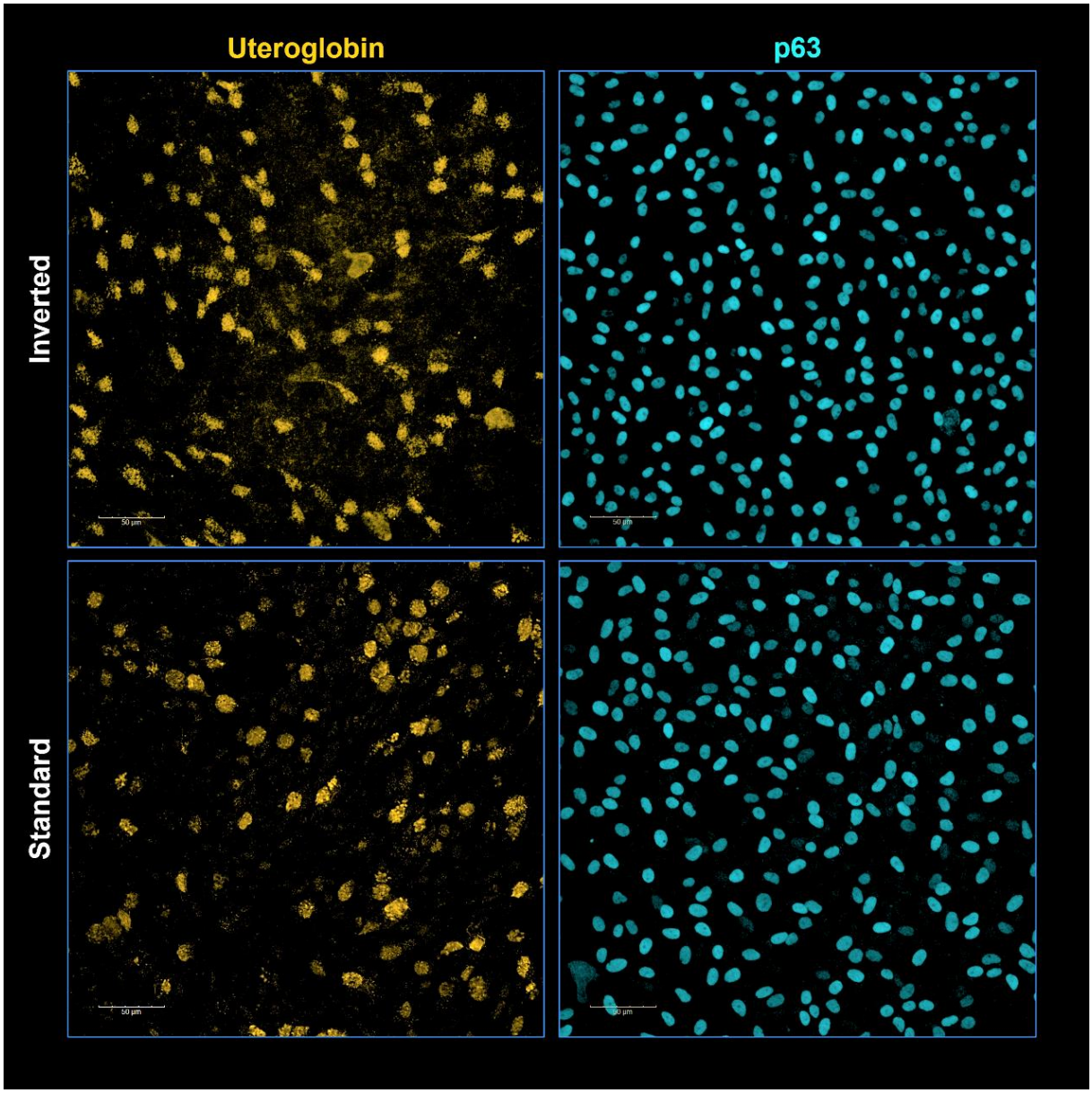

Figure 8 – Club and basal cells (respectively highlighted in orange and light blue) are present in both standard and inverted models. Images acquired with a 40x objective.

staining; tight junctions sealing together the epithelial cells were established, as highlighted by fluorescent staining of Zonula Occludens 1 (ZO-1) protein which was found properly delineating inter-cellular contours at the apical interface (Fig. 9). Cilia were evenly distributed along the apical surface; lower amounts of proportionally balanced goblet and club cells were found evenly distributed among ciliated cells, populating some areas with higher density; basal cell population uniformly lined the bottom of the epithelium. Both types of models exhibited sustained ciliary beating, mucus production and regeneration capacity after damage. Beyond

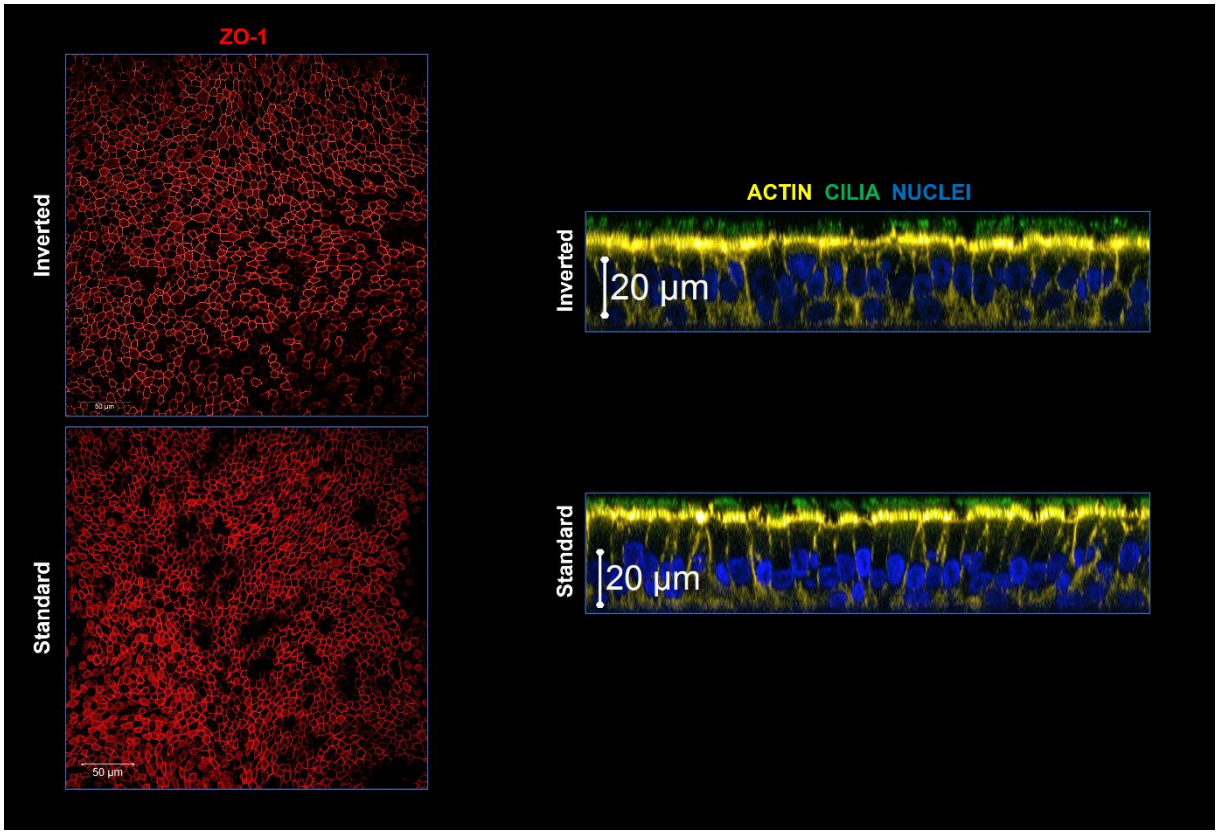

Figure 9 – Tight Junctions (highlighted in red) are fully developed in both configurations; epithelial thickness is slightly lower in inverted models.

the presence of differentiation markers, a quantification of the proportions of ciliated and goblet cells in each configuration was estimated by image analysis using Opera Phenix HCS System and Harmony HCI software. Entire samples stained for the respective marker (α-ß-tubulin IV or MUC5AC) were acquired with a 40x water objective. A specific image analysis pipeline was built for each marker as described in the Materials and Methods section. Figure 10 outlines single field virtual segregation adopted to develop the analysis pipeline for each marker. The total sum of the fluorescence-related areas of each field, calculated on the maximum projection of the acquired Z-stacks, was divided by the sum of the areas of all the analyzed fields in order to obtain a percentage value of the sample positive for the respective marker. The final evaluation was carried out on 144 fields representing the major central portion of the transwell membrane (Fig. 11). Results are summarized in figure 12. According to the analysis, cilia cover approximately 42-44% of the analyzed tissue area both in standard and inverted configuration, representing most of cell type found in our model. The analysis appears in accordance with the range reported for the human airways, according to which ciliated cells are the predominant type, representing 50-80% of epithelial cells (Crystal et al., 2008; Yaghi & Dolovich, 2016). Goblet cells are the most common

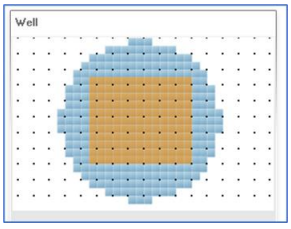

Figure 11

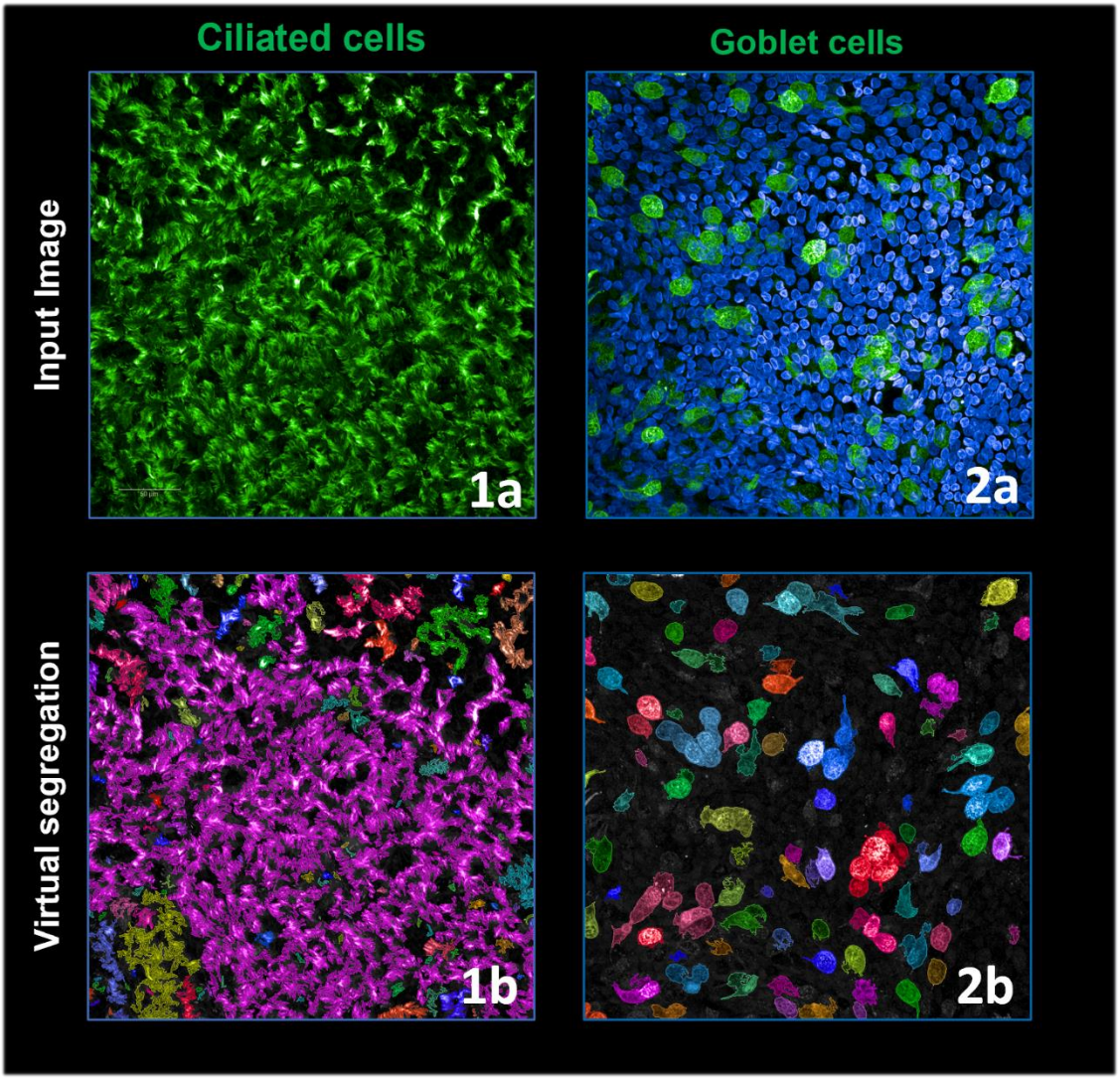

Figure 10 - The fluorescence signal related to each marker (1a, 2a,) allowed to virtually segregate the cell population of interest (1b, 2b) and measure, for each analyzed field, the total fluorescence area (µm2) related to each marker.

secretory cells in the tracheo-bronchial epithelium and their abundance can vary, ranging up to 25% of the columnar cells (Rogers, 2003), with their presence progressively decreasing with the airway degree of branching concurrently with the increase in club cell composition. Also in this case, regardless from the configuration, goblet cells were equivalently found along the tissue with variable density, representing approximately 20% of the total area.

Establishing that models grown in standard or inverted configuration have equivalent characteristics is an important prerequisite for being able to assess whether any differences in the response to experimental infections is effectively attributable to the tissue spatial arrangement. In the next paragraph, the assessment of colonization and infection is evaluated.

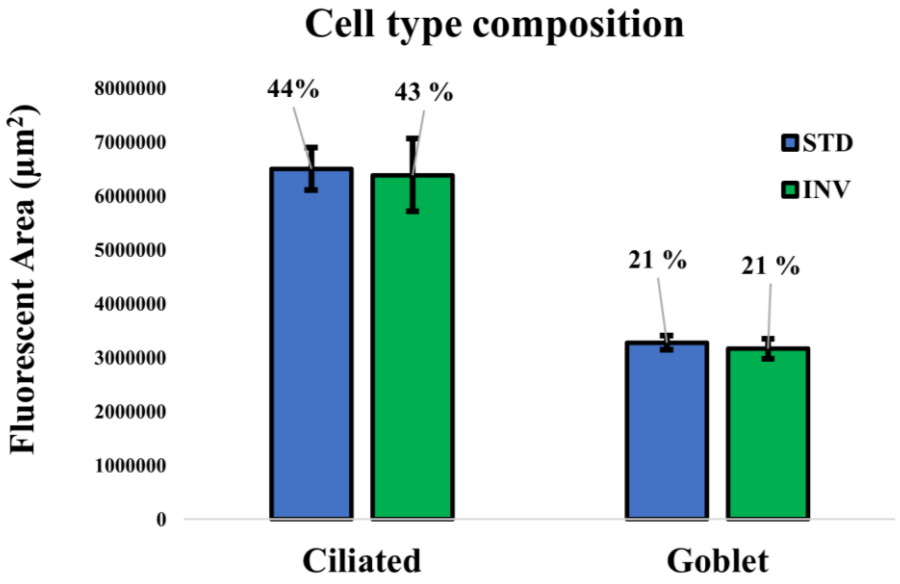

Figure 12 – Estimation of ciliated and goblet cell composition of standard and inverted models. Bars represent mean values plus standard deviation calculated on three replicates for each staining.

5.2 Small airway models cultured at an inverted air-liquid interface display delayed onset of *Moraxella catarrhalis* or NTHi infection and prolonged epithelial barrier resistance in respect to standard models

The human airway system is a complex organ that provide a critical line of defence against inhaled pathogens, representing the primary site for bacterial colonization. Moreover, conditions involving impaired tissue homeostasis as occurring in COPD patients can promote bacterial pathogenicity, leading to chronic infections of difficult eradication (Aghapour et al., 2018). Nontypeable *Haemophilus influenzae* (NTHi) and *Moraxella catarrhalis* (Mcat) are two pathogens frequently associated with AECOPD; several studies reported the ability of these bacteria to adopt persistence strategies such as biofilm formation and intracellular survival (Ahearn et al., 2017; Perez et al., 2014); however, despite extensive investigation, the ways by which these pathogens contribute to disease severity and airway inflammation have not yet been fully elucidated (Weeks et al., 2021).

To better understand the host-pathogen interplay occurring during NTHi and Mcat infection of the human airways, we performed *in vitro* infection experiments using organotypic air-liquid-interface (ALI) airway models; ALI tissue models closely mimic the structure and functions of the airway epithelium, providing a physiological environment to study the dynamics of bacterial colonization and host responses. However, the systems available to culture this tissues (e.g. Transwell) are characterized by a physically confined space that prevents the effective exploitation of natural epithelial clearance mechanisms (such as mucociliary escalator and cell extrusion) needed to contrast interaction with microorganisms; this aspect is particularly important with regard to the investigation of bacterial persistence strategies underlying chronic diseases, as *in vitro* cellular models do not tolerate bacterial presence for a prolonged period of time. We hypothesized that by inverting the epithelial configuration (as described previously) we could test bacterial-host interaction in a system devoid of any physical impediment to natural clearance, which better mimics *in vivo* conditions. In fact, although the surrogate tissue does not perfectly replicate the native environment (e.g., lack of immune system), this "unconfined" configuration could overcome the bounded aspect of the standard model in which the tissue is located within the well, rendering clearance mechanisms non-functional. Therefore, we infected standard and inverted models with NTHi FI 176 or Mcat AERIS 415 to compare disease onset in the two configurations. Trans-epithelial electrical resistance was monitored during the infection to evaluate epithelial barrier integrity; infection was characterized by LSCM, and cell

viability was evaluated by flow-cytometry. Measurements and sample processing were carried out according to specific experimental time plans tailored to each pathogen.

To evaluate the effect of infection on the integrity of the epithelial barrier, trans-epithelial electrical resistance (TEER) of standard and inverted models was monitored during the infection according to a previously defined time plan. Monitoring TEER variations over time allowed to observe a different response to infection between standard and inverted models challenged either with *Moraxella catarrhalis* or NTHi (Fig. 13). In both cases, inverted configuration appeared to increase the ability of the tissue to maintain barrier integrity despite bacterial invasion. Forty-eight hours after Mcat inoculum, a remarkable TEER decrease was

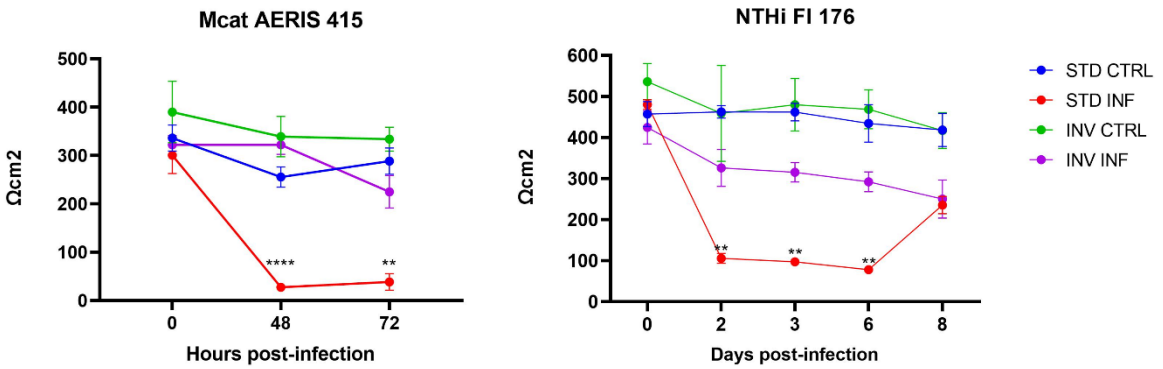

*Figure 13 – Transeptihelial electrical resistance variation over time in standard and inverted models challenged with Mcat or NTHi. Results are expressed as mean values plus standard deviation of four replicates per condition (STD CTRL = Standard Control; INV CTRL = Inverted Control; STD INF = Standard Infected; INV INF = Inverted Infected). Data were analyzed according to Welch and Brown-Forsythe ANOVA followed by a Dunnet's T3 post-hoc test. Statistical significance for the difference between the means of STD INF and INV INF is reported (** p < 0.005; **** p < 0.0001)*

observed in standard models, suggesting a complete loss of barrier function whereas equivalently inoculated inverted tissues maintained higher TEER values ($p < 0{,}0001$). NTHi showed a lower invasiveness of the tissues, allowing to extend the infection time frame up to 8 days; also in this case, TEER was observed to consistently fall earlier in standard models (72 hours) in respect to inverted samples, characterized by a slight decrease during the entire infection time-course. Interestingly, 8 days after infection, TEER of the standard models increased and values of the two configurations converged, indicating either the recovery of the barrier

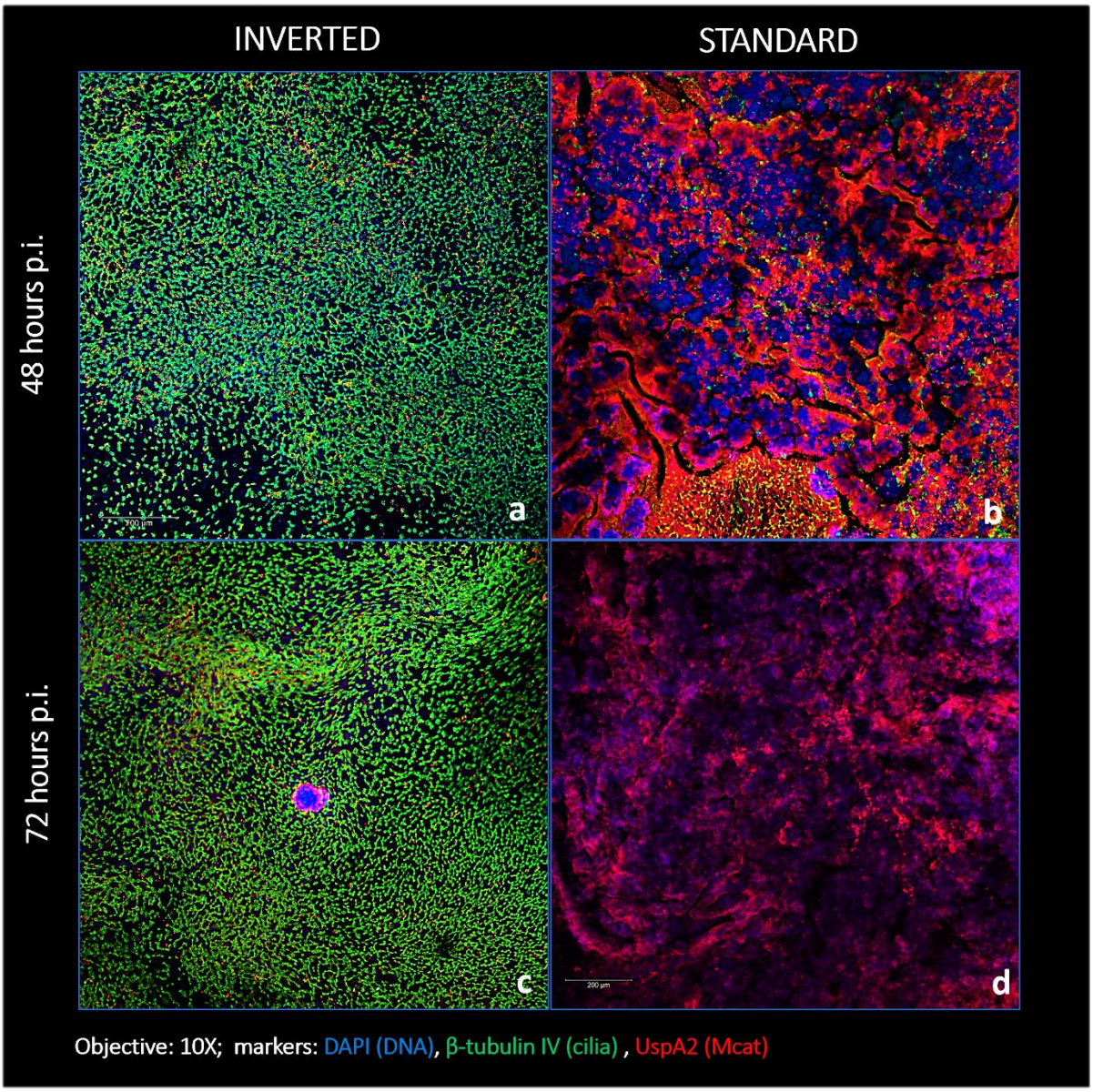

Figure 14 – Standard and inverted models 48 (a, b) and 72 (c, d) hours after Moraxella catarrhalis inoculum. In inverted samples, infection appears delayed in respect to the standard. Mcat (highlighted in red) exhibited high invasiveness in the standard model, largely colonizing the epithelium after 48 hours (b) and causing complete tissue disruption in 72 hours (d). In the inverted, tissue architecture is maintained during the infection time-course, with visible cilia (highlighted in green) lining the epithelial surface and bacteria present as single cells or small aggregates (a), starting to form macro-colonies at 72 hours p.i. Images are representative of three independent experiments.

function or the accumulation of bacteria and mucus, influencing the TEER readout. LSCM characterization supported the abovementioned observations, as shown in figures 14 and 15. Analysis conducted on Mcat infected samples showed how both at 48 and 72 hours the difference in bacterial colonization of standard and inverted models is quite noticeable. Indeed, after 48 hours of infection standard models challenged with Mcat appears widely covered by large bacterial aggregates (Fig. 14 – b), while in the inverted the pathogen is spotted mainly as a single cell or small bacterial aggregate (Fig. 14 – a). At 72 hours post-infection, Mcat completely took over the standard tissue (Fig. 14 – d) while, in the inverted, macro-colonies

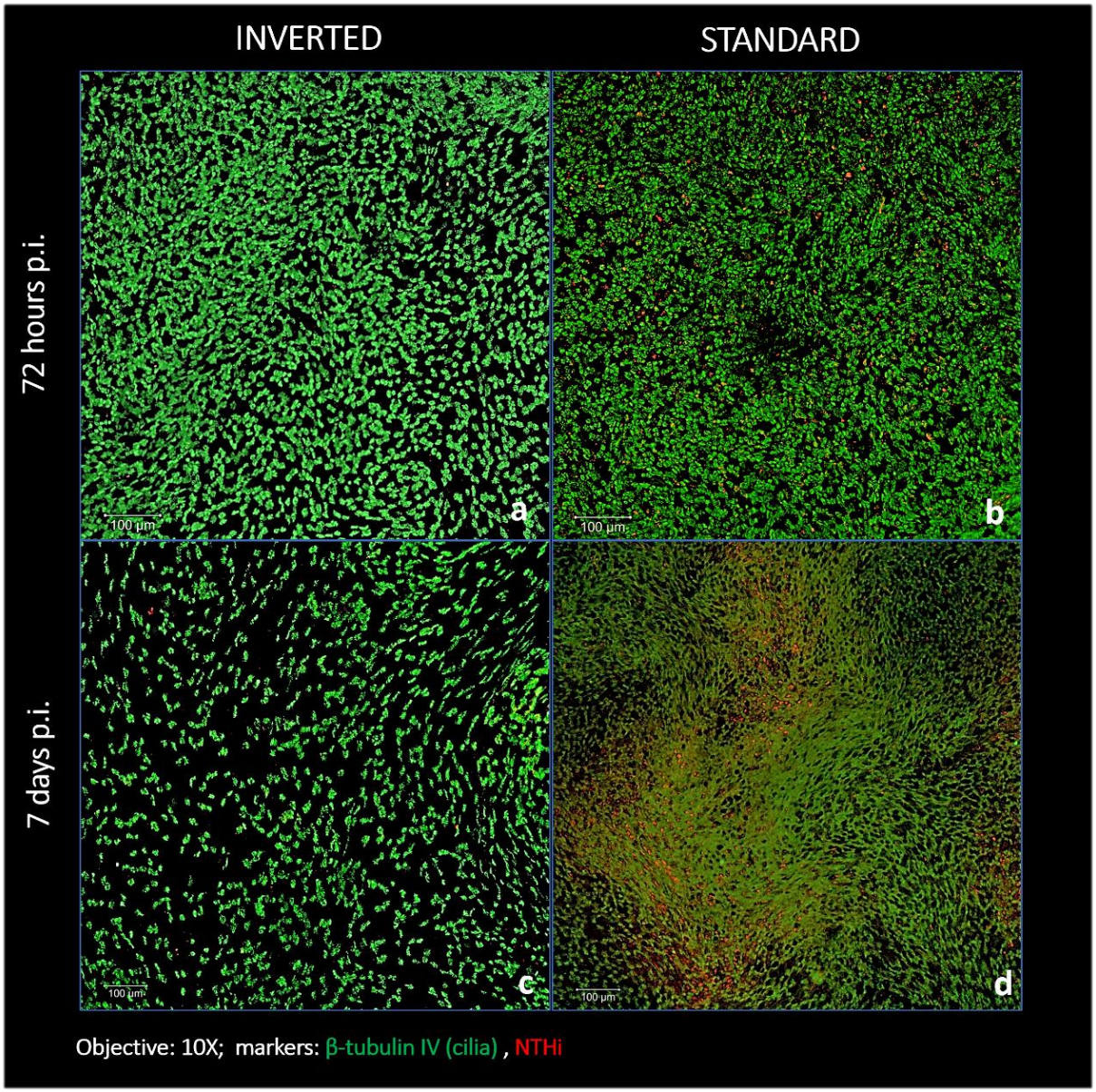

Figure 15 – Standard and inverted models 2 (a, b) and 7 (c, d) days after NTHi inoculum. In inverted samples, infection appears delayed in respect to the standard. NTHi is highlighted in red. Cilia are highlighted in green. Images are representative of two independent experiments.

start to appear on the epithelium, which is still maintaining tissue architecture with visible cilia (Fig. 14 – c). Analysis conducted on NTHi infected samples provided also in this case results in accordance with TEER variations. Despite NTHi did not display tissue invasiveness comparable to that of Mcat, LSCM analysis allowed to highlight differences in bacterial colonization of the tissue related to the model's configuration (Fig. 15). At the analyzed time points, bacterial colonization was lower in the inverted (Fig. 15 - a, c) in respect to the standard (Fig. 15 - b, d); the difference increases at later infection stage (7 days p.i.), when NTHi presence in standard models start to become appreciable (Fig. 16); in the inverted, the pathogen is scarcely detected and overall epithelial cell number appears lower, suggesting an ongoing infection-induced cell death (Fig. 15 – c). Together, these observations suggest that functional

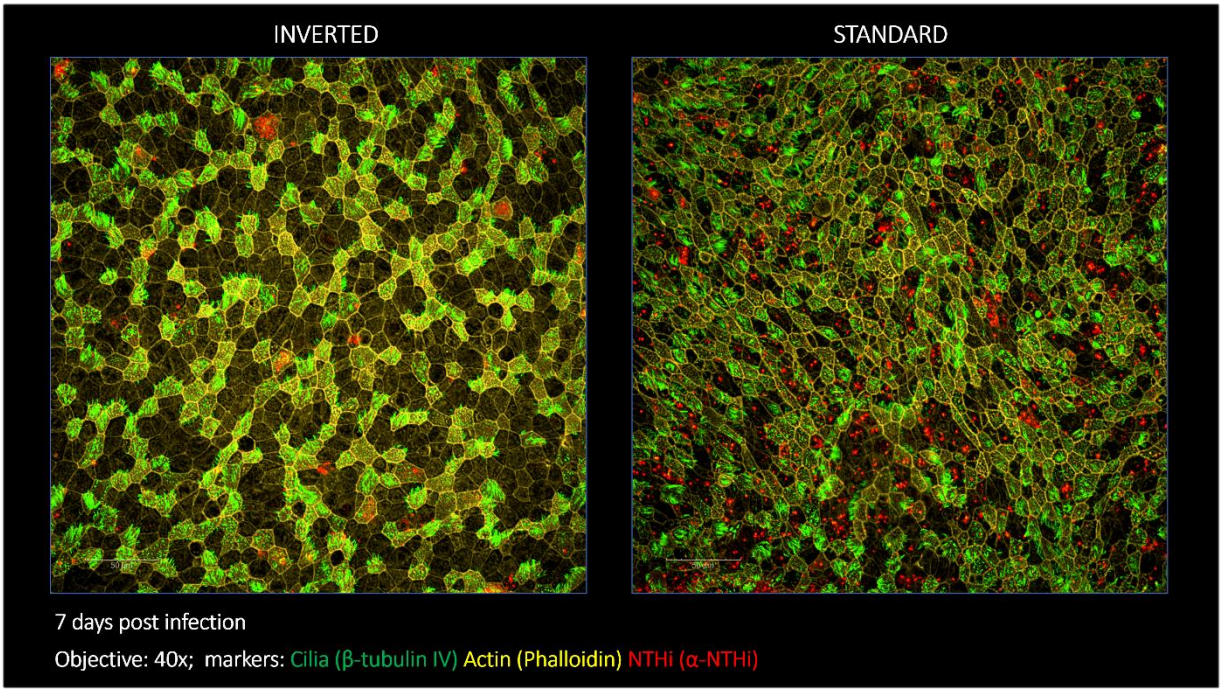

Figure 16 – Difference in tissue bacterial colonization between inverted and standard models seven days after infection.

epithelial clearance is occurring in inverted models; it can be speculated that the open configuration allows for removal of undesired, infected cells as well as of mucus entrapped bacteria.

To assess whether the configuration affects the cell viability of tissues infected with Mcat or NTHi, standard and inverted models were dissociated into single cell suspensions and analyzed by flow cytometry after staining with LIVE/DEAD Aqua Fixable Dead cell stain (Thermo Fisher) according to the time plan indicated in the figures. Figures 17, 18 and 19 summarize respectively the results obtained for Mcat or NTHi experimental infection time course. The Live/Dead analysis conducted on Mcat infected samples cells showed a remarkably higher death percentage in standard models in respect to the inverted (at 48 hours, 14 vs 4 %; at 72 hours, 26 vs 13 %); controls showed uniform death values both at 48 (3-6 %) and 72 hours post infection (16 %). However, even if death percentage values suggested a lower infection-induced cytotoxicity in the inverted configuration, these data alone do not appear to be fully representative of the overall cell death situation; indeed, comparing also the percentages of cellular debris, a more marked difference between the two configurations is observed. Debris were quantified subtracting the cell population of interest (morphology) to the total events per sample; at 48 hours post-infection, values were significantly higher in standard infected models in respect to inverted infected (44 vs 6 %), inverted control (26 %) and standard control (11 %). At 72 hours post infection the overall readout is similar: inverted control, inverted infected and standard control were characterized by uniform percentages of debris (20 %, 21 %, 29 %), while

in the standard infected configuration debris percentage was significantly higher (67 %) in respect to the other sample groups.

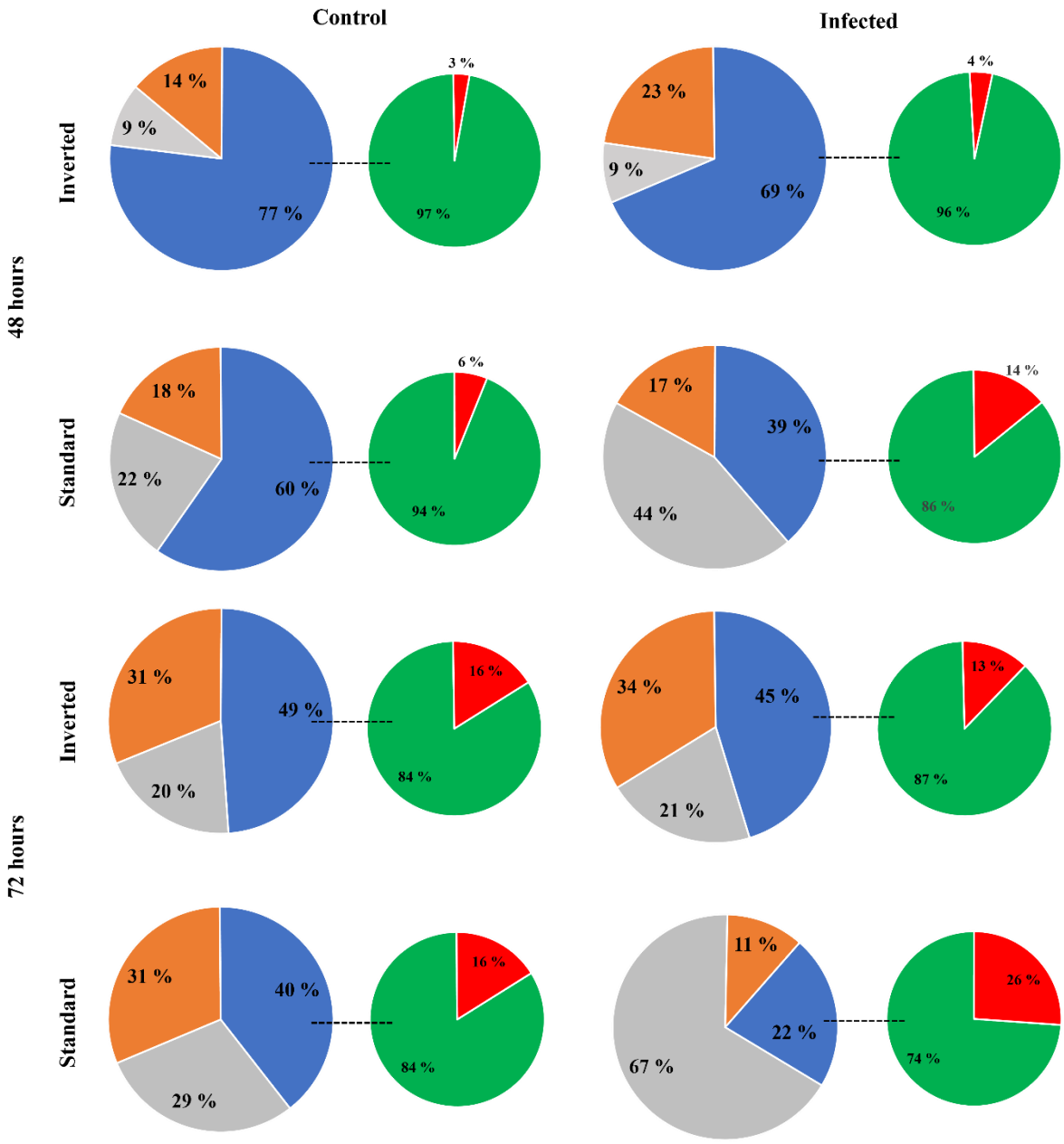

*Figure 17 – **Mcat infection - flow-cytometry analysis results overview**: gating strategy involved performing sequential gates on morphology, single cells and viability (LIVE/DEAD Fixable Aqua Dead cell Stain). Percentages are expressed as mean values calculated on three replicates for each condition; debris percentage was calculated on the total number of events per sample; aggregates percentage was calculated on the total cell population of interest (morphology); death percentage was calculated on the total single cells analyzed.*

On the contrary, the same analysis performed on models infected with NTHi FI 176 did not highlight a significant trend in the responses to infection between inverted and standard tissues (Fig. 18). At 72 hours, the pathogen did not induce cell death in infected tissues, that maintained levels of cytotoxicity analogous to the respective control. At a later stage, infection did not

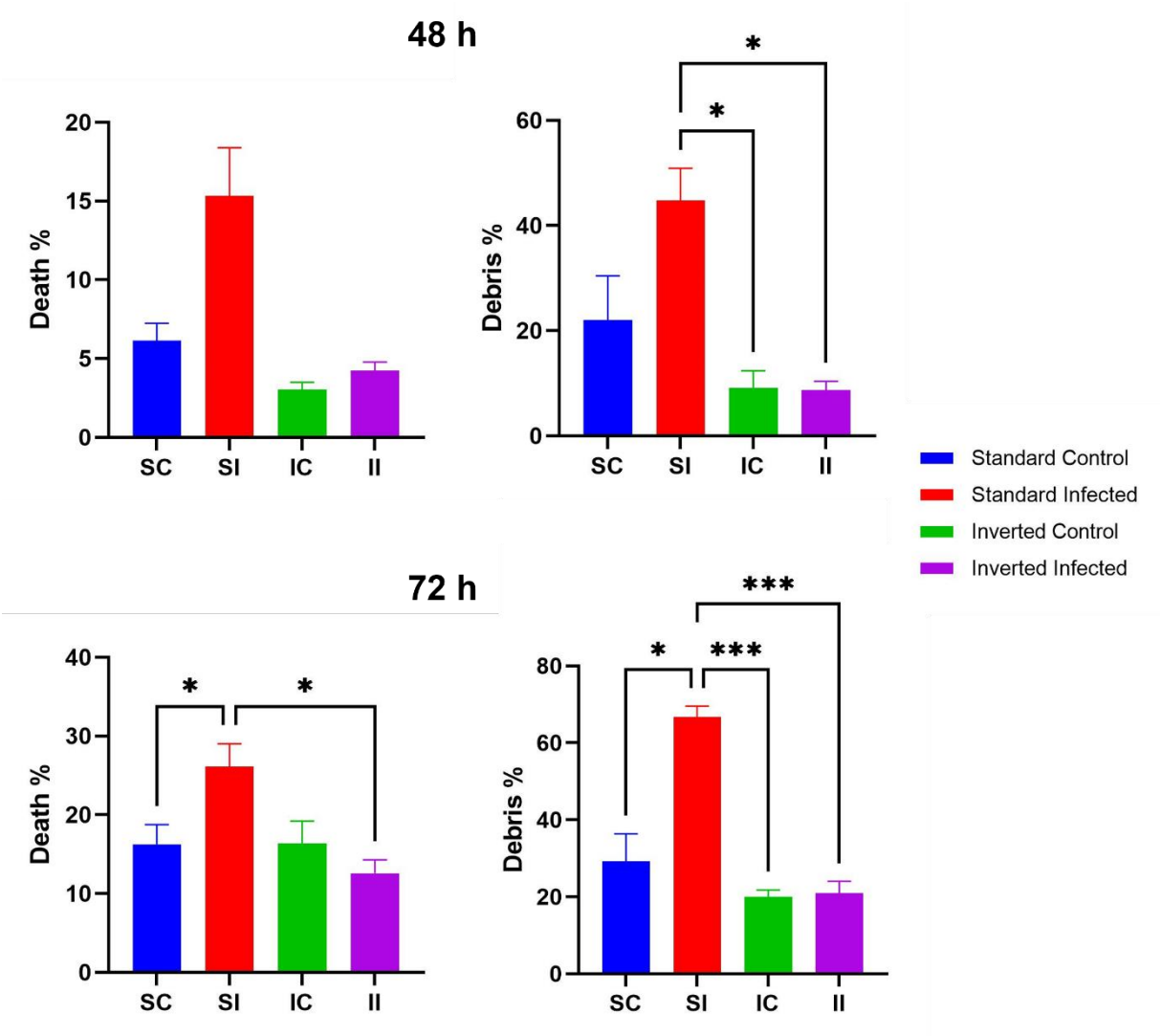

Figure 18 – Death and Debris percentages in standard and inverted models 48 and 72 hours after Mcat AERIS 415 challenge. Bars represent means plus standard deviation calculated on three replicates for each condition. Data were analyzed according to Welch and Brown-Forsythe ANOVA followed by a Dunnet's T3 post-hoc test. Statistical significance for the difference between the means is reported ($p < 0.05$; *** $p < 0.001$).*

appear to cause particular damage to the tissue, regardless of the configuration. It can be hypothesized that the adopted method does not allow to accurately detect all dead cells, for reasons related to the experimental protocol to detach and dissociate the tissue cells. Indeed, a number of damaged cells could be not enough resistant and consequently intact to be detected; moreover, extruded cells can be removed during washing procedures prior to sample processing. On the other hand, it is also possible that the used NTHi strain is adapting to the epithelial environment without causing remarkable cell death. Indeed, it has been reported that NTHi isolates have different capability to infect and induce inflammation in host tissues.

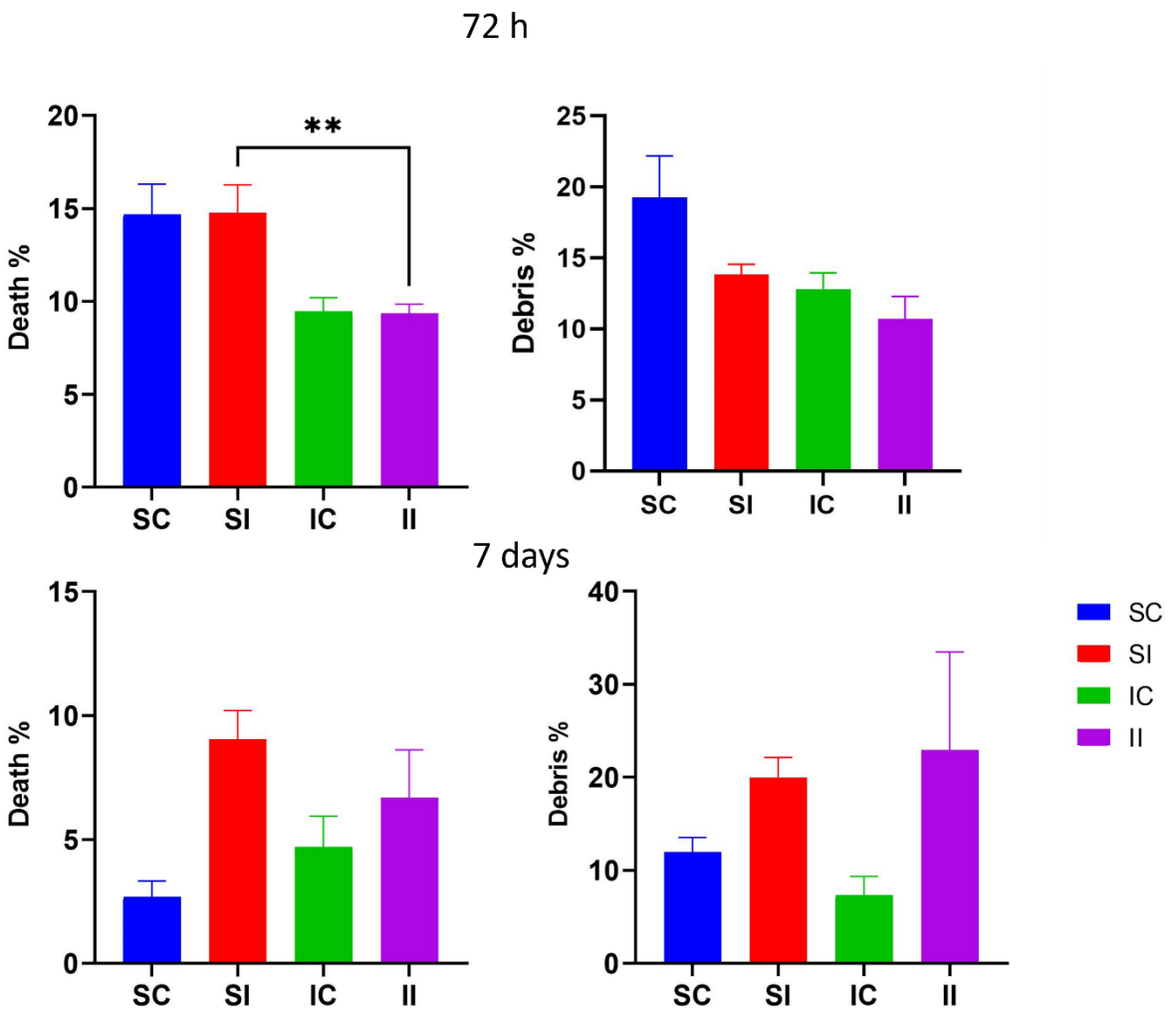

*Figure 19 – Death and Debris percentages of standard and inverted models 2 and 7 days after NTHi FI 176 challenge. Bars represent mean values plus standard deviation calculated on three replicates for each condition. Data is representative of two independent experiments. Data were analyzed according to Welch and Brown-Forsythe ANOVA followed by a Dunnet's T3 post-hoc test. Statistical significance for the difference between the means is reported (** $p < 0.01$).*

Our findings showed how inverted configuration delays NTHi or Mcat infection onset in differentiated airway epithelial cells, allowing to prolong epithelial barrier resistance and consequently the experimental infection timeframe. Despite the pathogens exhibited different invasiveness of the tissue, in both cases microscopy analysis showed a higher number of bacteria in standard models, suggesting that the delayed infection is apparently a consequence of an enhanced tissue clearance ability allowed by the inverted configuration.

5.3 *Moraxella catarrhalis* and Nontypeable *Haemophilus influenzae* colonization of differentiated airway epithelial cells involves the formation of intra-epithelial communities and biofilm structures

Given the evidence that inverted models have a lower susceptibility to bacterial infection, we performed long-term infections (up to two weeks) for a deeper characterization of Mcat or NTHi invasion and colonization of the airway epithelial tissue. Microscopy analysis (LSCM, TEM, SEM) of inverted airway models infected with *Moraxella catarrhalis* AERIS 415 allowed us to individuate unique infection features exhibited by the pathogen and consequently to speculate on its mechanism of pathogenesis. After invading the epithelium, Mcat starts growing intracellularly till the disruption/extrusion of infected cell clusters (Fig. 20 – 1), concurrently establishing biofilm-like structures that replace portions of the epithelium (Fig-

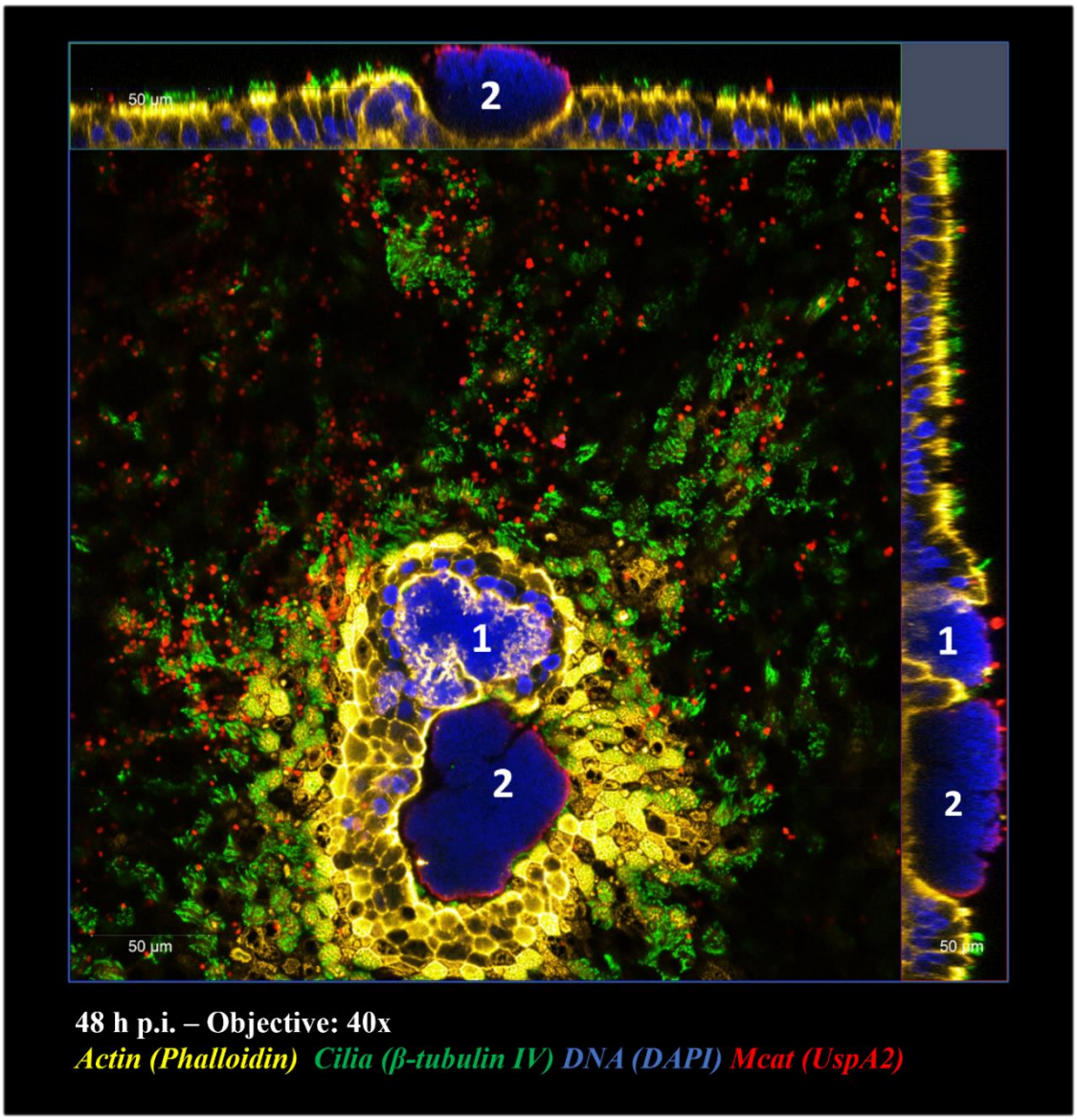

Figure 20 – Different stages of Moraxella catarrhalis colonization of airway epithelial cells. Intraepithelial bacterial growth is disrupting cellular actin (1) prior to establishing a dense aggregated mass replacing dead tissue portions (2).

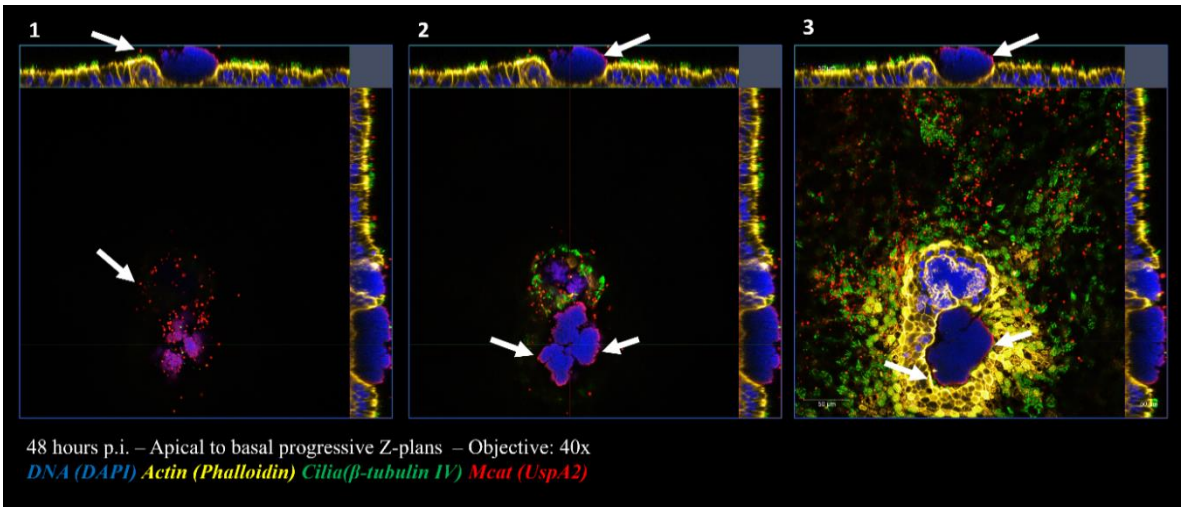

Figure 21 – Apical to basal progressive Z-plans show selective UspA2 staining for single bacteria (highlighted in red) (1) or the ones located on the perimeter of the aggregate (2, 3).

20 – 2). During this process, the analysis shows that Mcat growth is associated with macroscopical actin remodelling. Interestingly, the tissue does not appear to completely lose its cellular architecture and barrier function, since after the invasion and replacement of epithelial cells, where nuclei and actin tend to disappear progressively along with bacterial growth, mature Mcat aggregates rarely affect deeper cell layers (Fig. 20 – 2). The morphology of the epithelium surrounding the forming bacterial mass suggests that the tissue exerts forces in order to extrude it; however, these Mcat aggregates appear to be strongly associated to the epithelial surface. Interestingly, although samples were extensively permeabilized, only isolated bacteria or the ones that reside on the external perimeter of the aggregate can be efficiently immuno-stained. Indeed, even if bacteria that are embedded in these biofilm-like structures are labelled by DAPI, they appear to be recalcitrant to anti-UspA2 antibodies (Fig. 21). A more advanced infection stage (72 hours post-infection) is shown in figure 22. In the central zone of the infected area epithelial cells are completely absent, replaced by biofilm structures from which the infection is spreading to the neighbour tissue. In the surrounding area, immuno-staining recalcitrant bacteria are growing inside the epithelium, changing completely the morphology of the tissue and taking the control of that specific area from which Mcat diplococci or tetrads appear to be released from the inside of the epithelium in order to colonize other zones. Epithelial cells do not appear to extrude according to an active mechanism, as Z-stack analysis highlighted intracellularly growing bacteria that appear to push eukaryotic nuclei towards the apical surface. At two weeks post infection, the host-pathogen challenge is still ongoing, although Mcat macro colonies dominate the epithelium both intra- and extra-cellularly (Fig. 23); SEM analysis suggested the presence of an extra-polymeric substance enveloping bacterial clusters (Fig. 24), supporting the hypothesis that these macro-aggregates of bacterial cells represent effectively a biofilm. The selective labelling of the UspA2 surface protein of

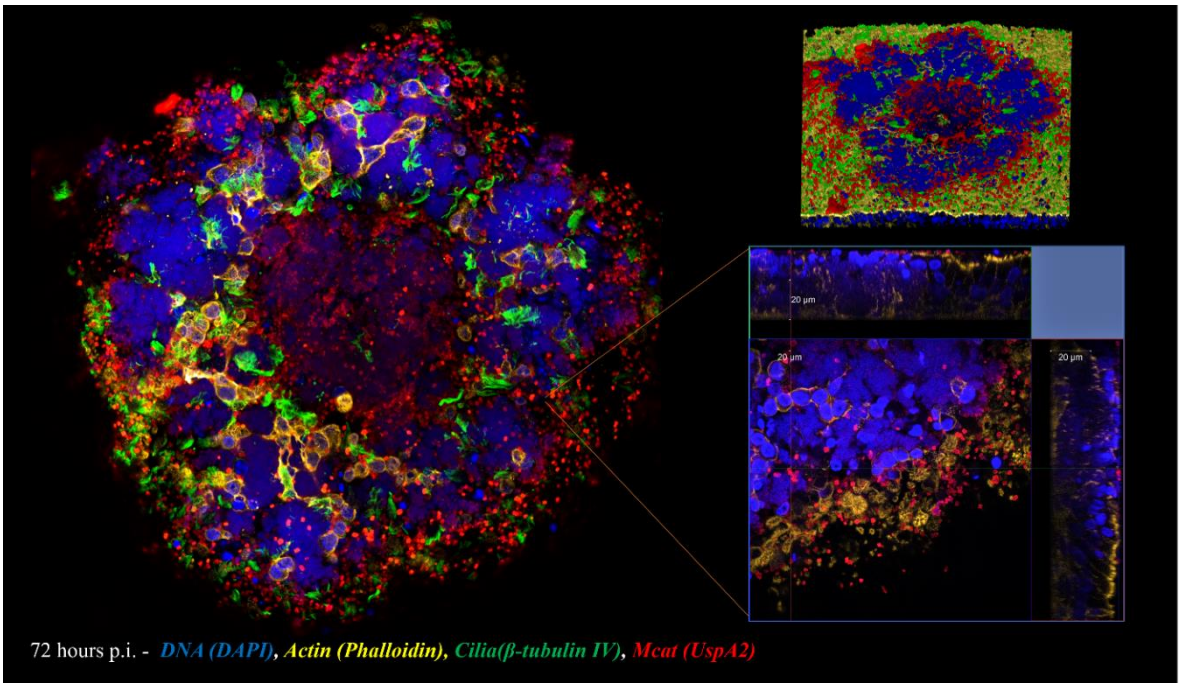

Figure 22 – Moraxella catarrhalis airway model infection spreading intra- and extra-cellularly.

unembedded bacterial cells in respect to the ones residing within the aggregated community suggested at first a differential expression pattern for the target, therefore an immunogold labelling assay was carried out to further investigate this hypothesis. The analysis allowed to detect the UspA2 antigen in the internal part of the Mcat communities, revealing the inability of the anti-UspA2 labelling antibodies to penetrate deeply into the biofilm structure; moreover, also dsDNA appeared to be part of the biofilm scaffold (Fig. 25), reinforcing the hypothesis that these structures constitute a complex host-bacterial biofilm-like structure. Microscopy analysis carried out on samples infected with NTHi FI 176 revealed at first a lower invasiveness of the tissue in respect to Mcat AERIS 415. At early infection stages (72 h post infection), NTHi was detected as a single intra- or extracellular bacteria, populating some areas with a higher density (Fig. 26) and infiltrating paracellularly between epithelial cells (Fig. 27). Bacterial cells that were observed to reside within epithelial cells, occasionally localized nearby eukaryotic nuclei and seemingly provoked their disruption (Fig. 28). With regard to the morphology of the epithelium, no particular

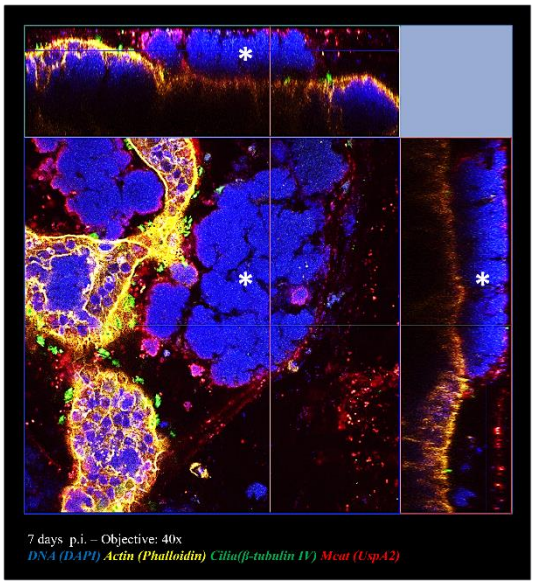

Figure 23 – At seven days post infection, Mcat persists on airway epithelial cells. Mature biofilm (indicated by the asterisk) is established on the apical surface of the epithelium.

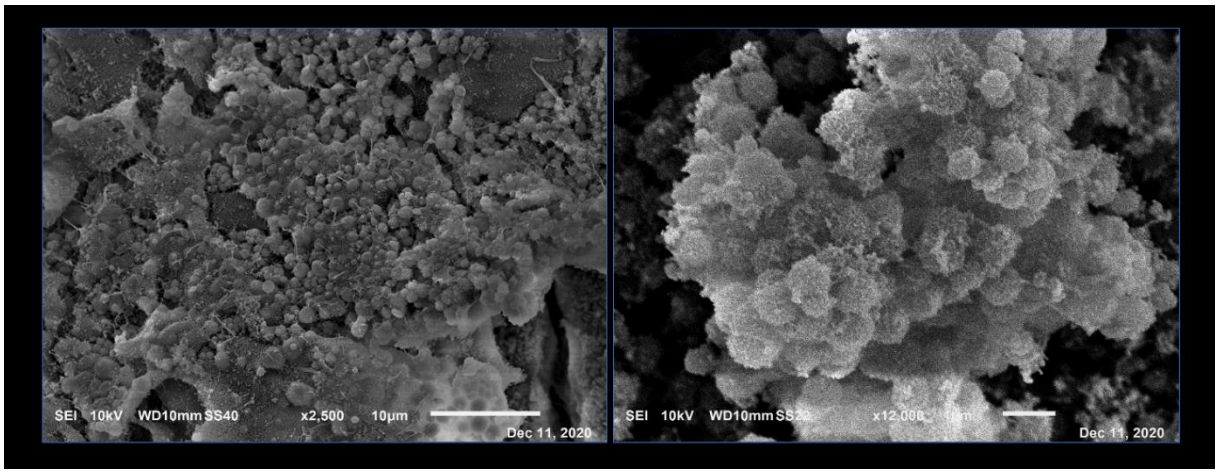

Figure 24 – Scanning Electron Microscopy analysis of inverted airway models after 14 days of Moraxella catarrhalis AERIS 415 infection

differences were observed between the standard and inverted infected models at this time point. In both configurations, the analysis highlighted the occurrence of infected cells extruding from

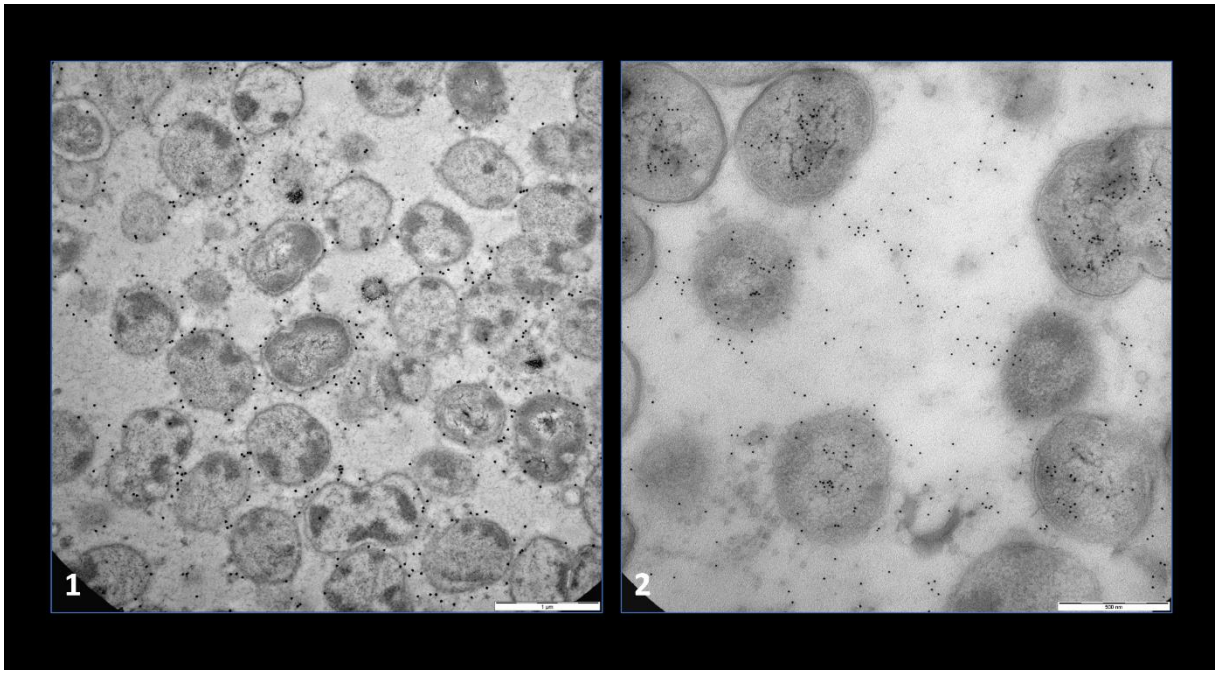

Figure 25 – Immunogold labeling assay conducted on Moraxella catarrhalis biofilm ultrathin sections reveals that UspA2 (1) is expressed by bacterial cells residing within the aggregate; dsDNA (2) is also part of the biofilm scaffold. Antibody targets are indicated by ***black dots****.*

the epithelium (Fig. 29); however, bacterial colonization was higher in the standard models (as shown previously in figure 15), suggesting that the inverted configuration effectively facilitates pathogen clearance through this mechanism. Intriguingly, we observed that NTHi FI 176 is capable to form intracellular bacterial communities that, similarly to Mcat, are recalcitrant to antibody staining; in this case the phenotype appears to be caused by a phenotypic switch rather than by a structure-related impermeancy, as also single NTHi cells are found negative to the staining (Fig. 30). Intracellular communities were found in standard models and not in the

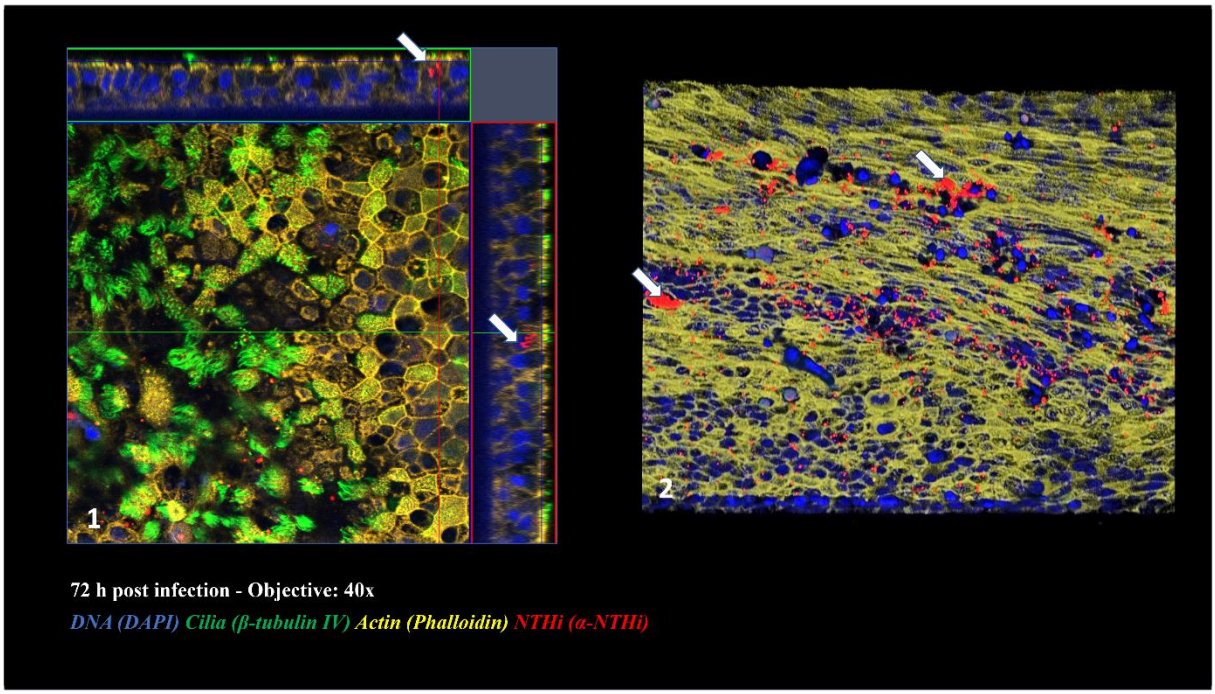

Figure 26 – At 72 hours post infection, single cell NTHi colonies (highlighted in red) were found inside host cells (1) and on the epithelium apical surface (2).

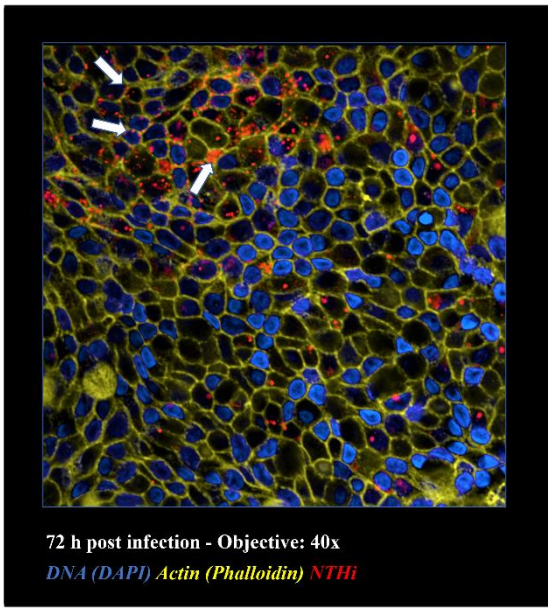

Figure 27 – NTHi (highlighted in red) colocalize intracellularly with cellular actin (highlighted in yellow)

inverted at 72 hours post infection. At seven days post infection, standard models were still characterized by a higher bacterial presence in respect to inverted models, with increased occurrence of intracellular NTHi communities that appear more densely packed in respect to the previous time point (Fig. 31, 32). In this case, differences with regard to the cellular architecture between standard and inverted tissues started to become appreciable. Large zones of the inverted epithelium exhibited reduced thickness and polarization, with the tissue appearing composed by a lower amount of cells, probably as a result of a remarkable infection-

induced cell extrusion; in support of this hypothesis, infected cell clusters surrounded by NTHi are found detached from the epithelial apical surface (Fig. 33, 34), suggesting that, in highly infected zones, cells are extruding in mass. A similar phenotype was recently characterized by Aparicio-Yuste et al. (2022) in MDCK monolayers infected with *Listeria monocytogenes*. Intraepithelial communitites were found in inverted models only at late time points (14 days

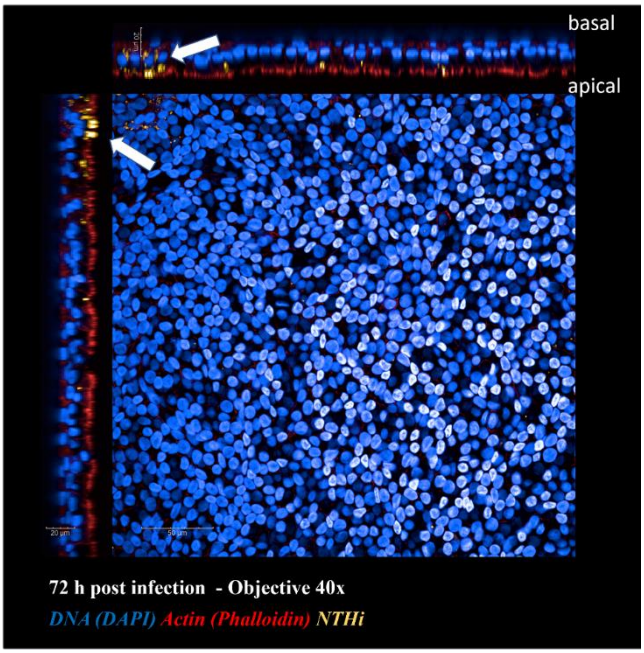

Figure 28 – NTHi (highlighted in yellow) interacting with eukaryotic nuclei (highlighted in blue).

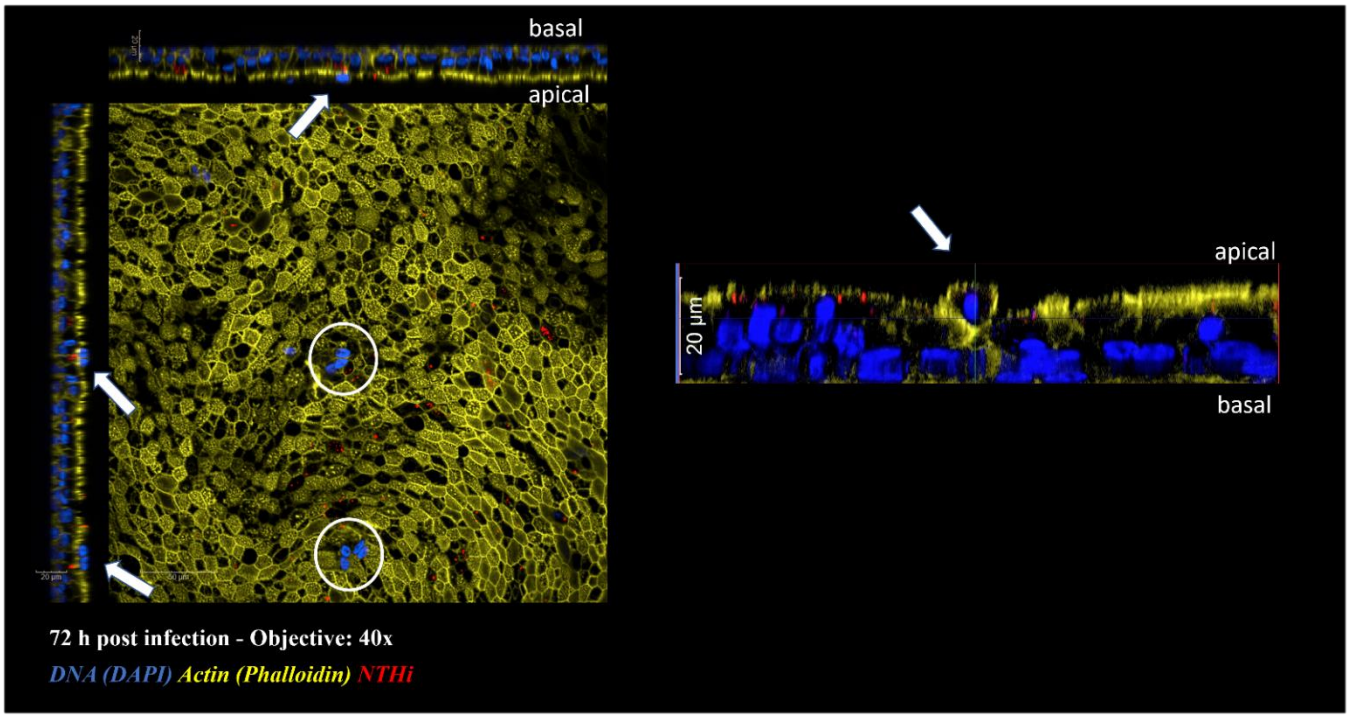

Figure 29 – Eukaryotic cells (highlighted by arrows circles) extruding from infected epithelial tissue.

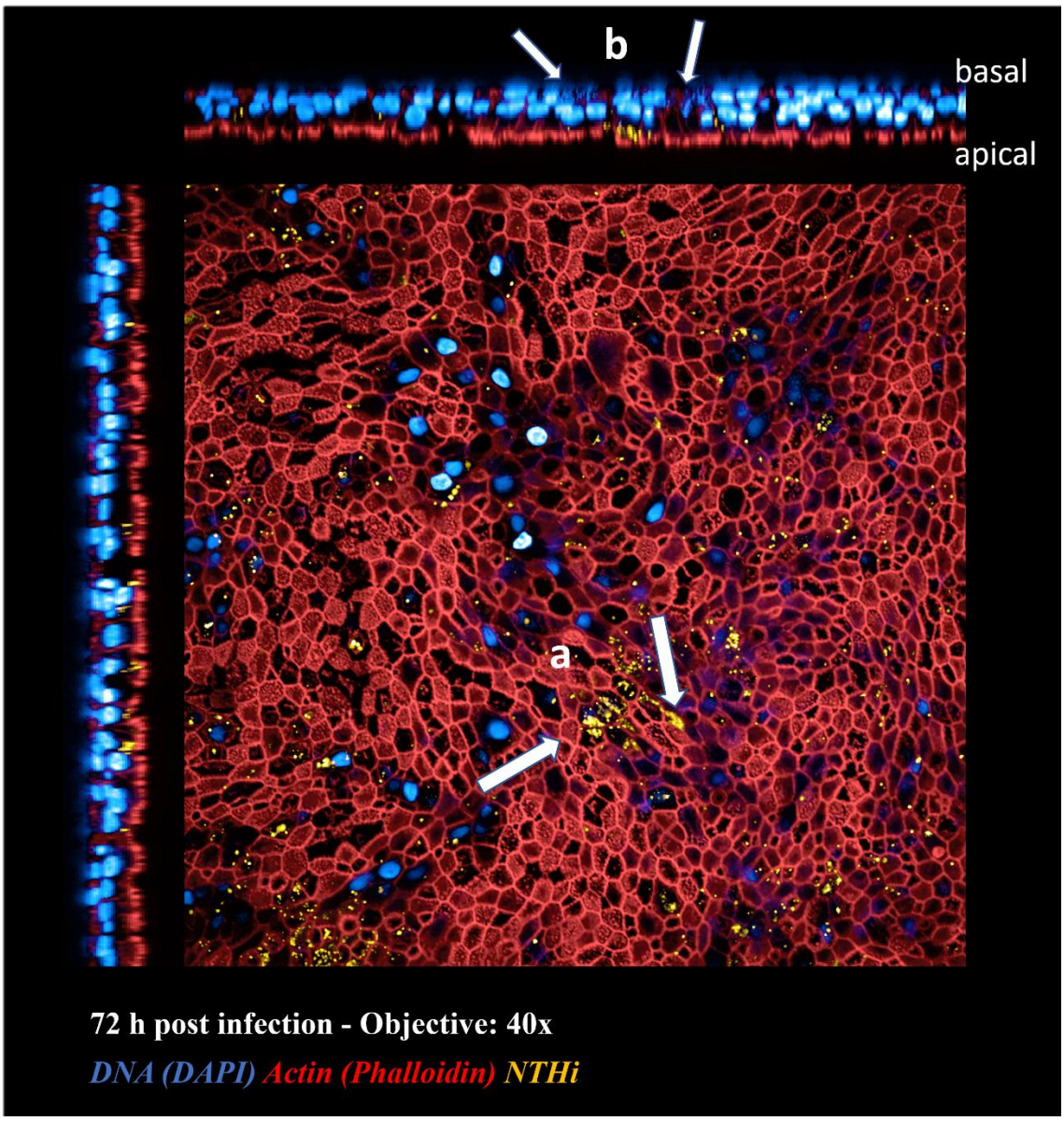

Figure 30 – NTHi FI 176 intra-epithelial communities started to form at 72 hours post infection in standard models. Bacterial single cells, highlighted in yellow (a) are positive to immuno-staining; on the other hand, NTHi microbial communities residing in the basal plan of the epithelium (b) are labeled only by DAPI (highlighted in blue).

p.i.), in correspondence of highly infected and compromised portions of the epithelium, where columnar morphology is completely lost (Fig. 35).

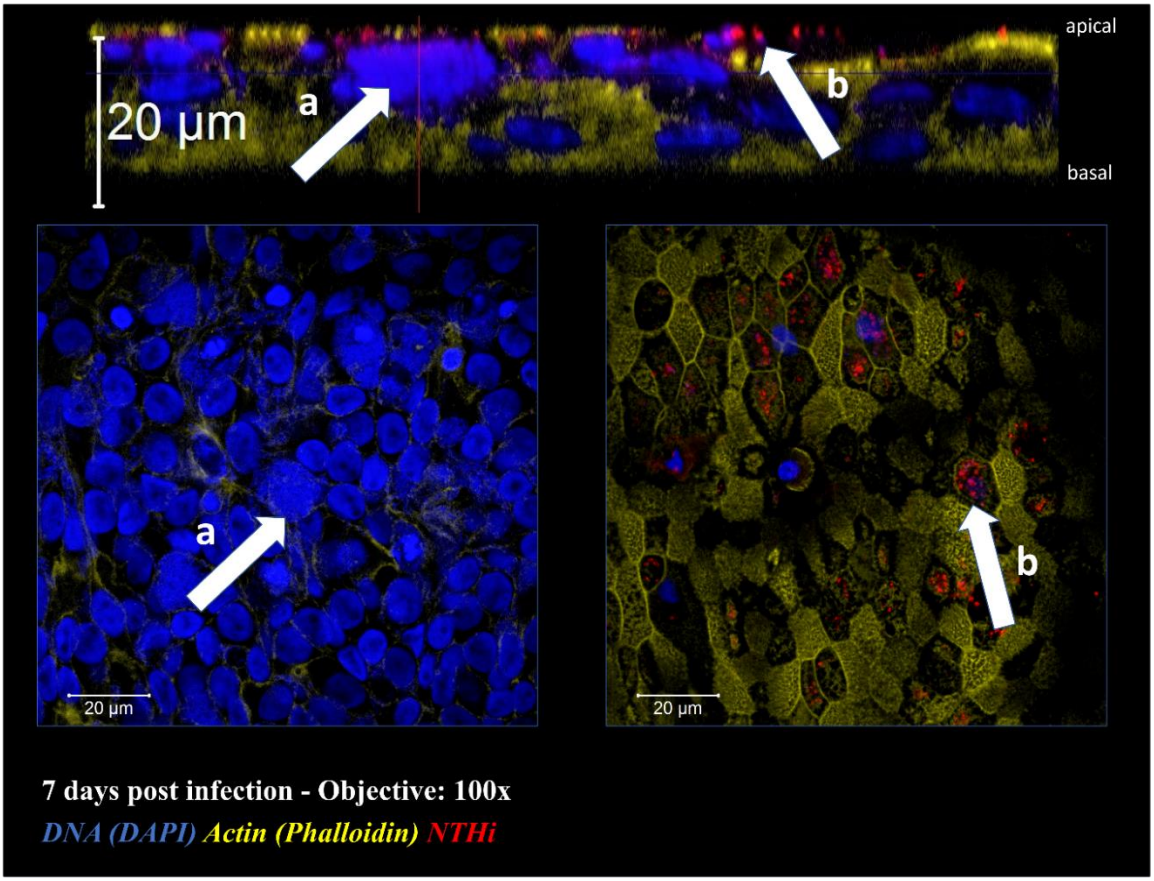

Figure 31 – 7 days post infection - Z-stack overview. NTHi intra-epithelial communities are recalcitrant to immuno-staining (a) and are labeled only by nucleic acid marker (highlighted in blue); single NTHi bacteria that do not reside within the structure (highlighted in red) are positive for the staining (b).

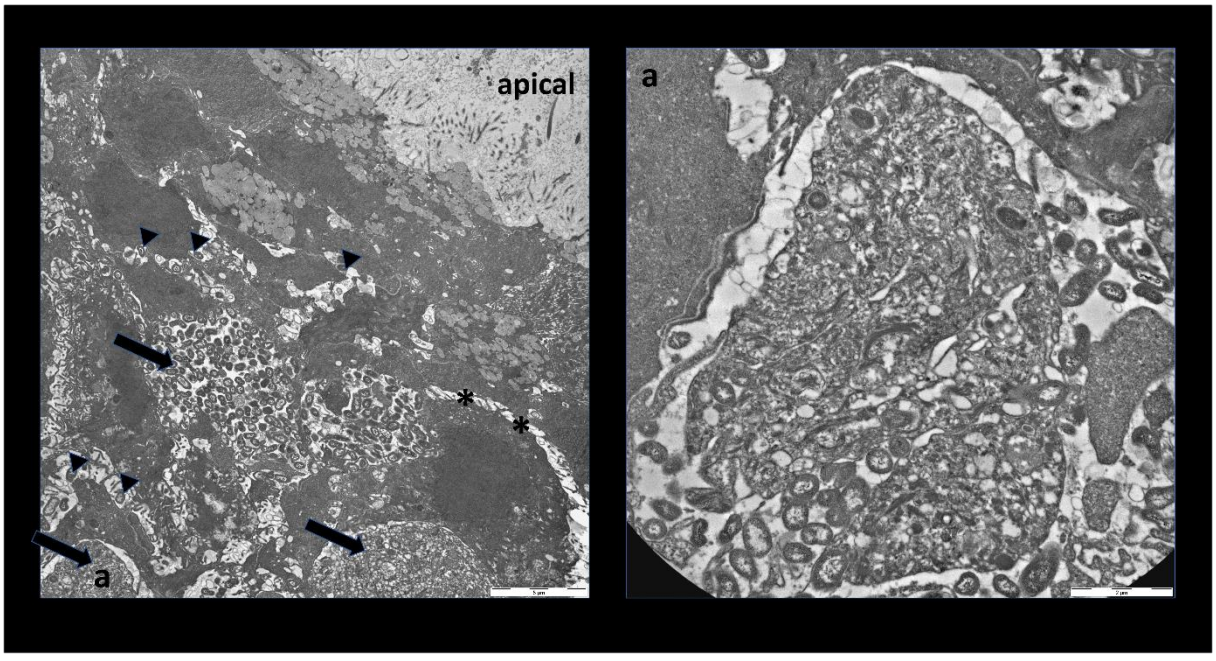

Figure 32 – TEM analysis confirms intra-epithelial localization of dense NTHi biofilm-like communities residing below the apical surface of the epithelium, as indicated by the black arrows. Bacteria localized paracellularly are indicated by black triangles; cell-to-cell junctions appear loose (highlighted by the asterisks). Higher magnification (a) shows NTHi organized in a densely packed structure.

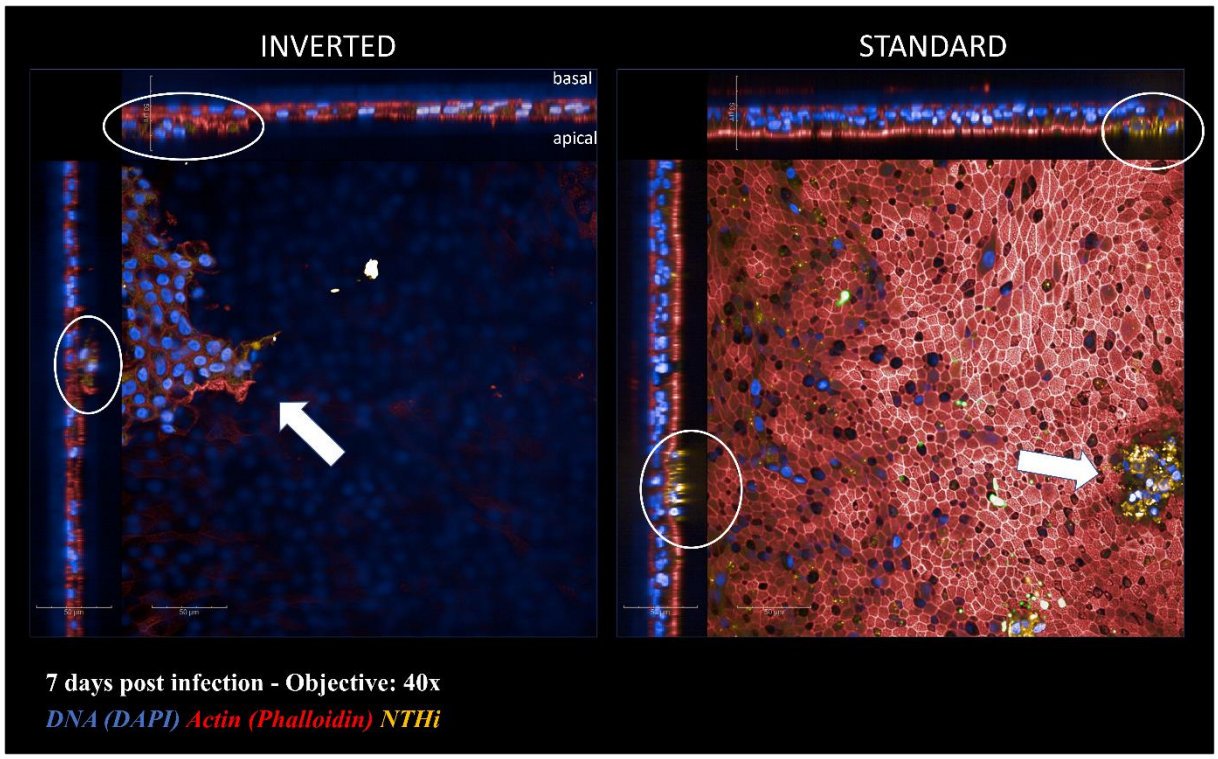

Figure 33 – At 7 days post infection, inverted models are characterized by a reduced thickness in respect to standard models, likely as a consequence of a more remarkable cellular extrusion. Infected cell clusters (indicated by arrows and circles) are found detached from the apical surface of the epithelium.

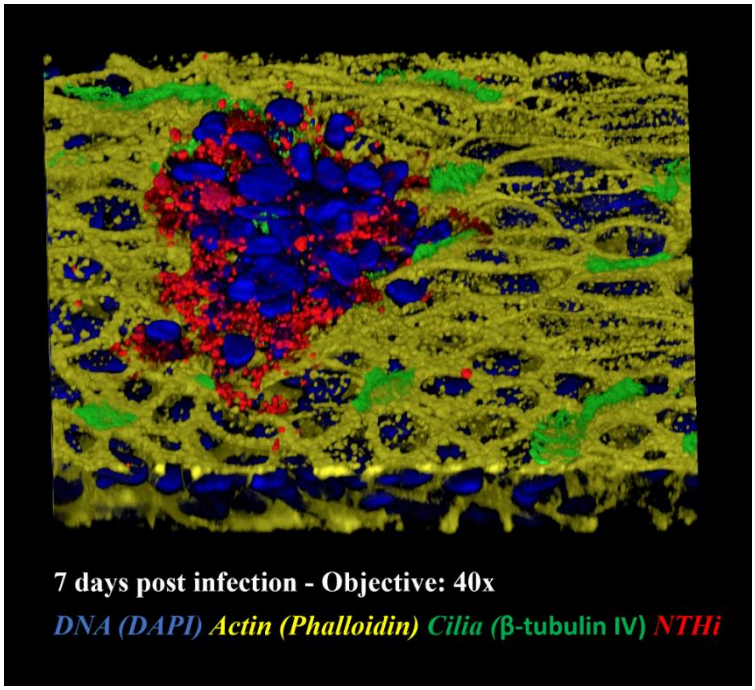

Figure 34 – Infected cell cluster detaching from the epithelium.

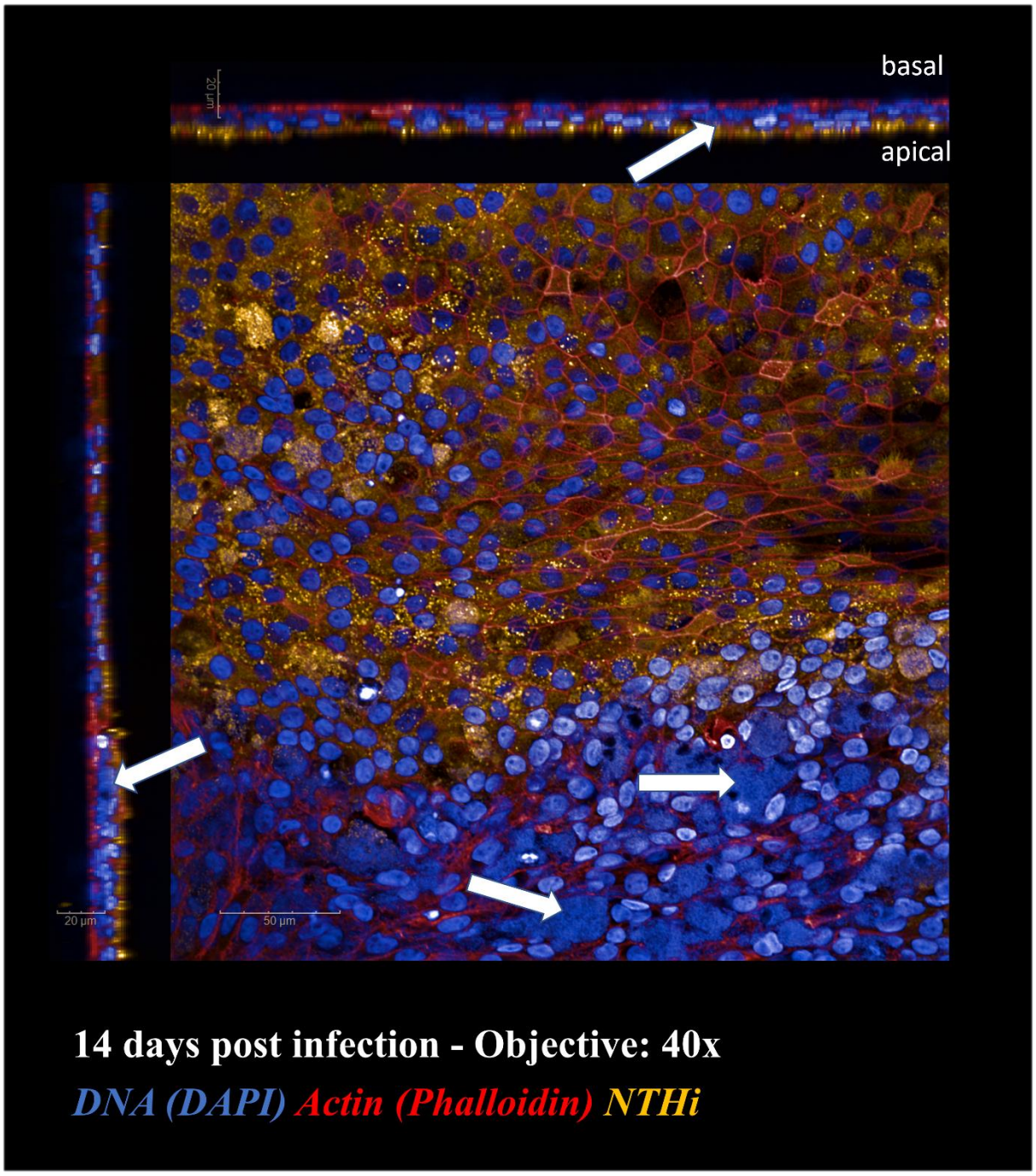

Figure 35 – Inverted model 14 days after NTHi inoculum. Intra-epithelial communities are indicated by the white arrows.

The investigation on the mechanisms by which bacteria colonize the host niches is crucial for the subsequent development of treatments against the provoked disease. Biofilms are complex communities of microorganisms embedded within a self-produced matrix that protects cells from the external environment, rendering bacteria less susceptible to treatments and immune defences (Flemming & Wingender, 2010). These structures can form on a wide range of biotic or abiotic surfaces and are generally characterized by a life cycle that is believed to involve four stages: bacterial adhesion to surfaces, formation of microcolonies, maturation of the biofilm and dispersal of bacterial cells (Tolker-Nielsen, 2015). In biofilm-associated infectious

diseases, this microbial lifestyle is thought to contribute to pathogen persistence and disease chronicity, as it allows bacterial survival within the host (Bjarnsholt, 2013).

To date, multiple evidence suggest that bacterial biofilms play a role in many infection-related human diseases, affecting several human districts including the auditory (otitis media), cardiovascular, digestive, reproductive, urinary and respiratory system (Vestby et al., 2020). Among other pathogens (*Escherichia coli, Pseudomonas aeruginosa, Streptococcus pneumonia*) Nontypeable *Haemophilus influenzae* and *Moraxella catarrhalis* have been shown to be capable of forming intracellular microbial aggregates displaying biofilm-like features, as reviewed by Mirzaei et al. (2020). Several studies have provided evidence for NTHi or *Moraxella catarrhalis* intracellular behavior, both in the context of otitis media and airway infections (Bandi et al., 2001; Clementi et al., 2014; Hall-Stoodley et al., 2006). Both pathogens exhibit biofilm lifestyle hallmarks (Armbruster et al., 2010; Weeks et al., 2021); however, with regards to respiratory diseases (e.g., COPD), the way these bacteria contribute to pathogenesis still remains unclear. Intracellular bacterial biofilm cycles were already described for other pathogens, with regard to the airway and the urogenital mucosa; Mirzaei et al. (2020) extensively reviewed the current knowledge of the bacteria that adopt this strategy, including *Pseudomonas aeruginosa* (Fleiszig et al., 1996; Garcia-Medina et al., 2005; Plotkowski et al., 1999; Schroeder et al., 2001; Zaas et al., 2005) and *Escherichia coli* (Abell-King et al., 2022; Anderson et al., 2004; Justice et al., 2004; Rosen et al., 2007).

Here, we have provided for the first-time direct evidence of NTHi or Mcat biofilm-like communities residing within differentiated airway epithelial tissue; moreover, we explored an alternative cell culturing approach that eases natural clearance mechanisms exhibited by organotypic Air-Liquid-Interface airway models and consequently extends the duration of the experimental infections time course. Our findings are in agreement with observations that these pathogens use this behavior as a strategy to persist within the host and cause chronic infections, as biofilm lifestyle enhances antibiotic resistance and immune evasion. In the case of Mcat, we demonstrated that the bacterial dense aggregates, although properly permeabilized, are impermeant to labeling immunoglobulins, suggesting a possible reduced efficacy of IgG-based host defences. In the case of NTHi, further research would be needed to assess if the recalcitrancy to antibody staining is due to bacterial expression changes or to the dense structure of the aggregate, not permitting the passage of labeling immunoglobulins. Microscopy analysis also suggested that NTHi infection induced remarkable epithelial cell extrusion; on the other hand, this phenomenon was not observed to a comparable extent in experimental Mcat

infections, suggesting that this pathogen could adopt strategies to inhibit cell extrusion tissue capability. Kim et al. (2010) highlighted that *Moraxella catarrhalis* and *Haemophilus influenzae* could inhibit the epithelial extrusion process through a mechanism involving upregulation of CD105 via CEACAM engagement; our findings are only partially in accordance with these speculations, suggesting that other mechanisms could underlie our observations.

5.5 mCherry complemented *Moraxella catarrhalis* does not uniformly express fluorescent protein during infection of airway epithelial cells

V-PIPE and I-PIPE reactions were performed according to the steps described in the Materials and Methods section in order to: clone the *ggt* pseudogene complementation locus comprising of 488 bp left and right flanking regions into a pET15-ccdb plasmid; clone a kanamycin resistance cassette and subsequently an mCherry expression cassette in the plasmid within the complementation locus flanking regions. The final result consisted in a pET15 plasmid encoding for kanamycin resistance and fluorescent protein mCherry expression cassette driven by a Mcat specific constitutive promoter (*OmpCD*). The construct was used to transform *Moraxella catarrhalis* AERIS 415. After transformation, bacteria were plated on chocolate agar plates supplemented with kanamycin; colonies that were observed to be pink were screened for mCherry cassette integration. Briefly, a PCR reaction with primers targeting the mCherry construct was carried out and the products were analyzed by gel electrophoresis (Fig. 36); all colonies tested showed expected bands in the expected bp range, confirming the integration of the construct into the Mcat 415 genome. Bacterial fluorescence was evaluated by confocal microscopy by comparing DAPI and mCherry fluorescent signal of bacteria in different growing conditions (Fig. 37). The entire bacteria population appeared to express the fluorescent protein in a variable manner: despite signal intensity was observed to be low after overnight agar growth, mid-log phase bacteria (0.5 OD_{600}) exhibited a more easily detectable fluorescence. Higher fluorescence was observed in bacteria grown at the Air-Liquid-Interface in the apical chamber of transwell inserts, suggesting that the intensity is related with the quantity of bacteria. With the aim of testing the fluorescence expression in more relevant conditions, we infected airway models with the transformed Mcat strain to

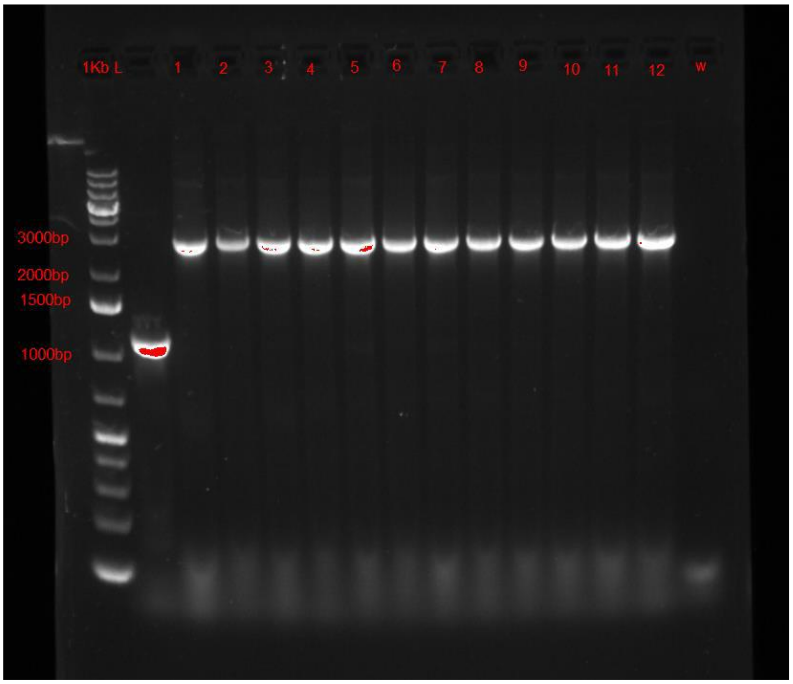

Figure 36 – Agarose gel electrophoresis of colony screening PCR products: successful integration of the final construct was observed for all the screened colonies.

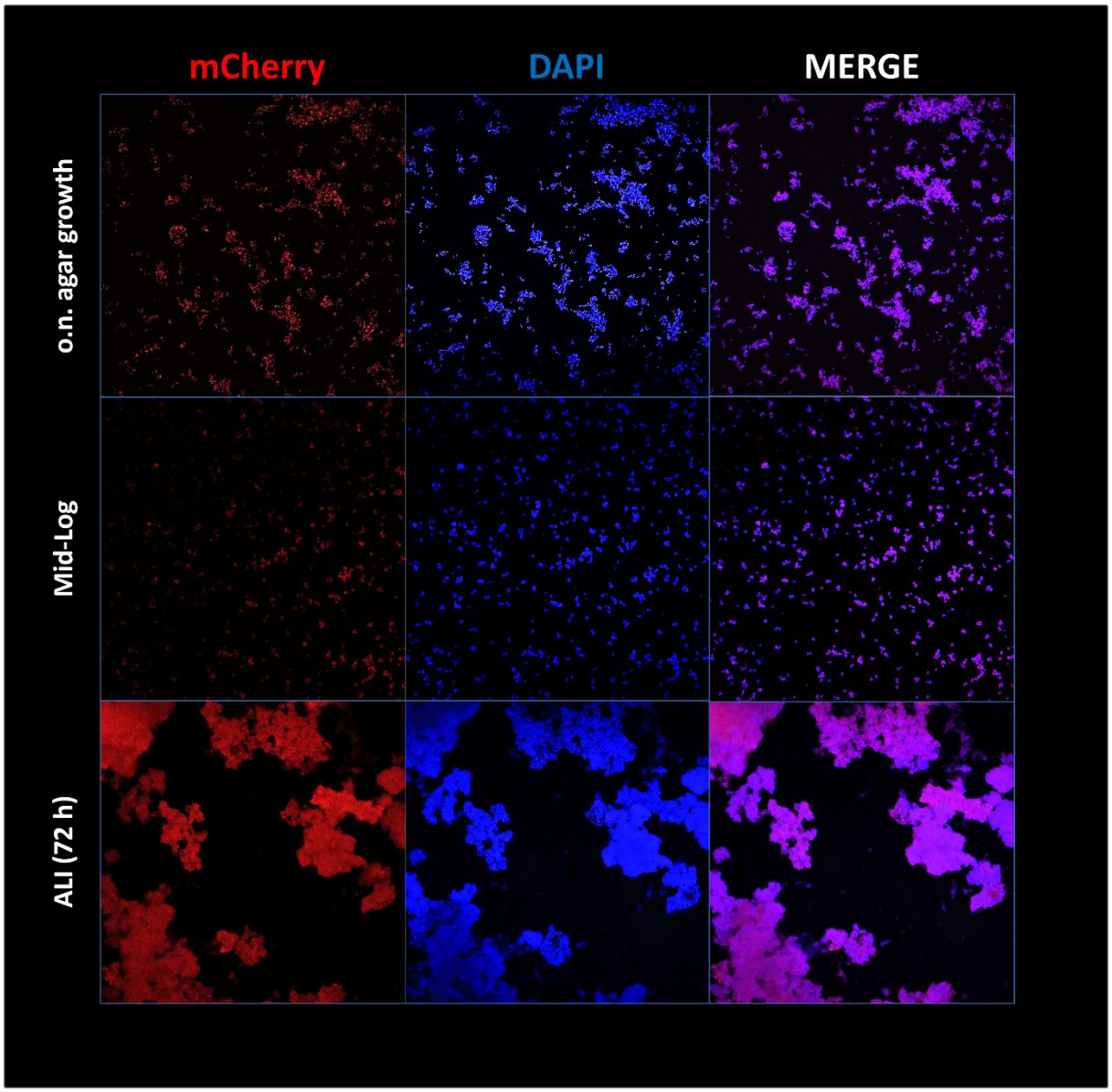

Figure 37 – Transformed Mcat strain fluorescence tests. The higher signal intensity was observed in bacteria grown at the air-liquid-interface.

perform a live imaging experiment. Endpoint imaging involves capturing images of fixed cells or tissues at a specific time point, providing only a snapshot of the host-pathogen interaction; on the other hand, live imaging (also known as time-lapse imaging) allows to capture images over time and directly observe dynamic processes. Briefly, MucilAir models purchased from Epithelix were infected with the fluorescent-strain and live monitored for 72 hours by using Opera Phenix Plus HCS System. Results showed how transformed Mcat did not uniformly express the mCherry protein, as Mcat colonies were distinguishable also with brightfield observation and the fluorescent signal did not completely overlap with growing bacteria, representing an obstacle for accurate fluorescence-based quantification (Fig. 38).

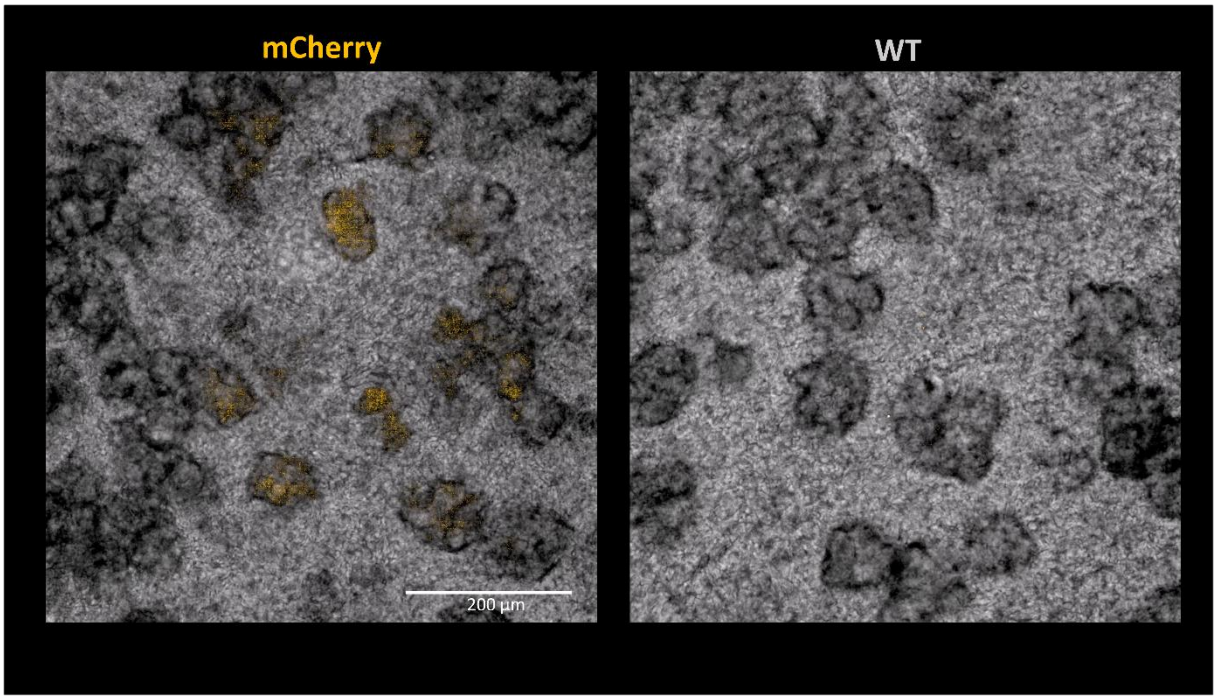

Figure 38 – mCherry fluorescent protein (highlighted in yellow) is not evenly expressed throughout the Moraxella catarrhalis population.

5.6 RT-qPCR for bacterial quantification in infected tissue models

It has been reported that *Moraxella catarrhalis* airway pathogenesis takes place through biofilm formation. Quantification of bacteria infecting *in vitro* tissues is required to evaluate the effect of antibodies or other treatments in counteracting the infection; however, Mcat biofilm-like phenotype represents an obstacle to traditional CFU counting methods (that work well when bacteria are in planktonic phase) as bacterial cells form aggregates that are difficult to disrupt leading to inconsistent data. For this reason, a RT-qPCR based method was explored to quantify bacteria on infected airway models. The approach aimed to quantify viable bacteria infecting the tissue samples by setting up a reference curve based on the amount of bacterial *16S rRNA*. The purpose of the experiments was to perform RT-qPCR targeting the *16s rRNA* gene on total RNA purified from tissue models that had been infected with defined amounts of bacteria, quantified in turn by 600-nm optical density readings and dilution plating. Two independent experiments were performed using different airway models obtained from different batches of differentiation. In each set of reactions, dissociation curves confirmed the absence of unspecific amplification products or primer-dimers. The obtained C_t values were plotted against the concentration of bacteria (expressed in CFU/ml) lysed and added to the airway models to simulate an infection. The 'power' regression model (non-linear) was adopted to fit the data and obtain the equation of a correlation curve, in order to calculate bacterial CFU through C_t interpolation. The first experiment (Fig. 39) showed a good correlation model ($R^2 = 0.97$), therefore the method was adopted to quantify bacteria in a pilot experiment; unfortunately, the bacterial concentration range used to build the reference curve was too low, as threshold values obtained from infected samples resulted below the lower C_t of the reference curve (data not shown). The experiment was repeated to obtain a reference curve with an extended range (Fig. 40). Also, in this case a correlation described by the power function was observed ($R^2 = 0.98$). However, a comparison with previous results showed a substantial difference in the obtained C_t values for each quantity of bacteria, beyond minor variations in the correspondence between defined optical densities and CFU values, likely due to Mcat aggregating phenotype. This difference could be explained by the diverse batch of models used for the experiments (MucilAir vs in-house developed SmallAir models), possibly affecting RNA purification procedure and yield. In conclusion, this method could be used for the established purpose only by associating each independent experiment with its own reference curve, allowing differences between the level of bacterial colonization of tissues to be revealed beyond absolute quantification. Methods that rely on absolute nucleic acid quantification (e.g., digital PCR) would overcome the problems associated with the data variation observed in this study.

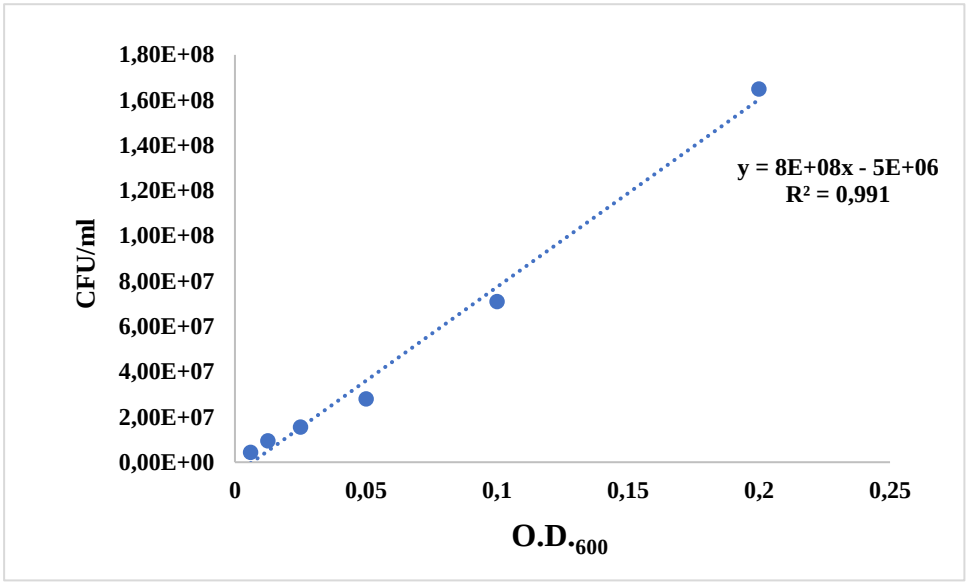

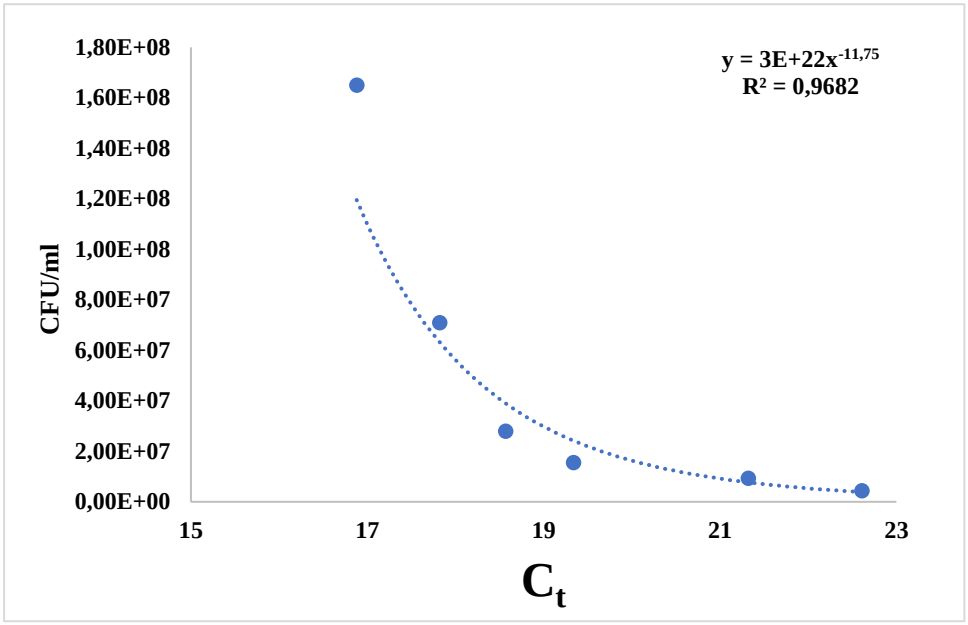

Ct	CFU/ml
16,88	1,65E+08
17,82	7,10E+07
18,57	2,80E+07
19,34	1,56E+07
21,32	9,40E+06
22,61	4,40E+06

Figure 39

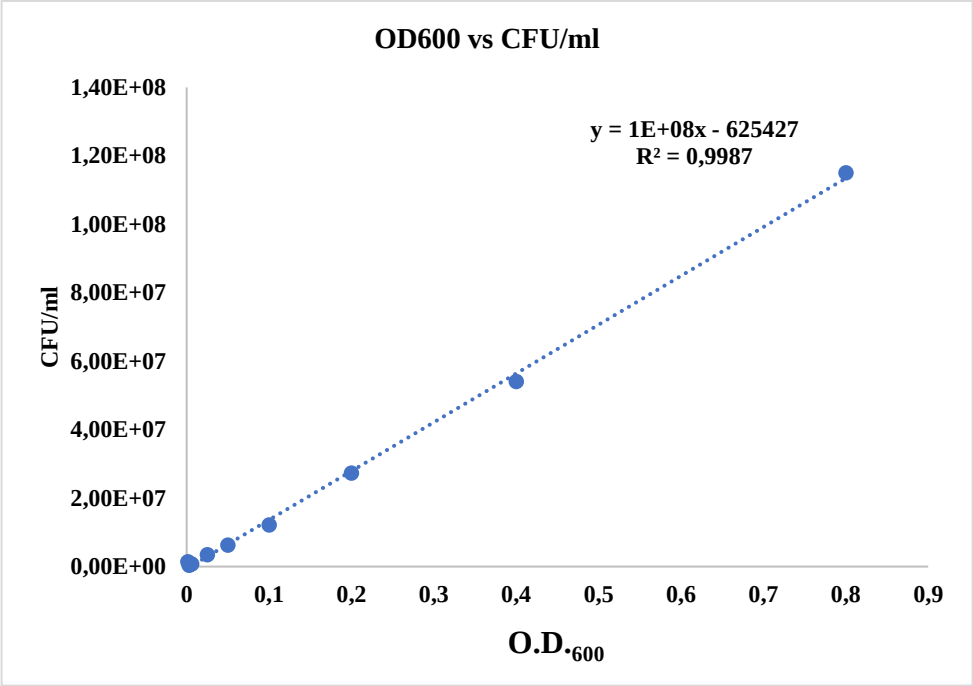

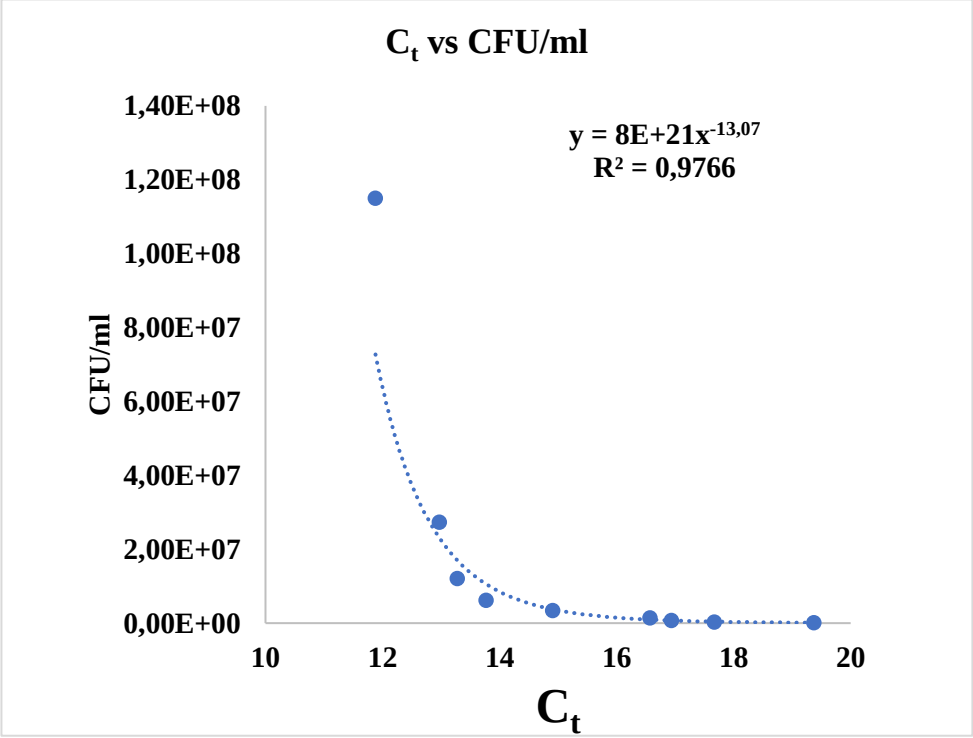

Ct	CFU/ml
11,88	1,15E+08
12,97	2,73E+07
13,28	1,21E+07
13,77	6,20E+06
14,91	3,40E+06
16,57	1,39E+06
16,94	7,10E+05
17,67	3,30E+05
19,37	1,42E+05

Figure 40

6. Conclusion and future perspectives

The present work aimed at implementing relevant cellular models for the characterization of respiratory tract bacterial infections caused by Nontypeable *Haemophilus influenzae* and *Moraxella catarrhalis*, bacteria frequently associated with AECOPD, Otitis Media and other diseases. Cellular models have been extensively used to study many biological processes including bacterial pathogenesis; however, differences between *in vitro* and *in vivo* conditions can affect the accuracy of the derived observations. In this context, advanced methods and technologies provide valuable alternatives to traditional *in vitro* systems. Organotypic airway tissue models grown at the Air-Liquid-Interface resemble multiple features of the human respiratory mucosa (presence of multiple cell types, mucus production, ciliary beating, regeneration capability) providing a physiological *in vivo*-like environment that is relevant for the investigation of host-pathogen interaction occurring at the human niche. However, despite traditional ALI models exhibit natural clearance mechanisms (such as the mucociliary escalator or the ability to extrude undesired cells) the culturing system spatial arrangement (e.g., Transwell) renders their occurrence non-functional. This aspect becomes of particular importance in the context of persistent infection modelling, as in general cellular *in vitro* systems do not tolerate bacterial presence for a prolonged period of time, representing an obstacle to mimicking pathogen adaptation to the host as well as long-term bacterial persistence strategies. Hence, we hypothesized that an alternative ALI culturing method, based on the inversion of the spatial arrangement of cells and medium in the Transwell system, could allow to facilitate tissue natural clearance mechanisms in response to bacterial infections. By monitoring infection time course in traditional and inverted ALI models, we showed that the spatial arrangement of traditional ALI systems hampers the natural clearance mechanisms exhibited by these pseudo-tissues, as proved by delayed onset of NTHi FI 76 or Mcat AERIS 415 infection in inverted models. Against this background, the functional integration of immune cells within our system represents the very next perspective to improve the relevance of this kind of models. The use of multiple microscopy-based approaches (LSCM, TEM, SEM) allowed us to deeply characterize the infection dynamics, visualizing the interactions between the pathogens and the airway epithelium. NTHi challenge appeared to trigger epithelial cell extrusion to a greater extent in respect to Mcat, suggesting that the latter could exploit inhibition of this mechanism to persist within epithelial cells. Our results demonstrate that Nontypeable *Haemophilus influenzae* and *Moraxella catarrhalis* can persist in the airways according to mechanisms involving the formation of biofilm-like communities residing within the epithelial tissue. In the case of Mcat, the strain tested was shown to form dense intraepithelial microbial

communities that resulted impermeant to labelling immunoglobulins, suggesting a role for this behavior in enhancing bacterial resistance to immune responses. Since both pathogens are able to adopt phase variation as well as other immune evasion mechanisms, further research would be required to deepen the molecular aspects of the microbial switch from planktonic to biofilm lifestyle, as differential antigen expression patterns could underlie this behavior. With the final scope of using the established infection models to evaluate the efficacy of specific treatments against pathogen infectivity, we explored alternative methods to quantify bacterial biomass associated with the respiratory models at different infection time points; traditional CFU counting methods were observed to produce inconsistent results if applied to biofilms, given the difficult disruption of the dense bacterial aggregates. Hence two strategies were adopted to provide more appropriate quantification methods. The first strategy was based on the generation of a fluorescence expressing Mcat strain in order to be quantified by LSCM and Image Analysis; this was done with the scope of overcoming the issues related to the biofilm impermeability to labelling antibodies. Moreover, it would have represented the possibility to perform live imaging experiments, taking a further step to the comprehensive understanding of the host-pathogen interplay. By using a transformation strategy based on PIPE method, we successfully complemented Mcat AERIS 415 with the mCherry fluorescent protein gene. Despite the strain exhibited a good fluorescence intensity in several growth conditions, it did not uniformly express the protein when interacting with the airway epithelium, rendering impractical an Image Analysis based quantification. The second strategy aimed to quantify viable bacteria infecting the tissue based on the amount of *16s rRNA* detected by RT-qPCR, according to the set-up of a reference curve to correlate bacterial concentrations and threshold cycle values obtained from the reactions. Results showed how although the relation between the two variables can be significantly described by mathematical functions, data variation among independent experiments represents an obstacle to repeatable results; for these reasons, an absolute nucleic acid quantification method such as digital PCR would be more attractive. In conclusion, this investigation provided valuable insights into persistent airway infections caused by Nontypeable *Haemophilus influenzae* and *Moraxella catarrhalis*. The use of relevant *in vitro* systems coupled to multiple imaging methods allowed for the first-time direct characterization of bacterial persistence mechanisms involving biofilm formation at the respiratory mucosal interface. Our findings could have implications for the development of effective therapies against bacterial infection-related airway chronic diseases.

7. Acknowledgements

I would like to express my sincere gratitude to my supervisors Alfredo Pezzicoli and Anna Rita Taddei, for their unwavering support, guidance, and encouragement throughout my PhD journey. Their expertise, patience, and willingness to share their knowledge have been instrumental in shaping my research and professional development. I am also extremely grateful to Martina Di Fede, who provided me with invaluable advice and assistance on a daily basis; her insights and critical feedbacks have been essential to the success of my research. I would like to acknowledge the contribution of my PhD colleague Martina Canè, who has been an excellent collaborator; her precious help inside and outside of the lab has been fundamental in accomplishing this work. Special thanks to Simona Tavarini, Giacomo Romagnoli, Kevin Pete Buno, Marco Spinsanti, and Giulia Realini for their technical assistance and dedication. Many thanks to Silvia Rossi Paccani for her encouraging feedbacks during my PhD. I would like to extend my sincere gratitude to Professors Simona Picchietti, Silvia Crognale and Francesco Buonocore, for providing me critical feedbacks allowing me to better shape my research. This research was funded by GlaxoSmithKline Biologicals SA, and I would like to express my gratitude for the financial support, which allowed me to pursue this research. I am grateful to all the staff at GSK and University of Tuscia for their support during my PhD program. Major thanks to Isabel Delany, always willing to listen and help me overcome the obstacles encountered during this journey; her encouragement was crucial to finalize this work. Finally, I would like to express my appreciation to Professor Antonio Tiezzi for his professional and personal mentoring, which has been with me since I started attending his laboratory four years ago; I have always viewed his approach in teaching and guiding students with deep appreciation and admiration.

8. References

Abell-King, C., Costas, A., Duggin, I. G., & Soderstrom, B. (2022). Bacterial filamentation during urinary tract infections. *PLoS Pathog*, *18*(12), e1010950. https://doi.org/10.1371/journal.ppat.1010950

Aebi, C., Lafontaine, E. R., Cope, L. D., Latimer, J. L., Lumbley, S. L., McCracken, G. H., Jr., & Hansen, E. J. (1998). Phenotypic effect of isogenic uspA1 and uspA2 mutations on Moraxella catarrhalis 035E. *Infect Immun*, *66*(7), 3113-3119. https://doi.org/10.1128/IAI.66.7.3113-3119.1998

Aghapour, M., Raee, P., Moghaddam, S. J., Hiemstra, P. S., & Heijink, I. H. (2018). Airway Epithelial Barrier Dysfunction in Chronic Obstructive Pulmonary Disease: Role of Cigarette Smoke Exposure. *Am J Respir Cell Mol Biol*, *58*(2), 157-169. https://doi.org/10.1165/rcmb.2017-0200TR

Aguilar, C., Alves da Silva, M., Saraiva, M., Neyazi, M., Olsson, I. A. S., & Bartfeld, S. (2021). Organoids as host models for infection biology - a review of methods. *Exp Mol Med*, *53*(10), 1471-1482. https://doi.org/10.1038/s12276-021-00629-4

Ahearn, C. P., Gallo, M. C., & Murphy, T. F. (2017). Insights on persistent airway infection by non-typeable Haemophilus influenzae in chronic obstructive pulmonary disease. *Pathog Dis*, *75*(4). https://doi.org/10.1093/femspd/ftx042

Ahearn, C. P., Kirkham, C., Chaves, L. D., Kong, Y., Pettigrew, M. M., & Murphy, T. F. (2019). Discovery and Contribution of Nontypeable Haemophilus influenzae NTHI1441 to Human Respiratory Epithelial Cell Invasion. *Infect Immun*, *87*(11). https://doi.org/10.1128/IAI.00462-19

Anderson, G. G., Martin, S. M., & Hultgren, S. J. (2004). Host subversion by formation of intracellular bacterial communities in the urinary tract. *Microbes and Infection*, *6*(12), 1094-1101. https://doi.org/https://doi.org/10.1016/j.micinf.2004.05.023

Aparicio-Yuste, R., Muenkel, M., Clark, A. G., Gómez-Benito, M. J., & Bastounis, E. E. (2022). A Stiff Extracellular Matrix Favors the Mechanical Cell Competition that Leads to Extrusion of Bacterially-Infected Epithelial Cells [Original Research]. *Frontiers in Cell and Developmental Biology*, *10*. https://doi.org/10.3389/fcell.2022.912318

Armbruster, C. E., Hong, W., Pang, B., Weimer, K. E., Juneau, R. A., Turner, J., & Swords, W. E. (2010). Indirect pathogenicity of Haemophilus influenzae and Moraxella catarrhalis in polymicrobial otitis media occurs via interspecies quorum signaling. *mBio*, *1*(3). https://doi.org/10.1128/mBio.00102-10

Artzy-Schnirman, A., Arber Raviv, S., Doppelt Flikshtain, O., Shklover, J., Korin, N., Gross, A., Mizrahi, B., Schroeder, A., & Sznitman, J. (2021). Advanced human-relevant in vitro pulmonary platforms for respiratory therapeutics. *Adv Drug Deliv Rev*, *176*, 113901. https://doi.org/10.1016/j.addr.2021.113901

Baddal, B., Muzzi, A., Censini, S., Calogero, R. A., Torricelli, G., Guidotti, S., Taddei, A. R., Covacci, A., Pizza, M., Rappuoli, R., Soriani, M., & Pezzicoli, A. (2015). Dual RNA-seq of Nontypeable Haemophilus influenzae and Host Cell Transcriptomes Reveals Novel Insights into Host-Pathogen Cross Talk. *mBio*, *6*(6), e01765-01715. https://doi.org/10.1128/mBio.01765-15

Bakaletz, L. O., & Novotny, L. A. (2018). Nontypeable Haemophilus influenzae (NTHi). *Trends Microbiol*, *26*(8), 727-728. https://doi.org/10.1016/j.tim.2018.05.001

Balder, R., Hassel, J., Lipski, S., & Lafontaine, E. R. (2007). Moraxella catarrhalis strain O35E expresses two filamentous hemagglutinin-like proteins that mediate adherence to human epithelial cells. *Infect Immun*, *75*(6), 2765-2775. https://doi.org/10.1128/IAI.00079-07

Balder, R., Krunkosky, T. M., Nguyen, C. Q., Feezel, L., & Lafontaine, E. R. (2009). Hag mediates adherence of Moraxella catarrhalis to ciliated human airway cells. *Infect Immun*, *77*(10), 4597-4608. https://doi.org/10.1128/iai.00212-09

Ball, M., Hossain, M., & Padalia, D. (2022). Anatomy, Airway. In *StatPearls*. https://www.ncbi.nlm.nih.gov/pubmed/29083624

Bandi, V., APICELLA, M. A., MASON, E., MURPHY, T. F., SIDDIQI, A., ATMAR, R. L., & GREENBERG, S. B. (2001). Nontypeable Haemophilus influenzae in the Lower Respiratory Tract of Patients with Chronic Bronchitis. *American Journal of Respiratory and Critical Care Medicine*, *164*(11), 2114-2119. https://doi.org/10.1164/ajrccm.164.11.2104093

Barnes, P. J., Bonini, S., Seeger, W., Belvisi, M. G., Ward, B., & Holmes, A. (2015). Barriers to new drug development in respiratory disease. *Eur Respir J*, *45*(5), 1197-1207. https://doi.org/10.1183/09031936.00007915

Barrila, J., Crabbe, A., Yang, J., Franco, K., Nydam, S. D., Forsyth, R. J., Davis, R. R., Gangaraju, S., Ott, C. M., Coyne, C. B., Bissell, M. J., & Nickerson, C. A. (2018). Modeling Host-Pathogen Interactions in the Context of the Microenvironment: Three-Dimensional Cell Culture Comes of Age. *Infect Immun*, *86*(11). https://doi.org/10.1128/IAI.00282-18

Barron, S. L., Saez, J., & Owens, R. M. (2021). In Vitro Models for Studying Respiratory Host–Pathogen Interactions. *Advanced Biology*, *5*(6), 2000624. https://doi.org/https://doi.org/10.1002/adbi.202000624

Bastounis, E. E., Serrano-Alcalde, F., Radhakrishnan, P., Engström, P., Gómez-Benito, M. J., Oswald, M. S., Yeh, Y.-T., Smith, J. G., Welch, M. D., García-Aznar, J. M., & Theriot, J. A. (2021). Mechanical competition triggered by innate immune signaling drives the collective extrusion of bacterially infected epithelial cells. *Developmental Cell*, *56*(4), 443-460.e411. https://doi.org/https://doi.org/10.1016/j.devcel.2021.01.012

Benam, K. H., Villenave, R., Lucchesi, C., Varone, A., Hubeau, C., Lee, H.-H., Alves, S. E., Salmon, M., Ferrante, T. C., Weaver, J. C., Bahinski, A., Hamilton, G. A., & Ingber, D. E. (2016). Small airway-on-a-chip enables analysis of human lung inflammation and drug responses in vitro. *Nature Methods*, *13*(2), 151-157. https://doi.org/10.1038/nmeth.3697

Berube, K., Prytherch, Z., Job, C., & Hughes, T. (2010). Human primary bronchial lung cell constructs: the new respiratory models. *Toxicology*, *278*(3), 311-318. https://doi.org/10.1016/j.tox.2010.04.004

Bjarnsholt, T. (2013). The role of bacterial biofilms in chronic infections. *APMIS Suppl*(136), 1-51. https://doi.org/10.1111/apm.12099

Blakeway, L. V., Tan, A., Peak, I. R., Atack, J. M., & Seib, K. L. (2020). Proteome of a Moraxella catarrhalis Strain under Iron-Restricted Conditions. *Microbiol Resour Announc*, *9*(12). https://doi.org/10.1128/mra.00064-20

Blakeway, L. V., Tan, A., Peak, I. R. A., & Seib, K. L. (2017). Virulence determinants of Moraxella catarrhalis: distribution and considerations for vaccine development. *Microbiology (Reading)*, *163*(10), 1371-1384. https://doi.org/10.1099/mic.0.000523

Blume, C., Reale, R., Held, M., Millar, T. M., Collins, J. E., Davies, D. E., Morgan, H., & Swindle, E. J. (2015). Temporal Monitoring of Differentiated Human Airway Epithelial Cells Using Microfluidics. *PLoS One*, *10*(10), e0139872. https://doi.org/10.1371/journal.pone.0139872

Boers, J. E., Ambergen, A. W., & Thunnissen, F. B. (1998). Number and proliferation of basal and parabasal cells in normal human airway epithelium. *Am J Respir Crit Care Med*, *157*(6 Pt 1), 2000-2006. https://doi.org/10.1164/ajrccm.157.6.9707011

Bouquet, J., Tabor, D. E., Silver, J. S., Nair, V., Tovchigrechko, A., Griffin, M. P., Esser, M. T., Sellman, B. R., & Jin, H. (2020). Microbial burden and viral exacerbations in a

longitudinal multicenter COPD cohort. *Respir Res*, *21*(1), 77. https://doi.org/10.1186/s12931-020-01340-0

Brooks, M. J., Sedillo, J. L., Wagner, N., Wang, W., Attia, A. S., Wong, H., Laurence, C. A., Hansen, E. J., & Gray-Owen, S. D. (2008). Moraxella catarrhalis binding to host cellular receptors is mediated by sequence-specific determinants not conserved among all UspA1 protein variants. *Infect Immun*, *76*(11), 5322-5329. https://doi.org/10.1128/IAI.00572-08

Broz, P., & Dixit, V. M. (2016). Inflammasomes: mechanism of assembly, regulation and signalling. *Nature Reviews Immunology*, *16*(7), 407-420. https://doi.org/10.1038/nri.2016.58

Bustamante-Marin, X. M., & Ostrowski, L. E. (2017). Cilia and Mucociliary Clearance. *Cold Spring Harb Perspect Biol*, *9*(4). https://doi.org/10.1101/cshperspect.a028241

Cao, X., Coyle, J. P., Xiong, R., Wang, Y., Heflich, R. H., Ren, B., Gwinn, W. M., Hayden, P., & Rojanasakul, L. (2021). Invited review: human air-liquid-interface organotypic airway tissue models derived from primary tracheobronchial epithelial cells-overview and perspectives. *In Vitro Cell Dev Biol Anim*, *57*(2), 104-132. https://doi.org/10.1007/s11626-020-00517-7

Cerutti, A., Chen, K., & Chorny, A. (2011). Immunoglobulin responses at the mucosal interface. *Annu Rev Immunol*, *29*, 273-293. https://doi.org/10.1146/annurev-immunol-031210-101317

Chakraborty, A., Mastalerz, M., Hatz, R., Behr, J., Lindner, M., Hilgendorff, A., & Staab-Weijnitz, C. (2021). Establishment of a human in vitro model for airway epithelial repair and regeneration. *European Respiratory Journal*, *58*(suppl 65), PA2039. https://doi.org/10.1183/13993003.congress-2021.PA2039

Chong, L. H., Li, H., Wetzel, I., Cho, H., & Toh, Y. C. (2018). A liver-immune coculture array for predicting systemic drug-induced skin sensitization. *Lab Chip*, *18*(21), 3239-3250. https://doi.org/10.1039/c8lc00790j

Churchill, M. J., Mitchell, P. S., & Rauch, I. (2022). Epithelial Pyroptosis in Host Defense. *J Mol Biol*, *434*(4), 167278. https://doi.org/10.1016/j.jmb.2021.167278

Clementi, C. F., Håkansson, A. P., & Murphy, T. F. (2014). Internalization and trafficking of nontypeable Haemophilus influenzae in human respiratory epithelial cells and roles of IgA1 proteases for optimal invasion and persistence. *Infect Immun*, *82*(1), 433-444. https://doi.org/10.1128/iai.00864-13

Co, J. Y., Margalef-Catala, M., Monack, D. M., & Amieva, M. R. (2021). Controlling the polarity of human gastrointestinal organoids to investigate epithelial biology and infectious diseases. *Nat Protoc*, *16*(11), 5171-5192. https://doi.org/10.1038/s41596-021-00607-0

Crystal, R. G., Randell, S. H., Engelhardt, J. F., Voynow, J., & Sunday, M. E. (2008). Airway epithelial cells: current concepts and challenges. *Proc Am Thorac Soc*, *5*(7), 772-777. https://doi.org/10.1513/pats.200805-041HR

Davis, J. D., & Wypych, T. P. (2021). Cellular and functional heterogeneity of the airway epithelium. *Mucosal Immunol*, *14*(5), 978-990. https://doi.org/10.1038/s41385-020-00370-7

de Vries, S. P., Eleveld, M. J., Hermans, P. W., & Bootsma, H. J. (2013). Characterization of the molecular interplay between Moraxella catarrhalis and human respiratory tract epithelial cells. *PLoS One*, *8*(8), e72193. https://doi.org/10.1371/journal.pone.0072193

Decramer, M., Janssens, W., & Miravitlles, M. (2012). Chronic obstructive pulmonary disease. *Lancet*, *379*(9823), 1341-1351. https://doi.org/10.1016/s0140-6736(11)60968-9

Dy, R., & Sethi, S. (2016). The lung microbiome and exacerbations of COPD. *Curr Opin Pulm Med*, *22*(3), 196-202. https://doi.org/10.1097/MCP.0000000000000268

Eisenhoffer, G. T., Loftus, P. D., Yoshigi, M., Otsuna, H., Chien, C.-B., Morcos, P. A., & Rosenblatt, J. (2012). Crowding induces live cell extrusion to maintain homeostatic cell numbers in epithelia. *Nature*, *484*(7395), 546-549. https://doi.org/10.1038/nature10999

Esch, E. W., Bahinski, A., & Huh, D. (2015). Organs-on-chips at the frontiers of drug discovery. *Nat Rev Drug Discov*, *14*(4), 248-260. https://doi.org/10.1038/nrd4539

Fleiszig, S. M., Zaidi, T. S., Preston, M. J., Grout, M., Evans, D. J., & Pier, G. B. (1996). Relationship between cytotoxicity and corneal epithelial cell invasion by clinical isolates of Pseudomonas aeruginosa. *Infection and Immunity*, *64*(6), 2288-2294. https://doi.org/doi:10.1128/iai.64.6.2288-2294.1996

Flemming, H.-C., & Wingender, J. (2010). The biofilm matrix. *Nature Reviews Microbiology*, *8*(9), 623-633. https://doi.org/10.1038/nrmicro2415

Galluzzi, L., Vitale, I., Aaronson, S. A., Abrams, J. M., Adam, D., Agostinis, P., Alnemri, E. S., Altucci, L., Amelio, I., Andrews, D. W., Annicchiarico-Petruzzelli, M., Antonov, A. V., Arama, E., Baehrecke, E. H., Barlev, N. A., Bazan, N. G., Bernassola, F., Bertrand, M. J. M., Bianchi, K., . . . Kroemer, G. (2018). Molecular mechanisms of cell death: recommendations of the Nomenclature Committee on Cell Death 2018. *Cell Death & Differentiation*, *25*(3), 486-541. https://doi.org/10.1038/s41418-017-0012-4

Ganesan, S., Comstock, A. T., & Sajjan, U. S. (2013). Barrier function of airway tract epithelium. *Tissue Barriers*, *1*(4), e24997. https://doi.org/10.4161/tisb.24997

Garcia-Medina, R., Dunne, W. M., Singh, P. K., & Brody, S. L. (2005). Pseudomonas aeruginosa Acquires Biofilm-Like Properties within Airway Epithelial Cells. *Infection and Immunity*, *73*(12), 8298-8305. https://doi.org/doi:10.1128/IAI.73.12.8298-8305.2005

Gard, A. L., Luu, R. J., Miller, C. R., Maloney, R., Cain, B. P., Marr, E. E., Burns, D. M., Gaibler, R., Mulhern, T. J., Wong, C. A., Alladina, J., Coppeta, J. R., Liu, P., Wang, J. P., Azizgolshani, H., Fezzie, R. F., Balestrini, J. L., Isenberg, B. C., Medoff, B. D., . . . Borenstein, J. T. (2021). High-throughput human primary cell-based airway model for evaluating influenza, coronavirus, or other respiratory viruses in vitro. *Sci Rep*, *11*(1), 14961. https://doi.org/10.1038/s41598-021-94095-7

Gohy, S., Hupin, C., Ladjemi, M. Z., Hox, V., & Pilette, C. (2020). Key role of the epithelium in chronic upper airways diseases. *Clin Exp Allergy*, *50*(2), 135-146. https://doi.org/10.1111/cea.13539

Goyal, M., Singh, M., Ray, P., Srinivasan, R., & Chakraborti, A. (2015). Cellular interaction of nontypeable Haemophilus influenzae triggers cytotoxicity of infected type II alveolar cells via apoptosis. *Pathogens and Disease*, *73*(2), 1-12. https://doi.org/10.1111/2049-632x.12215

Gudipaty, S. A., & Rosenblatt, J. (2017). Epithelial cell extrusion: Pathways and pathologies. *Semin Cell Dev Biol*, *67*, 132-140. https://doi.org/10.1016/j.semcdb.2016.05.010

Guenat, O. T., & Berthiaume, F. (2018). Incorporating mechanical strain in organs-on-a-chip: Lung and skin. *Biomicrofluidics*, *12*(4), 042207. https://doi.org/10.1063/1.5024895

Hall-Stoodley, L., Hu, F. Z., Gieseke, A., Nistico, L., Nguyen, D., Hayes, J., Forbes, M., Greenberg, D. P., Dice, B., Burrows, A., Wackym, P. A., Stoodley, P., Post, J. C., Ehrlich, G. D., & Kerschner, J. E. (2006). Direct detection of bacterial biofilms on the middle-ear mucosa of children with chronic otitis media. *JAMA*, *296*(2), 202-211. https://doi.org/10.1001/jama.296.2.202

Hammerschmidt, S., Wolff, S., Hocke, A., Rosseau, S., Müller, E., & Rohde, M. (2005). Illustration of Pneumococcal Polysaccharide Capsule during Adherence and Invasion of Epithelial Cells. *Infection and Immunity*, *73*(8), 4653-4667. https://doi.org/doi:10.1128/IAI.73.8.4653-4667.2005

Hartl, D., Tirouvanziam, R., Laval, J., Greene, C. M., Habiel, D., Sharma, L., Yildirim, A. O., Dela Cruz, C. S., & Hogaboam, C. M. (2018). Innate Immunity of the Lung: From Basic Mechanisms to Translational Medicine. *J Innate Immun*, *10*(5-6), 487-501. https://doi.org/10.1159/000487057

Hasan, S., Sebo, P., & Osicka, R. (2018). A guide to polarized airway epithelial models for studies of host–pathogen interactions. *The FEBS Journal*, *285*(23), 4343-4358. https://doi.org/https://doi.org/10.1111/febs.14582

Hegde, M., Jindal, R., Bhushan, A., Bale, S. S., McCarty, W. J., Golberg, I., Usta, O. B., & Yarmush, M. L. (2014). Dynamic interplay of flow and collagen stabilizes primary hepatocytes culture in a microfluidic platform. *Lab Chip*, *14*(12), 2033-2039. https://doi.org/10.1039/c4lc00071d

Hill, D. J., & Virji, M. (2003). A novel cell-binding mechanism of Moraxella catarrhalis ubiquitous surface protein UspA: specific targeting of the N-domain of carcinoembryonic antigen-related cell adhesion molecules by UspA1. *Mol Microbiol*, *48*(1), 117-129. https://doi.org/10.1046/j.1365-2958.2003.03433.x

Ho, C. T., Lin, R. Z., Chen, R. J., Chin, C. K., Gong, S. E., Chang, H. Y., Peng, H. L., Hsu, L., Yew, T. R., Chang, S. F., & Liu, C. H. (2013). Liver-cell patterning lab chip: mimicking the morphology of liver lobule tissue. *Lab Chip*, *13*(18), 3578-3587. https://doi.org/10.1039/c3lc50402f

Hoiby, N., Bjarnsholt, T., Moser, C., Bassi, G. L., Coenye, T., Donelli, G., Hall-Stoodley, L., Hola, V., Imbert, C., Kirketerp-Moller, K., Lebeaux, D., Oliver, A., Ullmann, A. J., Williams, C., Biofilms, E. S. G. f., & Consulting External Expert Werner, Z. (2015). ESCMID guideline for the diagnosis and treatment of biofilm infections 2014. *Clin Microbiol Infect*, *21 Suppl 1*, S1-25. https://doi.org/10.1016/j.cmi.2014.10.024

Holm, M. M., Vanlerberg, S. L., Foley, I. M., Sledjeski, D. D., & Lafontaine, E. R. (2004). The Moraxella catarrhalis porin-like outer membrane protein CD is an adhesin for human lung cells. *Infect Immun*, *72*(4), 1906-1913. https://doi.org/10.1128/iai.72.4.1906-1913.2004

Holm, M. M., Vanlerberg, S. L., Sledjeski, D. D., & Lafontaine, E. R. (2003). The Hag protein of Moraxella catarrhalis strain O35E is associated with adherence to human lung and middle ear cells. *Infect Immun*, *71*(9), 4977-4984. https://doi.org/10.1128/iai.71.9.4977-4984.2003

Holt, P. G., Strickland, D. H., Wikström, M. E., & Jahnsen, F. L. (2008). Regulation of immunological homeostasis in the respiratory tract. *Nat Rev Immunol*, *8*(2), 142-152. https://doi.org/10.1038/nri2236

Hotomi, M., Arai, J., Billal, D. S., Takei, S., Ikeda, Y., Ogami, M., Kono, M., Beder, L. B., Toya, K., Kimura, M., & Yamanaka, N. (2010). Nontypeable Haemophilus influenzae isolated from intractable acute otitis media internalized into cultured human epithelial cells. *Auris Nasus Larynx*, *37*(2), 137-144. https://doi.org/10.1016/j.anl.2009.03.012

Huang, Y. J., Erb-Downward, J. R., Dickson, R. P., Curtis, J. L., Huffnagle, G. B., & Han, M. K. (2017). Understanding the role of the microbiome in chronic obstructive pulmonary disease: principles, challenges, and future directions. *Transl Res*, *179*, 71-83. https://doi.org/10.1016/j.trsl.2016.06.007

Hubrecht, R. C., & Carter, E. (2019). The 3Rs and Humane Experimental Technique: Implementing Change. *Animals (Basel)*, *9*(10). https://doi.org/10.3390/ani9100754

Huh, D., Leslie, D. C., Matthews, B. D., Fraser, J. P., Jurek, S., Hamilton, G. A., Thorneloe, K. S., McAlexander, M. A., & Ingber, D. E. (2012). A human disease model of drug toxicity-induced pulmonary edema in a lung-on-a-chip microdevice. *Sci Transl Med*, *4*(159), 159ra147. https://doi.org/10.1126/scitranslmed.3004249

Huh, D., Matthews, B. D., Mammoto, A., Montoya-Zavala, M., Hsin, H. Y., & Ingber, D. E. (2010). Reconstituting organ-level lung functions on a chip. *Science*, *328*(5986), 1662-1668. https://doi.org/10.1126/science.1188302

Humayun, M., Chow, C. W., & Young, E. W. K. (2018). Microfluidic lung airway-on-a-chip with arrayable suspended gels for studying epithelial and smooth muscle cell interactions. *Lab Chip*, *18*(9), 1298-1309. https://doi.org/10.1039/c7lc01357d

Imura, Y., Asano, Y., Sato, K., & Yoshimura, E. (2009). A Microfluidic System to Evaluate Intestinal Absorption. *Analytical Sciences*, *25*(12), 1403-1407. https://doi.org/10.2116/analsci.25.1403

Jalili-Firoozinezhad, S., Gazzaniga, F. S., Calamari, E. L., Camacho, D. M., Fadel, C. W., Bein, A., Swenor, B., Nestor, B., Cronce, M. J., Tovaglieri, A., Levy, O., Gregory, K. E., Breault, D. T., Cabral, J. M. S., Kasper, D. L., Novak, R., & Ingber, D. E. (2019). A complex human gut microbiome cultured in an anaerobic intestine-on-a-chip. *Nat Biomed Eng*, *3*(7), 520-531. https://doi.org/10.1038/s41551-019-0397-0

Jang, K. J., Mehr, A. P., Hamilton, G. A., McPartlin, L. A., Chung, S., Suh, K. Y., & Ingber, D. E. (2013). Human kidney proximal tubule-on-a-chip for drug transport and nephrotoxicity assessment. *Integr Biol (Camb)*, *5*(9), 1119-1129. https://doi.org/10.1039/c3ib40049b

Jang, K. J., & Suh, K. Y. (2010). A multi-layer microfluidic device for efficient culture and analysis of renal tubular cells. *Lab Chip*, *10*(1), 36-42. https://doi.org/10.1039/b907515a

Jorgensen, I., Rayamajhi, M., & Miao, E. A. (2017). Programmed cell death as a defence against infection. *Nature Reviews Immunology*, *17*(3), 151-164. https://doi.org/10.1038/nri.2016.147

Justice, S. S., Hung, C., Theriot, J. A., Fletcher, D. A., Anderson, G. G., Footer, M. J., & Hultgren, S. J. (2004). Differentiation and developmental pathways of uropathogenic Escherichia coli in urinary tract pathogenesis. *Proceedings of the National Academy of Sciences*, *101*(5), 1333-1338. https://doi.org/doi:10.1073/pnas.0308125100

Kang, Y. B., Sodunke, T. R., Lamontagne, J., Cirillo, J., Rajiv, C., Bouchard, M. J., & Noh, M. (2015). Liver sinusoid on a chip: Long-term layered co-culture of primary rat hepatocytes and endothelial cells in microfluidic platforms. *Biotechnol Bioeng*, *112*(12), 2571-2582. https://doi.org/10.1002/bit.25659

Kasendra, M., Tovaglieri, A., Sontheimer-Phelps, A., Jalili-Firoozinezhad, S., Bein, A., Chalkiadaki, A., Scholl, W., Zhang, C., Rickner, H., Richmond, C. A., Li, H., Breault, D. T., & Ingber, D. E. (2018). Development of a primary human Small Intestine-on-a-Chip using biopsy-derived organoids. *Scientific Reports*, *8*(1), 2871. https://doi.org/10.1038/s41598-018-21201-7

Kaufhold, I., Osbahr, S., Shima, K., Marwitz, S., Rohmann, K., Dromann, D., Goldmann, T., Dalhoff, K., & Rupp, J. (2017). Nontypeable Haemophilus influenzae (NTHi) directly interfere with the regulation of E-cadherin in lung epithelial cells. *Microbes Infect*, *19*(11), 560-566. https://doi.org/10.1016/j.micinf.2017.07.002

Ketterer, M. R., Shao, J. Q., Hornick, D. B., Buscher, B., Bandi, V. K., & Apicella, M. A. (1999). Infection of primary human bronchial epithelial cells by Haemophilus influenzae: macropinocytosis as a mechanism of airway epithelial cell entry. *Infect Immun*, *67*(8), 4161-4170. https://doi.org/10.1128/IAI.67.8.4161-4170.1999

Kia'i, N., & Bajaj, T. (2022). Histology, Respiratory Epithelium. In *StatPearls*. https://www.ncbi.nlm.nih.gov/pubmed/31082105

Kim, H. J., Huh, D., Hamilton, G., & Ingber, D. E. (2012). Human gut-on-a-chip inhabited by microbial flora that experiences intestinal peristalsis-like motions and flow [10.1039/C2LC40074J]. *Lab on a Chip*, *12*(12), 2165-2174. https://doi.org/10.1039/C2LC40074J

Kim, J., Koo, B.-K., & Knoblich, J. A. (2020). Human organoids: model systems for human biology and medicine. *Nature Reviews Molecular Cell Biology*, *21*(10), 571-584. https://doi.org/10.1038/s41580-020-0259-3

Kim, M., Ashida, H., Ogawa, M., Yoshikawa, Y., Mimuro, H., & Sasakawa, C. (2010). Bacterial Interactions with the Host Epithelium. *Cell Host & Microbe*, *8*(1), 20-35. https://doi.org/https://doi.org/10.1016/j.chom.2010.06.006

Klock, H. E., & Lesley, S. A. (2009). The Polymerase Incomplete Primer Extension (PIPE) method applied to high-throughput cloning and site-directed mutagenesis. *Methods Mol Biol*, *498*, 91-103. https://doi.org/10.1007/978-1-59745-196-3_6

Knodler, L. A., Vallance, B. A., Celli, J., Winfree, S., Hansen, B., Montero, M., & Steele-Mortimer, O. (2010). Dissemination of invasive Salmonella via bacterial-induced extrusion of mucosal epithelia. *Proceedings of the National Academy of Sciences*, *107*(41), 17733-17738. https://doi.org/doi:10.1073/pnas.1006098107

Ko, J., Park, D., Lee, S., Gumuscu, B., & Jeon, N. L. (2022). Engineering Organ-on-a-Chip to Accelerate Translational Research. *Micromachines (Basel)*, *13*(8). https://doi.org/10.3390/mi13081200

Kolpen, M., Kragh, K. N., Enciso, J. B., Faurholt-Jepsen, D., Lindegaard, B., Egelund, G. B., Jensen, A. V., Ravn, P., Mathiesen, I. H. M., Gheorge, A. G., Hertz, F. B., Qvist, T., Whiteley, M., Jensen, P., & Bjarnsholt, T. (2022). Bacterial biofilms predominate in both acute and chronic human lung infections. *Thorax*, *77*(10), 1015-1022. https://doi.org/10.1136/thoraxjnl-2021-217576

Koval, M. (2017). Junctional interplay in lung epithelial barrier function. In *Lung Epithelial Biology in the Pathogenesis of Pulmonary Disease* (pp. 1-20). Elsevier.

Lacroix, G., Koch, W., Ritter, D., Gutleb, A. C., Larsen, S. T., Loret, T., Zanetti, F., Constant, S., Chortarea, S., Rothen-Rutishauser, B., Hiemstra, P. S., Frejafon, E., Hubert, P., Gribaldo, L., Kearns, P., Aublant, J. M., Diabate, S., Weiss, C., de Groot, A., & Kooter, I. (2018). Air-Liquid Interface In Vitro Models for Respiratory Toxicology Research: Consensus Workshop and Recommendations. *Appl In Vitro Toxicol*, *4*(2), 91-106. https://doi.org/10.1089/aivt.2017.0034

Lafontaine, E. R., Cope, L. D., Aebi, C., Latimer, J. L., McCracken, G. H., Jr., & Hansen, E. J. (2000). The UspA1 protein and a second type of UspA2 protein mediate adherence of Moraxella catarrhalis to human epithelial cells in vitro. *J Bacteriol*, *182*(5), 1364-1373. https://doi.org/10.1128/JB.182.5.1364-1373.2000

Lawrence, A.-L. E., Berger, R. P., Hill, D. R., Huang, S., Yadagiri, V. K., Bons, B., Fields, C., Sule, G. J., Knight, J. S., Wobus, C. E., Spence, J. R., Young, V. B., O'Riordan, M. X., & Abuaita, B. H. (2022). Human neutrophil IL1β directs intestinal epithelial cell extrusion during Salmonella infection. *PLOS Pathogens*, *18*(10), e1010855. https://doi.org/10.1371/journal.ppat.1010855

Lechner, J. F., Haugen, A., Autrup, H., McClendon, I. A., Trump, B. F., & Harris, C. C. (1981). Clonal growth of epithelial cells from normal adult human bronchus. *Cancer Res*, *41*(6), 2294-2304.

Lee, H., Kim, D. S., Ha, S. K., Choi, I., Lee, J. M., & Sung, J. H. (2017). A pumpless multi-organ-on-a-chip (MOC) combined with a pharmacokinetic–pharmacodynamic (PK–PD) model. *Biotechnology and Bioengineering*, *114*(2), 432-443. https://doi.org/https://doi.org/10.1002/bit.26087

Lee, P. J., Hung, P. J., & Lee, L. P. (2007). An artificial liver sinusoid with a microfluidic endothelial-like barrier for primary hepatocyte culture. *Biotechnol Bioeng*, *97*(5), 1340-1346. https://doi.org/10.1002/bit.21360

Leiva-Juárez, M. M., Kolls, J. K., & Evans, S. E. (2018). Lung epithelial cells: therapeutically inducible effectors of antimicrobial defense. *Mucosal Immunol*, *11*(1), 21-34. https://doi.org/10.1038/mi.2017.71

Leung, C. M., de Haan, P., Ronaldson-Bouchard, K., Kim, G.-A., Ko, J., Rho, H. S., Chen, Z., Habibovic, P., Jeon, N. L., Takayama, S., Shuler, M. L., Vunjak-Novakovic, G., Frey, O., Verpoorte, E., & Toh, Y.-C. (2022). A guide to the organ-on-a-chip. *Nature Reviews Methods Primers*, *2*(1), 33. https://doi.org/10.1038/s43586-022-00118-6

Liesman, R. M., Buchholz, U. J., Luongo, C. L., Yang, L., Proia, A. D., DeVincenzo, J. P., Collins, P. L., & Pickles, R. J. (2014). RSV-encoded NS2 promotes epithelial cell shedding and distal airway obstruction. *J Clin Invest*, *124*(5), 2219-2233. https://doi.org/10.1172/JCI72948

Lu, S., Cuzzucoli, F., Jiang, J., Liang, L. G., Wang, Y., Kong, M., Zhao, X., Cui, W., Li, J., & Wang, S. (2018). Development of a biomimetic liver tumor-on-a-chip model based on decellularized liver matrix for toxicity testing. *Lab Chip*, *18*(22), 3379-3392. https://doi.org/10.1039/c8lc00852c

Ma, L. D., Wang, Y. T., Wang, J. R., Wu, J. L., Meng, X. S., Hu, P., Mu, X., Liang, Q. L., & Luo, G. A. (2018). Design and fabrication of a liver-on-a-chip platform for convenient, highly efficient, and safe in situ perfusion culture of 3D hepatic spheroids. *Lab Chip*, *18*(17), 2547-2562. https://doi.org/10.1039/c8lc00333e

Malvisi, L., Taddei, L., Yarraguntla, A., Wilkinson, T. M. A., Arora, A. K., & Group, A. S. (2021). Sputum sample positivity for Haemophilus influenzae or Moraxella catarrhalis in acute exacerbations of chronic obstructive pulmonary disease: evaluation of association with positivity at earlier stable disease timepoints. *Respir Res*, *22*(1), 67. https://doi.org/10.1186/s12931-021-01653-8

Marrazzo, P., Maccari, S., Taddei, A., Bevan, L., Telford, J., Soriani, M., & Pezzicoli, A. (2016). 3D Reconstruction of the Human Airway Mucosa In Vitro as an Experimental Model to Study NTHi Infections. *PLoS One*, *11*(4), e0153985. https://doi.org/10.1371/journal.pone.0153985

Marsano, A., Conficconi, C., Lemme, M., Occhetta, P., Gaudiello, E., Votta, E., Cerino, G., Redaelli, A., & Rasponi, M. (2016). Beating heart on a chip: a novel microfluidic platform to generate functional 3D cardiac microtissues. *Lab Chip*, *16*(3), 599-610. https://doi.org/10.1039/c5lc01356a

Mayhew, D., Devos, N., Lambert, C., Brown, J. R., Clarke, S. C., Kim, V. L., Magid-Slav, M., Miller, B. E., Ostridge, K. K., Patel, R., Sathe, G., Simola, D. F., Staples, K. J., Sung, R., Tal-Singer, R., Tuck, A. C., Van Horn, S., Weynants, V., Williams, N. P., . . . Wilkinson, T. M. A. (2018). Longitudinal profiling of the lung microbiome in the AERIS study demonstrates repeatability of bacterial and eosinophilic COPD exacerbations. *Thorax*, *73*(5), 422-430. https://doi.org/10.1136/thoraxjnl-2017-210408

Miller, A. J., & Spence, J. R. (2017). In Vitro Models to Study Human Lung Development, Disease and Homeostasis. *Physiology (Bethesda)*, *32*(3), 246-260. https://doi.org/10.1152/physiol.00041.2016

Mirzaei, R., Mohammadzadeh, R., Sholeh, M., Karampoor, S., Abdi, M., Dogan, E., Moghadam, M. S., Kazemi, S., Jalalifar, S., Dalir, A., Yousefimashouf, R., Mirzaei, E., Khodavirdipour, A., & Alikhani, M. Y. (2020). The importance of intracellular bacterial biofilm in infectious diseases. *Microb Pathog*, *147*, 104393. https://doi.org/10.1016/j.micpath.2020.104393

Montoro, D. T., Haber, A. L., Biton, M., Vinarsky, V., Lin, B., Birket, S. E., Yuan, F., Chen, S., Leung, H. M., Villoria, J., Rogel, N., Burgin, G., Tsankov, A. M., Waghray, A., Slyper, M., Waldman, J., Nguyen, L., Dionne, D., Rozenblatt-Rosen, O., . . . Rajagopal, J. (2018). A revised airway epithelial hierarchy includes CFTR-expressing ionocytes. *Nature*, *560*(7718), 319-324. https://doi.org/10.1038/s41586-018-0393-7

Moreira, A., Müller, M., Costa, P. F., & Kohl, Y. (2022). Advanced In Vitro Lung Models for Drug and Toxicity Screening: The Promising Role of Induced Pluripotent Stem Cells. *Advanced Biology*, *6*(2), 2101139. https://doi.org/https://doi.org/10.1002/adbi.202101139

Morey, P., Cano, V., Martí-Lliteras, P., López-Gómez, A., Regueiro, V., Saus, C., Bengoechea, J. A., & Garmendia, J. (2011). Evidence for a non-replicative intracellular stage of nontypable Haemophilus influenzae in epithelial cells. *Microbiology (Reading)*, *157*(Pt 1), 234-250. https://doi.org/10.1099/mic.0.040451-0

Morgenroth, & Ebsen. (2008). Anatomy. In B. L. PETER J. PAPADAKOS, Laraine Visser-Isles (Ed.), *Mechanical Ventilation*. W.B., Saunders.
Moysidou, C. M., Barberio, C., & Owens, R. M. (2020). Advances in Engineering Human Tissue Models. *Front Bioeng Biotechnol*, *8*, 620962. https://doi.org/10.3389/fbioe.2020.620962
Muenzner , P., Rohde , M., Kneitz , S., & Hauck , C. R. (2005). CEACAM engagement by human pathogens enhances cell adhesion and counteracts bacteria-induced detachment of epithelial cells. *Journal of Cell Biology*, *170*(5), 825-836. https://doi.org/10.1083/jcb.200412151
Murphy, T. F., & Parameswaran, G. I. (2009). Moraxella catarrhalis, a human respiratory tract pathogen. *Clin Infect Dis*, *49*(1), 124-131. https://doi.org/10.1086/599375
N'Guessan, P. D., Vigelahn, M., Bachmann, S., Zabel, S., Opitz, B., Schmeck, B., Hippenstiel, S., Zweigner, J., Riesbeck, K., Singer, B. B., Suttorp, N., & Slevogt, H. (2007). The UspA1 protein of Moraxella catarrhalis induces CEACAM-1-dependent apoptosis in alveolar epithelial cells. *J Infect Dis*, *195*(11), 1651-1660. https://doi.org/10.1086/514820
Nicchi, S., Giusti, F., Carello, S., Utrio Lanfaloni, S., Tavarini, S., Frigimelica, E., Ferlenghi, I., Rossi Paccani, S., Merola, M., Delany, I., Scarlato, V., Maione, D., & Brettoni, C. (2022). Moraxella catarrhalis evades neutrophil oxidative stress responses providing a safer niche for nontypeable Haemophilus influenzae. *iScience*, *25*(3), 103931. https://doi.org/10.1016/j.isci.2022.103931
Nieskens, T. T. G., & Sjogren, A. K. (2019). Emerging In Vitro Systems to Screen and Predict Drug-Induced Kidney Toxicity. *Semin Nephrol*, *39*(2), 215-226. https://doi.org/10.1016/j.semnephrol.2018.12.009
Njoku, C. M., Alqahtani, J. S., Wimmer, B. C., Peterson, G. M., Kinsman, L., Hurst, J. R., & Bereznicki, B. J. (2020). Risk factors and associated outcomes of hospital readmission in COPD: A systematic review. *Respir Med*, *173*, 105988. https://doi.org/10.1016/j.rmed.2020.105988
Ohsawa, S., Vaughen, J., & Igaki, T. (2018). Cell Extrusion: A Stress-Responsive Force for Good or Evil in Epithelial Homeostasis. *Dev Cell*, *44*(4), 532. https://doi.org/10.1016/j.devcel.2018.02.007
Osei, E. T., Booth, S., & Hackett, T. L. (2020). What Have In Vitro Co-Culture Models Taught Us about the Contribution of Epithelial-Mesenchymal Interactions to Airway Inflammation and Remodeling in Asthma? *Cells*, *9*(7). https://doi.org/10.3390/cells9071694
Palma Medina, L. M., Becker, A. K., Michalik, S., Surmann, K., Hildebrandt, P., Gesell Salazar, M., Mekonnen, S. A., Kaderali, L., Volker, U., & van Dijl, J. M. (2020). Interaction of Staphylococcus aureus and Host Cells upon Infection of Bronchial Epithelium during Different Stages of Regeneration. *ACS Infect Dis*, *6*(8), 2279-2290. https://doi.org/10.1021/acsinfecdis.0c00403
Parker, D., & Prince, A. (2011). Innate immunity in the respiratory epithelium. *Am J Respir Cell Mol Biol*, *45*(2), 189-201. https://doi.org/10.1165/rcmb.2011-0011RT
Pentecost, M., Otto, G., Theriot, J. A., & Amieva, M. R. (2006). Listeria monocytogenes Invades the Epithelial Junctions at Sites of Cell Extrusion. *PLOS Pathogens*, *2*(1), e3. https://doi.org/10.1371/journal.ppat.0020003
Perez, A. C., Pang, B., King, L. B., Tan, L., Murrah, K. A., Reimche, J. L., Wren, J. T., Richardson, S. H., Ghandi, U., & Swords, W. E. (2014). Residence of Streptococcus pneumoniae and Moraxella catarrhalis within polymicrobial biofilm promotes antibiotic resistance and bacterial persistence in vivo. *Pathog Dis*, *70*(3), 280-288. https://doi.org/10.1111/2049-632X.12129
Phuong, M. S., Hernandez, R. E., Wolter, D. J., Hoffman, L. R., & Sad, S. (2021). Impairment in inflammasome signaling by the chronic Pseudomonas aeruginosa

isolates from cystic fibrosis patients results in an increase in inflammatory response. *Cell Death & Disease*, *12*(3), 241. https://doi.org/10.1038/s41419-021-03526-w

Pilette, C., Durham, S. R., Vaerman, J. P., & Sibille, Y. (2004). Mucosal immunity in asthma and chronic obstructive pulmonary disease: a role for immunoglobulin A? *Proc Am Thorac Soc*, *1*(2), 125-135. https://doi.org/10.1513/pats.2306032

Pinkerton, J. W., Kim, R. Y., Robertson, A. A. B., Hirota, J. A., Wood, L. G., Knight, D. A., Cooper, M. A., O'Neill, L. A. J., Horvat, J. C., & Hansbro, P. M. (2017). Inflammasomes in the lung. *Mol Immunol*, *86*, 44-55. https://doi.org/10.1016/j.molimm.2017.01.014

Plasschaert, L. W., Žilionis, R., Choo-Wing, R., Savova, V., Knehr, J., Roma, G., Klein, A. M., & Jaffe, A. B. (2018). A single-cell atlas of the airway epithelium reveals the CFTR-rich pulmonary ionocyte. *Nature*, *560*(7718), 377-381. https://doi.org/10.1038/s41586-018-0394-6

Plotkowski, M. C., de Bentzmann, S., Pereira, S. H., Zahm, J. M., Bajolet-Laudinat, O., Roger, P., & Puchelle, E. (1999). Pseudomonas aeruginosa internalization by human epithelial respiratory cells depends on cell differentiation, polarity, and junctional complex integrity. *Am J Respir Cell Mol Biol*, *20*(5), 880-890. https://doi.org/10.1165/ajrcmb.20.5.3408

Proud, D. (2008). *The pulmonary epithelium in health and disease*. Wiley.

Prytherch, Z., Job, C., Marshall, H., Oreffo, V., Foster, M., & BéruBé, K. (2011). Tissue-Specific stem cell differentiation in an in vitro airway model. *Macromol Biosci*, *11*(11), 1467-1477. https://doi.org/10.1002/mabi.201100181

Puchelle, E., Zahm, J. M., Tournier, J. M., & Coraux, C. (2006). Airway epithelial repair, regeneration, and remodeling after injury in chronic obstructive pulmonary disease. *Proc Am Thorac Soc*, *3*(8), 726-733. https://doi.org/10.1513/pats.200605-126SF

Raffel, F. K., Szelestey, B. R., Beatty, W. L., & Mason, K. M. (2013). The Haemophilus influenzae Sap transporter mediates bacterium-epithelial cell homeostasis. *Infect Immun*, *81*(1), 43-54. https://doi.org/10.1128/iai.00942-12

Reynolds, S. D., & Malkinson, A. M. (2010). Clara cell: progenitor for the bronchiolar epithelium. *Int J Biochem Cell Biol*, *42*(1), 1-4. https://doi.org/10.1016/j.biocel.2009.09.002

Ritchie, A. I., & Wedzicha, J. A. (2020). Definition, Causes, Pathogenesis, and Consequences of Chronic Obstructive Pulmonary Disease Exacerbations. *Clin Chest Med*, *41*(3), 421-438. https://doi.org/10.1016/j.ccm.2020.06.007

Roberts, A. E., Kragh, K. N., Bjarnsholt, T., & Diggle, S. P. (2015). The Limitations of In Vitro Experimentation in Understanding Biofilms and Chronic Infection. *J Mol Biol*, *427*(23), 3646-3661. https://doi.org/10.1016/j.jmb.2015.09.002

Robinson, K. S., Teo, D. E. T., Tan, K. S., Toh, G. A., Ong, H. H., Lim, C. K., Lay, K., Au, B. V., Lew, T. S., Chu, J. J. H., Chow, V. T. K., Wang, Y., Zhong, F. L., & Reversade, B. (2020). Enteroviral 3C protease activates the human NLRP1 inflammasome in airway epithelia. *Science*, *370*(6521). https://doi.org/10.1126/science.aay2002

Rogers, D. F. (2003). The airway goblet cell. *Int J Biochem Cell Biol*, *35*(1), 1-6. https://doi.org/10.1016/s1357-2725(02)00083-3

Rosen, D. A., Hooton, T. M., Stamm, W. E., Humphrey, P. A., & Hultgren, S. J. (2007). Detection of Intracellular Bacterial Communities in Human Urinary Tract Infection. *PLOS Medicine*, *4*(12), e329. https://doi.org/10.1371/journal.pmed.0040329

Sachs, N., Papaspyropoulos, A., Zomer-van Ommen, D. D., Heo, I., Böttinger, L., Klay, D., Weeber, F., Huelsz-Prince, G., Iakobachvili, N., Amatngalim, G. D., de Ligt, J., van Hoeck, A., Proost, N., Viveen, M. C., Lyubimova, A., Teeven, L., Derakhshan, S., Korving, J., Begthel, H., . . . Clevers, H. (2019). Long-term expanding human airway organoids for disease modeling. *Embo j*, *38*(4). https://doi.org/10.15252/embj.2018100300

Satoh, T., Sugiura, S., Shin, K., Onuki-Nagasaki, R., Ishida, S., Kikuchi, K., Kakiki, M., & Kanamori, T. (2017). A multi-throughput multi-organ-on-a-chip system on a plate formatted pneumatic pressure-driven medium circulation platform. *Lab Chip*, *18*(1), 115-125. https://doi.org/10.1039/c7lc00952f

Saw, T. B., Doostmohammadi, A., Nier, V., Kocgozlu, L., Thampi, S., Toyama, Y., Marcq, P., Lim, C. T., Yeomans, J. M., & Ladoux, B. (2017). Topological defects in epithelia govern cell death and extrusion. *Nature*, *544*(7649), 212-216. https://doi.org/10.1038/nature21718

Schleimer, R. P., Kato, A., Kern, R., Kuperman, D., & Avila, P. C. (2007). Epithelium: at the interface of innate and adaptive immune responses. *J Allergy Clin Immunol*, *120*(6), 1279-1284. https://doi.org/10.1016/j.jaci.2007.08.046

Schneider, O., Zeifang, L., Fuchs, S., Sailer, C., & Loskill, P. (2019). User-Friendly and Parallelized Generation of Human Induced Pluripotent Stem Cell-Derived Microtissues in a Centrifugal Heart-on-a-Chip. *Tissue Eng Part A*, *25*(9-10), 786-798. https://doi.org/10.1089/ten.TEA.2019.0002

Schroeder, T. H., Reiniger, N., Meluleni, G., Grout, M., Coleman, F. T., & Pier, G. B. (2001). Transgenic cystic fibrosis mice exhibit reduced early clearance of Pseudomonas aeruginosa from the respiratory tract. *J Immunol*, *166*(12), 7410-7418. https://doi.org/10.4049/jimmunol.166.12.7410

Schutgens, F., Rookmaaker, M. B., Margaritis, T., Rios, A., Ammerlaan, C., Jansen, J., Gijzen, L., Vormann, M., Vonk, A., Viveen, M., Yengej, F. Y., Derakhshan, S., de Winter-de Groot, K. M., Artegiani, B., van Boxtel, R., Cuppen, E., Hendrickx, A. P. A., van den Heuvel-Eibrink, M. M., Heitzer, E., . . . Clevers, H. (2019). Tubuloids derived from human adult kidney and urine for personalized disease modeling. *Nature Biotechnology*, *37*(3), 303-313. https://doi.org/10.1038/s41587-019-0048-8

Serafini, S. M., & Michaelson, E. D. (1977). Length and distribution of cilia in human and canine airways. *Bull Eur Physiopathol Respir*, *13*(4), 551-559.

Shanks, N., Greek, R., & Greek, J. (2009). Are animal models predictive for humans? *Philosophy, Ethics, and Humanities in Medicine*, *4*(1), 2. https://doi.org/10.1186/1747-5341-4-2

Shi, D., Mi, G., Wang, M., & Webster, T. J. (2019). In vitro and ex vivo systems at the forefront of infection modeling and drug discovery. *Biomaterials*, *198*, 228-249. https://doi.org/10.1016/j.biomaterials.2018.10.030

Shin, W., Hinojosa, C. D., Ingber, D. E., & Kim, H. J. (2019). Human Intestinal Morphogenesis Controlled by Transepithelial Morphogen Gradient and Flow-Dependent Physical Cues in a Microengineered Gut-on-a-Chip. *iScience*, *15*, 391-406. https://doi.org/10.1016/j.isci.2019.04.037

Sivarajan, R., Kessie, D. K., Oberwinkler, H., Pallmann, N., Walles, T., Scherzad, A., Hackenberg, S., & Steinke, M. (2021). Susceptibility of Human Airway Tissue Models Derived From Different Anatomical Sites to Bordetella pertussis and Its Virulence Factor Adenylate Cyclase Toxin. *Front Cell Infect Microbiol*, *11*, 797491. https://doi.org/10.3389/fcimb.2021.797491

Spaniol, V., Heiniger, N., Troller, R., & Aebi, C. (2008). Outer membrane protein UspA1 and lipooligosaccharide are involved in invasion of human epithelial cells by Moraxella catarrhalis. *Microbes Infect*, *10*(1), 3-11. https://doi.org/10.1016/j.micinf.2007.09.014

Starner, T. D., Zhang, N., Kim, G., Apicella, M. A., & McCray, P. B., Jr. (2006). Haemophilus influenzae forms biofilms on airway epithelia: implications in cystic fibrosis. *Am J Respir Crit Care Med*, *174*(2), 213-220. https://doi.org/10.1164/rccm.200509-1459OC

Stroulios, G., Brown, T., Moreni, G., Kondro, D., Dei, A., Eaves, A., Louis, S., Hou, J., Chang, W., Pajkrt, D., Wolthers, K. C., Sridhar, A., & Simmini, S. (2022). Apical-out

airway organoids as a platform for studying viral infections and screening for antiviral drugs. *Scientific Reports*, *12*(1), 7673. https://doi.org/10.1038/s41598-022-11700-z

Stucki, A. O., Stucki, J. D., Hall, S. R., Felder, M., Mermoud, Y., Schmid, R. A., Geiser, T., & Guenat, O. T. (2015). A lung-on-a-chip array with an integrated bio-inspired respiration mechanism. *Lab Chip*, *15*(5), 1302-1310. https://doi.org/10.1039/c4lc01252f

Sung, J. H., Yu, J., Luo, D., Shuler, M. L., & March, J. C. (2011). Microscale 3-D hydrogel scaffold for biomimetic gastrointestinal (GI) tract model. *Lab Chip*, *11*(3), 389-392. https://doi.org/10.1039/c0lc00273a

Tan, A., Li, W. S., Verderosa, A. D., Blakeway, L. V., T, D. M., Totsika, M., & Seib, K. L. (2019). Moraxella catarrhalis NucM is an entry nuclease involved in extracellular DNA and RNA degradation, cell competence and biofilm scaffolding. *Sci Rep*, *9*(1), 2579. https://doi.org/10.1038/s41598-019-39374-0

Tan, T. T., Forsgren, A., & Riesbeck, K. (2006). The respiratory pathogen moraxella catarrhalis binds to laminin via ubiquitous surface proteins A1 and A2. *J Infect Dis*, *194*(4), 493-497. https://doi.org/10.1086/505581

Tan, T. T., Nordstrom, T., Forsgren, A., & Riesbeck, K. (2005). The respiratory pathogen Moraxella catarrhalis adheres to epithelial cells by interacting with fibronectin through ubiquitous surface proteins A1 and A2. *J Infect Dis*, *192*(6), 1029-1038. https://doi.org/10.1086/432759

Thacker, V. V., Dhar, N., Sharma, K., Barrile, R., Karalis, K., & McKinney, J. D. (2020). A lung-on-chip model of early Mycobacterium tuberculosis infection reveals an essential role for alveolar epithelial cells in controlling bacterial growth. *Elife*, *9*. https://doi.org/10.7554/eLife.59961

Tolker-Nielsen, T. (2015). Biofilm Development. In *Microbial Biofilms* (pp. 51-66). https://doi.org/https://doi.org/10.1128/9781555817466.ch3

van der Vaart, J., & Clevers, H. (2021). Airway organoids as models of human disease. *J Intern Med*, *289*(5), 604-613. https://doi.org/10.1111/joim.13075

van Midwoud, P. M., Merema, M. T., Verpoorte, E., & Groothuis, G. M. (2010). A microfluidic approach for in vitro assessment of interorgan interactions in drug metabolism using intestinal and liver slices. *Lab Chip*, *10*(20), 2778-2786. https://doi.org/10.1039/c0lc00043d

Van Norman, G. A. (2020). Limitations of Animal Studies for Predicting Toxicity in Clinical Trials: Part 2: Potential Alternatives to the Use of Animals in Preclinical Trials. *JACC Basic Transl Sci*, *5*(4), 387-397. https://doi.org/10.1016/j.jacbts.2020.03.010

Vestby, L. K., Gronseth, T., Simm, R., & Nesse, L. L. (2020). Bacterial Biofilm and its Role in the Pathogenesis of Disease. *Antibiotics (Basel)*, *9*(2). https://doi.org/10.3390/antibiotics9020059

Vladimer, G. I., Marty-Roix, R., Ghosh, S., Weng, D., & Lien, E. (2013). Inflammasomes and host defenses against bacterial infections. *Curr Opin Microbiol*, *16*(1), 23-31. https://doi.org/10.1016/j.mib.2012.11.008

Walters, J. A., Tang, J. N., Poole, P., & Wood-Baker, R. (2017). Pneumococcal vaccines for preventing pneumonia in chronic obstructive pulmonary disease. *Cochrane Database Syst Rev*, *1*, CD001390. https://doi.org/10.1002/14651858.CD001390.pub4

Wang, B., Lim, D. J., Han, J., Kim, Y. S., Basbaum, C. B., & Li, J.-D. (2002). Novel Cytoplasmic Proteins of Nontypeable *Haemophilus influenzae* Up-regulate Human MUC5AC Mucin Transcription via a Positive p38 Mitogen-activated Protein Kinase Pathway and a Negative Phosphoinositide 3-Kinase-Akt Pathway *Journal of Biological Chemistry*, *277*(2), 949-957. https://doi.org/10.1074/jbc.M107484200

Wang, J., Sahoo, M., Lantier, L., Warawa, J., Cordero, H., Deobald, K., & Re, F. (2018). Caspase-11-dependent pyroptosis of lung epithelial cells protects from melioidosis

while caspase-1 mediates macrophage pyroptosis and production of IL-18. *PLOS Pathogens*, *14*(5), e1007105. https://doi.org/10.1371/journal.ppat.1007105
Weeks, J. R., Staples, K. J., Spalluto, C. M., Watson, A., & Wilkinson, T. M. A. (2021). The Role of Non-Typeable Haemophilus influenzae Biofilms in Chronic Obstructive Pulmonary Disease. *Front Cell Infect Microbiol*, *11*, 720742. https://doi.org/10.3389/fcimb.2021.720742
Wen, J., Xuan, B., Liu, Y., Wang, L., He, L., Meng, X., Zhou, T., & Wang, Y. (2021). Updating the NLRC4 Inflammasome: from Bacterial Infections to Autoimmunity and Cancer. *Front Immunol*, *12*, 702527. https://doi.org/10.3389/fimmu.2021.702527
Wilkinson, T. M. A., Aris, E., Bourne, S., Clarke, S. C., Peeters, M., Pascal, T. G., Schoonbroodt, S., Tuck, A. C., Kim, V., Ostridge, K., Staples, K. J., Williams, N., Williams, A., Wootton, S., & Devaster, J.-M. (2017). A prospective, observational cohort study of the seasonal dynamics of airway pathogens in the aetiology of exacerbations in COPD. *Thorax*, *72*(10), 919-927. https://doi.org/10.1136/thoraxjnl-2016-209023
Wisnivesky, J., & De-Torres, J. P. (2019). The Global Burden of Pulmonary Diseases: Most Prevalent Problems and Opportunities for Improvement. *Ann Glob Health*, *85*(1). https://doi.org/10.5334/aogh.2411
Wu, Q., Liu, J., Wang, X., Feng, L., Wu, J., Zhu, X., Wen, W., & Gong, X. (2020). Organ-on-a-chip: recent breakthroughs and future prospects. *BioMedical Engineering OnLine*, *19*(1), 9. https://doi.org/10.1186/s12938-020-0752-0
Wurster, S., Ruiz, O. E., Samms, K. M., Tatara, A. M., Albert, N. D., Kahan, P. H., Nguyen, A. T., Mikos, A. G., Kontoyiannis, D. P., & Eisenhoffer, G. T. (2021). EGF-mediated suppression of cell extrusion during mucosal damage attenuates opportunistic fungal invasion. *Cell Rep*, *34*(12), 108896. https://doi.org/10.1016/j.celrep.2021.108896
Xu, F., Wen, Z., Shi, X., & Fan, J. (2018). Inflammasome in the Pathogenesis of Pulmonary Diseases. *Exp Suppl*, *108*, 111-151. https://doi.org/10.1007/978-3-319-89390-7_6
Xu, Z., Gao, Y., Hao, Y., Li, E., Wang, Y., Zhang, J., Wang, W., Gao, Z., & Wang, Q. (2013). Application of a microfluidic chip-based 3D co-culture to test drug sensitivity for individualized treatment of lung cancer. *Biomaterials*, *34*(16), 4109-4117. https://doi.org/10.1016/j.biomaterials.2013.02.045
Yaghi, A., & Dolovich, M. B. (2016). Airway Epithelial Cell Cilia and Obstructive Lung Disease. *Cells*, *5*(4). https://doi.org/10.3390/cells5040040
Yang, X., Li, K., Zhang, X., Liu, C., Guo, B., Wen, W., & Gao, X. (2018). Nanofiber membrane supported lung-on-a-chip microdevice for anti-cancer drug testing. *Lab Chip*, *18*(3), 486-495. https://doi.org/10.1039/c7lc01224a
Yonker, L. M., Mou, H., Chu, K. K., Pazos, M. A., Leung, H., Cui, D., Ryu, J., Hibbler, R. M., Eaton, A. D., Ford, T. N., Falck, J. R., Kinane, T. B., Tearney, G. J., Rajagopal, J., & Hurley, B. P. (2017). Development of a Primary Human Co-Culture Model of Inflamed Airway Mucosa. *Sci Rep*, *7*(1), 8182. https://doi.org/10.1038/s41598-017-08567-w
Zaas, D. W., Duncan, M. J., Li, G., Wright, J. R., & Abraham, S. N. (2005). Pseudomonas Invasion of Type I Pneumocytes Is Dependent on the Expression and Phosphorylation of Caveolin-2 *. *Journal of Biological Chemistry*, *280*(6), 4864-4872. https://doi.org/10.1074/jbc.M411702200
Zhang, D., Shadrin, I. Y., Lam, J., Xian, H. Q., Snodgrass, H. R., & Bursac, N. (2013). Tissue-engineered cardiac patch for advanced functional maturation of human ESC-derived cardiomyocytes. *Biomaterials*, *34*(23), 5813-5820. https://doi.org/10.1016/j.biomaterials.2013.04.026
Zhang, J., Zhu, Z., Zuo, X., Pan, H., Gu, Y., Yuan, Y., Wang, G., Wang, S., Zheng, R., Liu, Z., Wang, F., & Zheng, J. (2020). The role of NTHi colonization and infection in the

pathogenesis of neutrophilic asthma. *Respir Res*, *21*(1), 170. https://doi.org/10.1186/s12931-020-01438-5

Zhang, X., Wang, T., Wang, P., & Hu, N. (2016). High-Throughput Assessment of Drug Cardiac Safety Using a High-Speed Impedance Detection Technology-Based Heart-on-a-Chip. *Micromachines (Basel)*, *7*(7). https://doi.org/10.3390/mi7070122

Zhang, Y. S., Arneri, A., Bersini, S., Shin, S. R., Zhu, K., Goli-Malekabadi, Z., Aleman, J., Colosi, C., Busignani, F., Dell'Erba, V., Bishop, C., Shupe, T., Demarchi, D., Moretti, M., Rasponi, M., Dokmeci, M. R., Atala, A., & Khademhosseini, A. (2016). Bioprinting 3D microfibrous scaffolds for engineering endothelialized myocardium and heart-on-a-chip. *Biomaterials*, *110*, 45-59. https://doi.org/10.1016/j.biomaterials.2016.09.003